

NASA Contractor Report 4448

Advanced Composites Structural Concepts and Materials Technologies for Primary Aircraft Structures

Structural Response and Failure Analysis

W. J. Dorris, J. W. Hairr,
J. T. Huang, J. E. Ingram,
and B. M. Shah
Lockheed Aeronautical Systems Company
Marietta, Georgia

Prepared for
Langley Research Center
under Contract NAS1-18888



National Aeronautics and
Space Administration

Office of Management

Scientific and Technical
Information Program

1992



FOREWORD

This final technical report covers the work performed under Phase I, Evaluation and Initial Development, Task 2 Structural Response and Failure Analysis, of NASA Contract NAS1-18888, entitled, "Advanced Composite Structural Concepts and Materials Technology for Primary Aircraft Structures", between May 1989 to May 1992. This contract is administered under the management direction of Dr. John G. Davis and under the technical direction of Dr. Randall C. Davis, NASA/SPO, NASA Langley Research Center, Hampton, Virginia 23665.

Lockheed Aeronautical Systems Company (LASC) is the prime contractor. Mr. A. C. Jackson is the LASC Program Manager, directing all the contract activities. Mr. Bharat M. Shah of Advanced Structures and Materials Division was the technical thrust leader in the performance of this task.

Other key LASC (Or as indicated) contributors to the Methods Development Task are listed below:

Non-Linear Analysis Methods

Norm Cyr	(LMSC)
Glen Sahrman	(LMSC)
Jui-Tien Huang	
Bill Dorris	
Bharat Shah	

"ISPAN" Modules Development

Wayne Brown	(LMSC)
Tony Wei	(LMSC)
Ed Ingram	
Jui-Tien Huang	
John Hairr	

Bolted Joint Strength Prediction Methodolgy

Dr. Fu-Kuo Chang	(Stanford University)
Bharat Shah	
Jui-Tien Huang	

Table of Contents

Foreword.....	iii
List of Figures	vii
List of Tables.....	x
Abbreviations and Symbols.....	xi
Summary	xiii
1.0 Introduction	1
2.0 Non-linear Analysis Methodology.....	4
2.1 Post-Buckling Analysis	5
2.2 DIAL Implementation of the Arc Length Method.....	8
2.2.1 Target Point Analysis	9
2.3 Interface Analysis.....	11
3.0 'ISPAN' Module Development.....	15
3.1 Flat Stiffened Panel.....	16
3.1.1 DIAL Shell Element	18
3.1.2 Model Geometry	19
3.1.3 Loads.....	20
3.1.4 Boundary Conditions	21
3.1.5 Solutions.....	23
3.2 Curved Stiffened Panel	25
3.2.1 Example Problems.....	26
3.2.1.1 Example 1 Linear Static Analysis	26
3.2.1.2 Example 2 Bifurcation Buckling Analysis	31
3.3 Flat Rectangular Tubular Truss Core Panel.....	35
3.3.1 Program Components.....	35
3.3.1.1 Command Module	35
3.3.1.2 Pre-processor.....	36
3.3.1.3 Post-processor.....	36
3.3.2 Modeling Concepts.....	36
3.3.2.1 Shell Model	36
3.3.2.2 Mesh Generation	37
3.3.2.3 Boundary Conditions.....	38
3.3.2.4 Load Application and Displacement Coupling.....	39
3.3.3 Examples	39
3.3.3.1 Material Properties.....	40
3.3.4 Example 1. Static Analysis of a Panel Strip	41
3.3.4.1 Non-Finite Element Calculations.....	42
3.3.4.2 DIAL Solution.....	43
3.3.5 Example 2. Static Analysis of a Panel Subjected to Inplane Shear Loads ..	45
3.3.6 Example 3. Local Buckling of a Panel Strip.....	47
3.3.7 Example 4. Overall Buckling of a Panel Strip.....	48
3.3.8 Example 5. Overall Buckling of a Square Panel	49
3.3.9 Closure.....	50

3.4 Geodesically Stiffened Rectangular Panel	51
3.4.1 Example.....	52
3.4.2 Closure.....	54
4.0 Failure Analysis.....	55
4.1 AML Failure Analysis Procedure	56
4.1.1 Example.....	57
4.1.2 AML within DIAL.....	58
4.2 Hashin's Failure Criterion	59
4.2.1 Hashin's Criterion within DIAL.....	60
5.0 Bolted Joint Strength Prediction.....	62
5.1 Introduction to Bolted Joint Prediction.....	63
5.2 Statement of Problem.....	64
5.3 Analysis.....	65
5.3.1 Stress Analysis.....	66
5.3.2 Failure Analysis.....	69
5.3.2.1 Failure Criteria.....	69
5.3.2.2 Property Degradation Models.....	71
5.4 TEXTJOINT Code	77
5.5 Numerical Results and Verifications.....	78
5.6 Summary.....	84
6.0 Concluding Remarks	85
7.0 References	86
Appendix A TEXTJOINT Example Input	A1

List of Figures

Figure 1	ACT Program Master Schedule - Phase I.....	2
Figure 2	Load Deflection Curve	5
Figure 3	Limit Point.....	6
Figure 4	Simply Supported Shallow Spherical Cap.....	8
Figure 5	DIAL Computed Load Deflection Curve.....	9
Figure 6	Three Dimensional Lap Shear joint Specimen.....	11
Figure 7	DIAL Three Dimensional Lap Shear Joint Model.....	12
Figure 8	Lap Shear Joint Problem, Peel Stress Comparison.....	12
Figure 9	Lap Shear Joint Problem, Shear Strain Comparison	13
Figure 10	Lap Shear Joint Problem, Shear Stress Comparison	13
Figure 11	Flat Panel Stiffener Geometry.....	16
Figure 12	Shell Element Connectives, Reference Vector and Sign Convention.....	18
Figure 13	Typical Flat Panel Model with Closed Hat Stiffeners	19
Figure 14	Flange Attach Region.....	20
Figure 15	Applied Loads Definition	20
Figure 16	CONODE Command	21
Figure 17	Typical Constraint Vectors for Flat Panel.....	22
Figure 18	Rib/Frame Elastic Support, Column Analogy.....	23
Figure 19	Geometry of Curved Panel	25
Figure 20	Curved Panel, DIAL Model with Applied Loads, Example 1	26
Figure 21	Curved Panel, Deflected Shape, Example 1	27
Figure 22	Curved Panel Contour Plot, N_x Average.....	29
Figure 23	Curved Panel Contour Plot ϵ_x Average, Example 1.....	30
Figure 24	Curved Panel Margin of Safety, Example 1	30
Figure 25	Curved Panel ϵ_x Average, Typical Stiffener, Example 1	31

Figure 26	Curved Panel, Geometry and Applied Load Vectors, Example 2.....	32
Figure 27	Curved Panel Deflected Shape, Example 2.....	32
Figure 28	Curved Panel Contour Plot, ϵ_x , Example 2.....	33
Figure 29	Curved Panel Contour Plot, ϵ_{xy} , Example 2.....	33
Figure 30	Curved Panel Buckled Mode Shape, Example 2.....	34
Figure 31	Truss Core Panel.....	35
Figure 32	Generic Truss Core Panel with Ply orientations.....	37
Figure 33	Truss Core Mesh Generation Sequence.....	37
Figure 34	Truss Core Panel, Kinematic Boundary Conditions.....	38
Figure 35	Truss Core Example Panel Geometry.....	41
Figure 36	Finite Element Mode of Truss Core Panel, Example 1.....	43
Figure 37	Truss Core Panel Deflected Geometry, Example 1.....	43
Figure 38	Truss Core Panel Contour Plot, ϵ_x , Example 1.....	44
Figure 39	Truss Core Panel Margin of Safety Plot, Example 1.....	44
Figure 40	Truss Core Panel Geometry and Deflected Plot, Example 2.....	46
Figure 41	Truss Core Panel Coutour Plot, ϵ_x Example 2.....	46
Figure 42	Truss Core Panel Coutour Plot, ϵ_{xy} , Example 2.....	47
Figure 43	Truss Core Panel Strip Geometry, Example 3.....	47
Figure 44	Truss Core Panel Strip, First Mode Shape, Example 3.....	48
Figure 45	Truss Core Panel Strip, Second Mode Shape, Example 3.....	48
Figure 46	Truss Core Panel Strip, First Mode Shape, Example 4.....	49
Figure 47	Truss Core Panel Strip, Second Mode Shape Example 4.....	49
Figure 48	Truss Core Panel Geometry and First Mode Shape, Example 5.....	50
Figure 49	Geodesic Panel General Structural Arrangement.....	51
Figure 50	Geodesic Panel Geometry and Deflected Shape.....	53
Figure 51	Geodesic Panel N_x Contour Plot.....	54
Figure 52	AML Hypothetical Allowable Strains.....	57

Figure 53	Description of Bolted Composite Joint Problem	64
Figure 54	Bolted Joint, Typical Finite Element Mesh	68
Figure 55	Measures verses Predicted Bearing Loads T300/934 Net-Tension or Shear-out.....	79
Figure 56	Predicted Damage Progression in a $[0/\pm 45/90]_{3S}$ Bolted Composite Joint	80
Figure 57	Predicted Damage Progression in a $[0/90]_{6S}$ Bolted Composite Joint.....	80
Figure 58	Predicted Load-Deflection Response of IM8/APC-HTA Bearing Failure Mode	81
Figure 59	Predicted Load-Deflection Response of IM8/APC-HTA Bearing Failure Mode	81
Figure 60	Predicted Load-Deflection Response $[0/90]_{6S}$, two holes in parallel.....	83
Figure 61	Predicted Load-Deflection Response $[0/90]_{6S}$, two holes in series.....	83

List of Tables

Table 1	Curved panel material properties, AML Values and strain allowables.....	27
Table 2	Comparison of Average Results from LAMSTR and DIAL: Curved Panel.....	31
Table 3	AML Values, Tensile and Compressive Strains.....	41
Table 4	Geodesic Panel, Material Properties.....	53
Table 5	Laminate Layups for Skin and Stiffeners.....	54
Table 6	Material Properties of T300/934 and IM8/APC-HTA Composites.....	78
Table 7	Measured verses Predicted Bearing Load of IM8/APC-HTA Bearing Failure.....	82

Abbreviations and Symbols

A	=	In-situ matrix strength constant
AML	=	Angle minus Longitudinal or Load
AML _n	=	AML value with the load in the direction n degrees from the 1 axis
B	=	In-situ matrix strength constant
C	=	In-situ shear strength constant
D	=	In-situ shear strength constant
E	=	Modulus of elasticity (isotropic)
E ₁	=	Young's modulus of elasticity of lamina in the fiber direction
E ₂	=	Young's modulus of elasticity of lamina transverse to fiber direction
E _x	=	Young's Longitudinal modulus of laminate along reference axis X
E _y	=	Young's Transverse modulus of laminate along reference axis Y
F _{ij}	=	Coefficients for failure criteria
G ₁₂	=	Inplane shear modulus of lamina
G _{xy}	=	Inplane shear modulus of laminate in reference plane X-Y
IML	=	Inner Mold Line
K	=	Spring constant
L	=	Length
M.S.	=	Margin of Safety
N _x	=	Inplane longitudinal Axial Lind load (lb/in)
N _{xy}	=	Inplane shear load (lb/in)
N _y	=	Inplane Transverse Axial Line load (lb/in)
P	=	Uniform pressure loading
q	=	Distributed line load
R	=	Radius of curvature
w	=	Out-of-plane deflection

X_c	=	Longitudinal compression strength of Crossplied Laminate
X_t	=	Longitudinal tension strength of Crossplied Laminate
Y_c	=	Logitudinal Shear strength, of Crossplied Laminate
Y_t^0	=	Transverse tension strength

Greek

α	=	Stiffener angle (geodesic panel)
α_s	=	Nonlinearity parameter
β	=	Shape parameter for fiber tension failure
δ	=	Fiber interaction zone size
ϵ_C	=	Compressive Strain allowable
ϵ_T	=	Tensive Strain allowable
ϵ_x	=	Axial strain
ϵ_y	=	Lateral strain
γ	=	Shape parameter for bearing failure
γ_{xy}	=	Shear Strain
γ_{yld}	=	Yield shear strain
η	=	Critical bearing area coefficient
ν_{12}	=	Poisson's ratio of lamina
ν_{xy}	=	Poisson's ratio of laminate
σ_{ij}	=	Stress on the i^{th} face in the j^{th} direction
σ_{yld}	=	Yield stress

Summary

The documentation of the work performed in Phase I, Task 2, "Structural Response and Failure Analysis", is contained in the final technical report.

The primary objective of this task was to develop analysis methods and modeling techniques to accurately evaluate the response of stiffened structures under combined in-plane and out-of-plane loadings. The contents of this technical report are briefly summarized.

Section 2.0 describes the non-linear analysis methods that were adapted and incorporated in the Lockheed finite element code DIAL. These methods include, the arc length Method, target point analysis procedures, and skin-stiffener interface analysis. The finite element based approach was taken to address the complex interaction of nonlinearities due to pressurization, postbuckling and geometric configurations for stiffened structures representative of wing cover panels, fuselage shells, spar webs, bulkheads, and ribs.

In order to produce an efficient solution and effective computer utilization during non-linear analysis, the Arc Length method was implemented in the DIAL finite element code. This method allows the unstable branch of the postbuckling response to be predicted. The implementation of the arc-length solution method has several unique features such as automatic shifting between load and displacement control to ensure numerical stability and tracing out the full response curve.

In order to develop a relatively simple analysis method for bonded structures, a new material model was implemented in the DIAL finite element code for use with the 2-D and 3-D interface elements. This material model enables the interface elements to model a thin layer of bonding material with non-linear shear stress-strain relationship. The stress components for the interface elements include a normal stress perpendicular to the plane of the element, and longitudinal and transverse interlaminar shear stresses.

Section 3.0 describes the developmental work related to the DIAL interactive pre-processor modules. In order to streamline the analyst's work during concepts analysis/trade study, ISPAN (Interactive Stiffened Panel ANalysis) modules were developed. Each ISPAN module is an interactive design tool that is intended to provide the means of performing a self-initiated preliminary analysis of specific primary composite structures such as flat and curved stiffened panel, corrugated sandwich panel and curved geodesic fuselage panel. The ISPAN module requires the user to simply specify basic geometric parameters, material properties, loads

information, boundary conditions, and types of analysis. The ISPAN utilizes this information to generate the finite element model automatically and perform the analysis. The output is in the form of summary tables of stress or margin of safety, contour plots of loads or stresses or strains and deflected shape plots which can be used to determine the adequacy of the specific design concept.

Section 4.0 describes the incorporation of the AML failure analysis procedure and Hashin's failure criterion in the DIAL finite element package. Incorporation of Hashin's criterion is for predicting skin/stiffener interface strength. The AML (% Angle plies Minus % Longitudinal plies) laminate failure method is a simplified approach to obtain the design allowable strains which account for fastener holes, barely visible impact damage, and the internal defects in symmetric and balanced laminates.

Section 5.0 describes the development of bolted composite joint strength prediction methodology. The motivation for this task was in direct response to the need for an accurate strength prediction for multifastener composite joints and to alleviate significant costs associated with obtaining joint strength data through testing. The methodology developed is a 2-D non-linear finite element based analysis considering material and geometrical non-linearity. It also conducts failure analysis and applies material degradation models. The code is interactive and has the capacity to analyze matrix tension and compression failure, shear-out failure, fiber failure, and bearing failure modes. Validation of the code (called TEXTJOINT-X) through the correlation of the predicted versus test results is excellent.

Section 6.0 includes of the concluding remarks and recommendations.

1.0 Introduction

The use of graphite/epoxy for primary and secondary structures in military as well as commercial transport aircraft has been demonstrated to save weight compared to conventional metal structures. However, the goal of cost-effective use of composite on the primary structure is not realized yet.

The Advanced Composite Technology (ACT) Program was initiated to provide creative research and innovative concepts to meet the goal of "cost-effective composite structures", in particular concepts for wing and fuselage primary structures. The developed technologies are meant for the future transcentury aircraft. The new structural concepts are to take advantage of tougher improved organic matrix materials, and advanced fabrication techniques. The validated structures technology being developed under the ACT program is necessary to provide the confidence essential for the use of polymeric composite materials for future primary aircraft structures.

The Lockheed ACT contract was programmed in two phases. Phase I, Evaluation and Initial Development, was initiated in May 1989 and ran through May 1992. Phase II, Development and Verification of Technology, was initiated in October 1991 and is schedule to run through April 1995. The total program span is 72 months.

Phase I consists of five tasks: Task 1. Design/Manufacturing Concept Assessment, Task 2. Structural Response and Failure Analysis, Task 3. Advanced Material Concepts, Task 4. Assessment Review, and Task 5. Composite Transport Wing Technology Developments.

Phase II consists of four tasks: Task 1. Advanced Resin Systems for Textile Technology, Task 2. Preform Development and Processing, Task 3. Design, Analysis, Fabrication and Test, and Task 4. Low-Cost Fabrication Development. The ACT Program Phase I Master Schedule is shown in Figure 1.

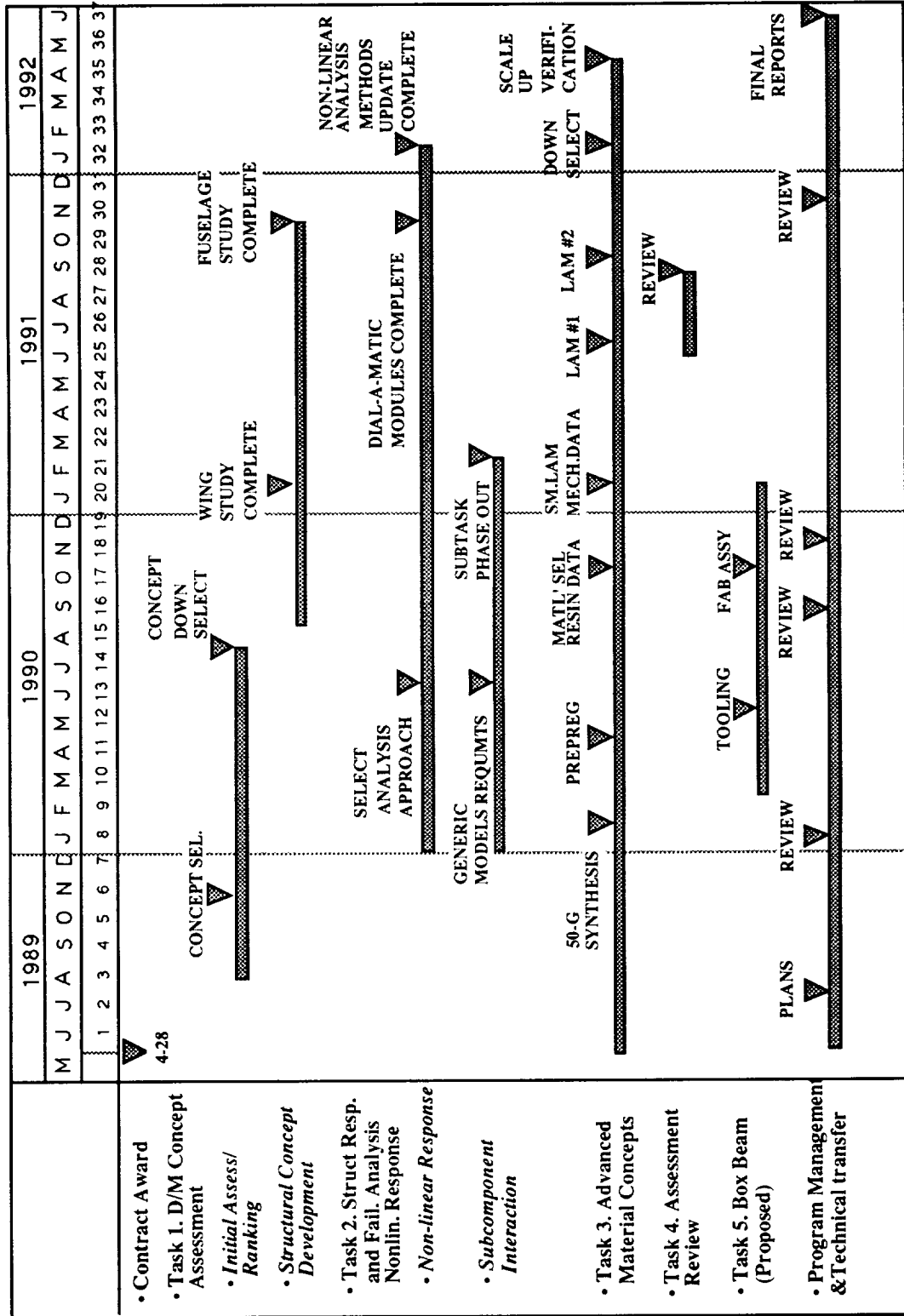


Figure 1 ACT Program Master Schedule - Phase I

Phase I has been completed and Final Technical Reports are published for Tasks 1,2, and 3. Task 4 was an assessment of Phase I results and the plans for Phase II. Task 5 has no final report.

The results of this phase were published in papers presented at the First and Second ACT Conferences.[1,2]. This report covers the work performed in Phase I Task 2.

Throughout this program technical information generated during the performance of the contract is being disseminated all through the aircraft industry and to the government. This information is being distributed through monthly technical reports and final task reports. Oral reviews have been conducted to acquaint the aircraft industry and government with progress on the program.

Use of commercial products or names of manufactures in this report does not constitute official endorsement of such products or manufactures, either expressed or implied by the National Aeronautical and Space Administration.

2.0 Nonlinear Analysis Methodology

The design of safe and efficient structures depends on the ability to accurately analyze the behavior of the structure. In order to make cost-effective use of material, structural components must be loaded as close as possible to their failure load. An accurate prediction of the failure load is a vital part of the design process. Consequently, since most structures exhibit nonlinear behavior as they approach failure, a reliable nonlinear solution technique is an important part of the structural analyst's capabilities. One of the main goals of the work presented in this report is the enhancement of the nonlinear analysis methodology. This section of the report presents the achievements made during Phase I Task 2 of this Contract.

2.1 Post-Buckling Analysis

Structures loaded in compression and/or shear are susceptible to instability failures. In some cases, the ultimate load for the structure is taken to be the load at which buckling initiates. However, in most cases the structure is capable of safely carrying load beyond initial buckling. In order to safely utilize this additional strength, the analyst must be able to predict the behavior of the structure past the initial buckling load. This task is complicated by the fact that the structural response is nonlinear after this point. Many of the general purpose finite element codes, including DIAL (developed at LMSC) are capable of solving geometrically nonlinear problems. However, the standard solution techniques in these codes usually require an experienced user, which makes routine solution of nonlinear problems difficult.

In order to illustrate the standard nonlinear solution techniques, consider the load deflection curve shown in Figure 2.

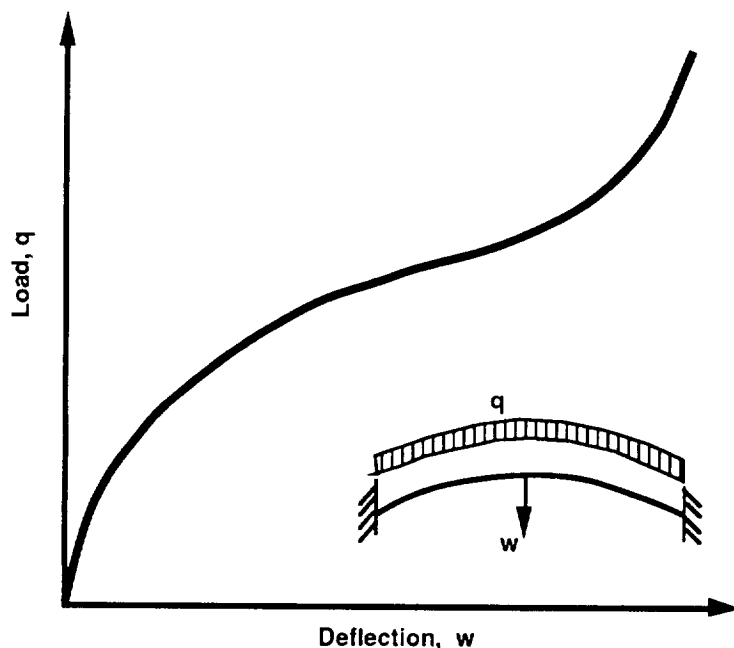


Figure 2 Load Deflection Curve

One method of finding the equilibrium curve is to specify a series of load steps and solve for the corresponding set of displacements. This technique works well for cases where there is a unique displacement configuration for each of the specified load steps. However, many structures do not behave in this manner and possess a limit point, such as Point A in Figure 3.

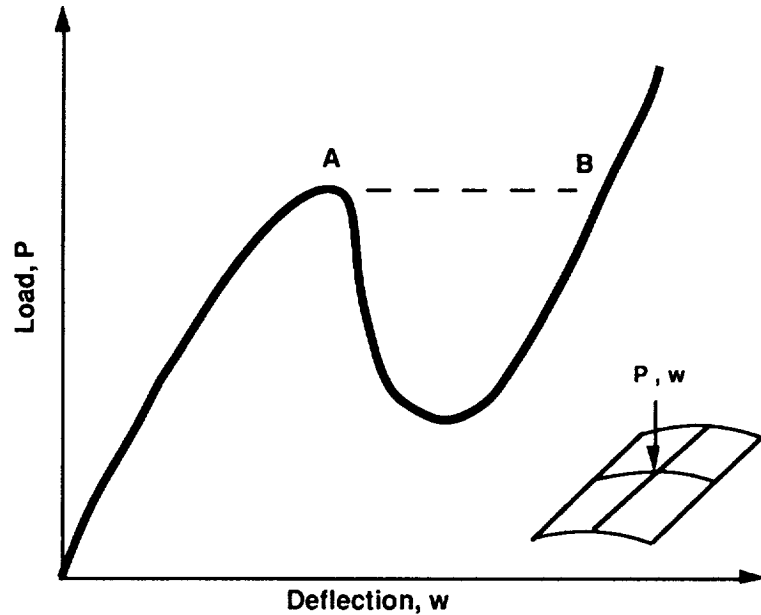


Figure 3 Limit Point

Increasing the load past the limit point causes the solution to jump across the equilibrium curve to Point B, completely missing the AB section of the curve. In some cases, it is possible to alter the solution procedure by specifying a series of displacements that define the loading process and then calculate the corresponding magnitude of the applied loads. This technique (“load control”) will usually work for structures exhibiting limit point behavior, provided it is possible to make the change of independent variables from load to displacements.

The solution techniques described above can be used to solve many of the nonlinear problems that are encountered in practical structural analysis, but they must be applied by an experienced user with an a priori knowledge of the structural response. The user must be able to determine if load or displacement control is appropriate and choose a suitable step size. Many times, the problem must be solved with several piecewise solutions obtained with different sizes and solution techniques. The user skill and interaction required to solve a problem in this manner makes nonlinear analysis difficult to incorporate into the design process.

In 1971, Wempner [3] suggested a solution technique that did not require a priori knowledge of the structural behavior and did not encounter difficulty at limit points. The method, implemented by Riks[4] is essentially a combination of load and displacement control. The technique involves taking steps of a specified length along the equilibrium curve. A much wider range of problems can be solved with this technique, with less user interaction. Therefore it is more suitable for use

in a design environment. Unfortunately, this technique generally requires more computer time than either of the other techniques discussed.

2.2 DIAL Implementation of the Arc Length Method

The DIAL finite element system was improved by the addition of an arc length solution capability. This enhancement means that postbuckling solutions can be attained with much less user interaction. This capability, together with generic modelling capabilities already in DIAL, provides a very powerful analytical tool that can be useful in the design environment.

The DIAL implementation of the arc length method is initiated with a minimum amount of user input. The starting load factor and the final value of the independent variable (load or displacement) are the only required parameters. The code is able to pick an appropriate step size and can change the step size as the solution progresses. If so desired, the user can specify the step size. Several other parameters, such as error tolerances, can be specified by the user, but appropriate default values are set or computed by the code if the user does not want to specify them.

In conjunction with the arc length solver, several additional features have been added to the DIAL solution capabilities. The arc length solver can be requested to solve for exact values of limit points as part of the solution process. The user can request that a limit point be calculated for either the load factor or the value of a particular displacement degree of freedom.

As a demonstration of the DIAL arc length solver, consider the simply supported shallow spherical cap shown in Figure 4.

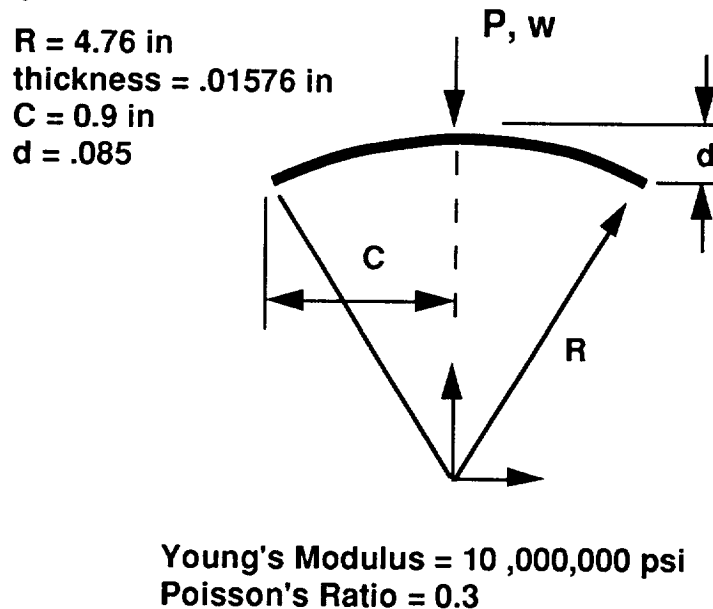


Figure 4 Simply Supported Shallow Spherical Cap

The spherical cap is loaded by a concentrated force at the central point. A total of six axisymmetric, three-noded shell elements were used to construct a symmetric model of the shell. The load-deflection curve computed by DIAL is shown in Figure 5.

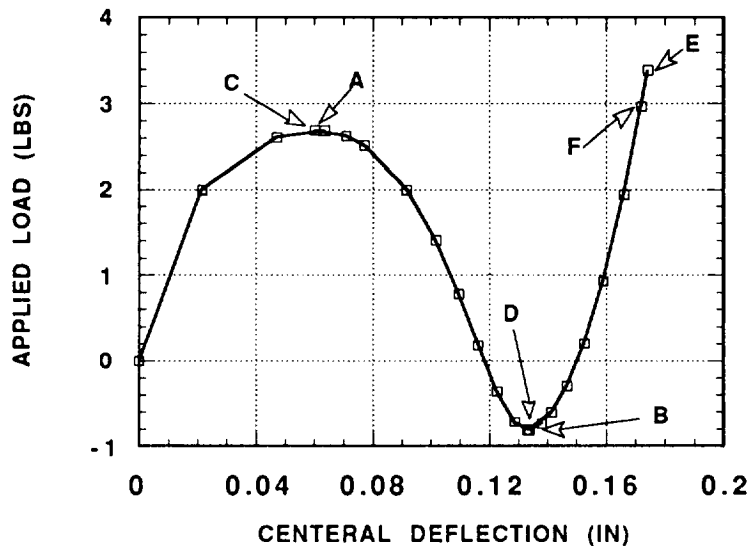


Figure 5 DIAL Computed Load Deflection Curve

It is important to note that the solver was able to detect that limit points had been passed at points A and B and was able to back up and calculate the actual limit points at C and D.

2.2.1 Target Point Analysis

As part of the arc length solution procedure, the user specifies the end of the desired solution by defining a “target point”. The target point is the unique point on the solution path at which the user wants the solution to end. Definition of the target point is made by specifying either the load factor, the value of a particular displacement degree of freedom or the value of the Margin of Safety for a particular element. During the solution process, the arc length solver monitors the value of the target point variable. If the solver detects that the target point has been passed, the solution backs up to find the exact location of the target point.

The load-deflection curve for the spherical cap, shown in Figure 5 illustrates the calculation of a displacement target point. The solver was directed to continue the analysis until the shell was

completely inverted which corresponds to a displacement of 0.172 in. The solver actually went past the target point to point E which corresponds to a central displacement of 0.174 in. In a manner similar to the limit point calculation, the solver backed up to the desired target point at point F.

2.3 Interface Analysis

Another type of failure of particular importance for composite structures is failure at subcomponent interfaces. Test results have demonstrated that the failure of bonded or co-cured skin/stiffener interfaces has been the primary cause of post-buckled failure for fuselage shell structures. The DIAL system has been improved by the addition of a bond material model to the material library. The material is assumed to be elasto-plastic in shear and linear in normal stress. This nonlinear, non-isothermal model is appropriate for predicting bond failures.

The material model has been verified by comparing DIAL results for a three dimensional lap shear joint specimen (Figure 6) with those obtained by Shariffi and Sable [5].

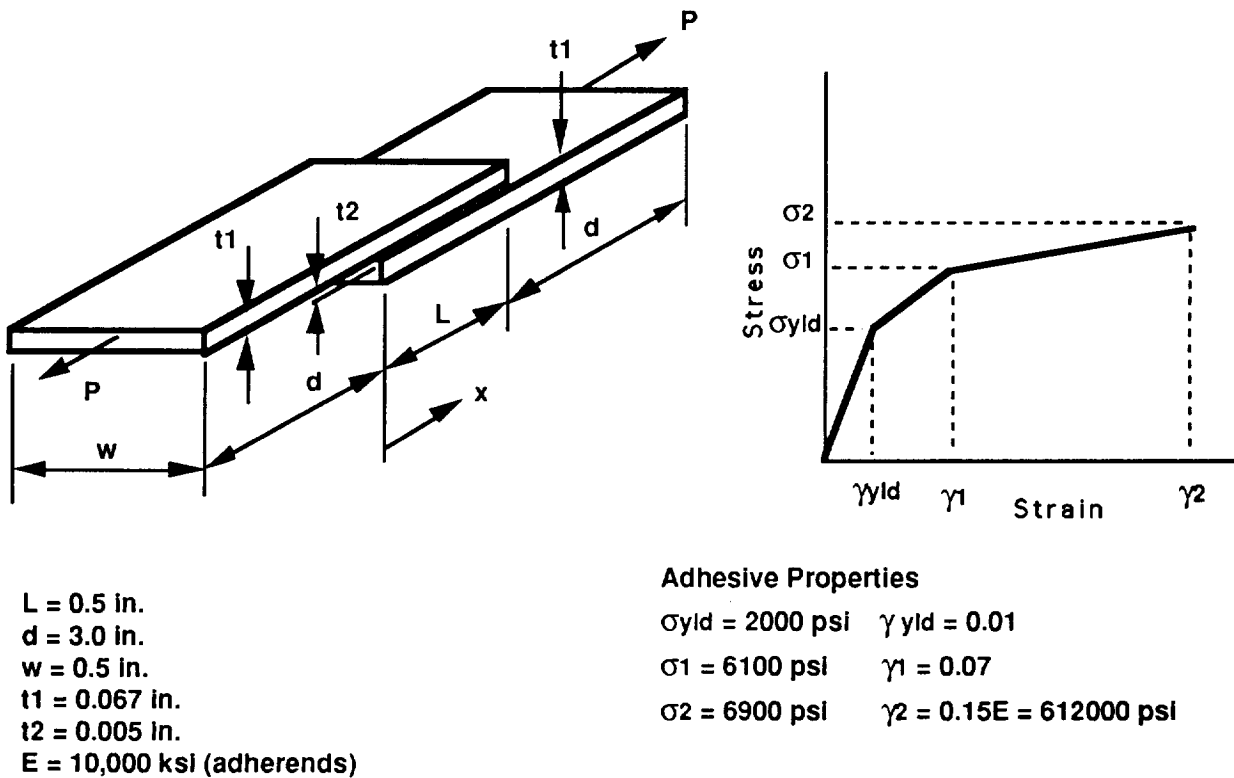


Figure 6 Three Dimensional Lap Shear Joint Specimen

The finite element mesh used by Shariffi and Sable was constructed using linear solid elements. Their mesh consisted of two layers of solid elements through the thickness of the adherends. The DIAL solution was generated using thick shell elements to model the adherends. The change to shell elements for the adherends yields a computer time savings that is especially important for

the nonlinear analysis that is required to predict the bond failure. The DIAL model is shown in Figure 7.

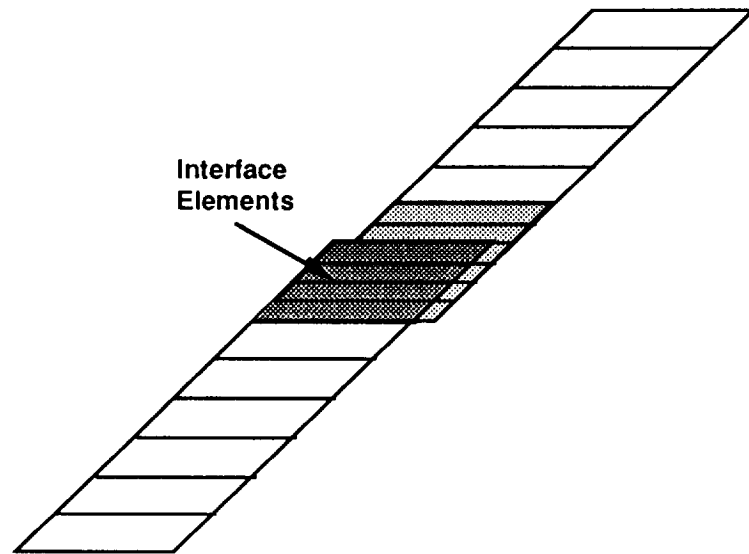


Figure 7 DIAL Three Dimensional Lap Shear Joint Model

The peel stress values computed by DIAL at the failure load of 4200 lb/in are compared with the results of Shariffi and Sable in Figure 8.

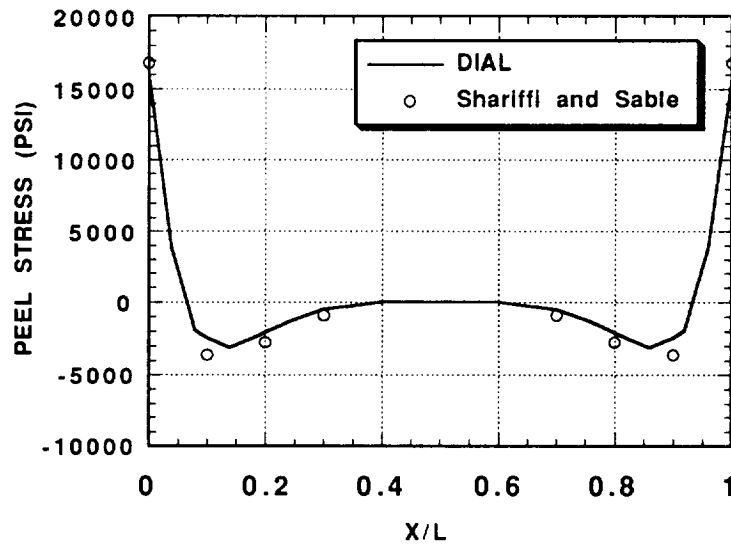


Figure 8 Lap Shear Joint Problem - Peel Stress Comparison

Figure 9 and Figure 10 show the shear strain and shear stress comparisons, respectively.

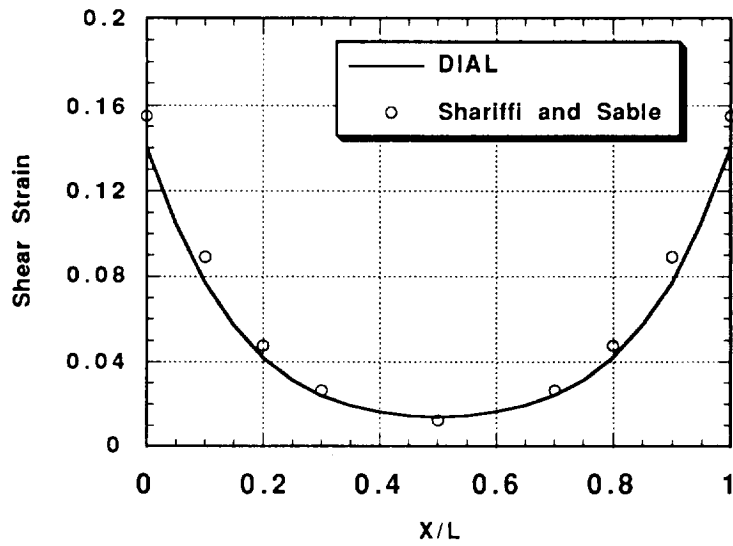


Figure 9 Lap Shear Joint Problem - Shear Strain Comparison

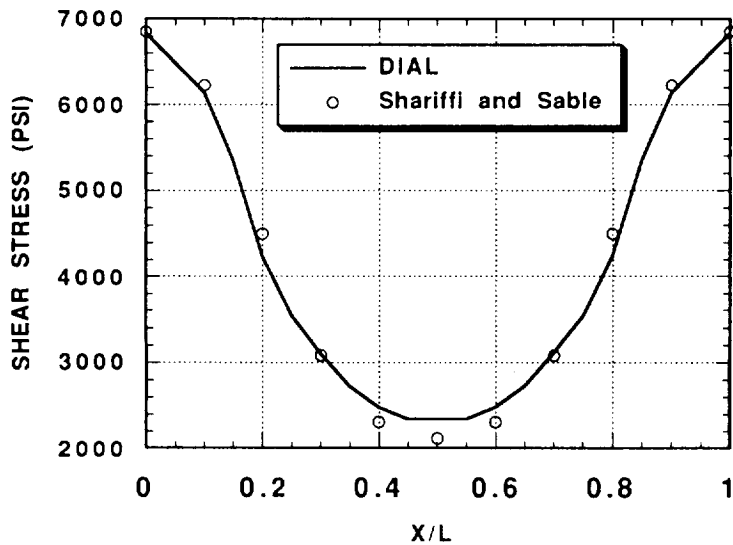


Figure 10 Lap Shear Joint Problem - Shear Stress Comparison

The two solutions compare very well, except some lack of agreement is evident at the edge of the bond for the shear strain. This variation can be attributed to different ways in which the two programs compute strains. DIAL computes strains at the element integration points, while the code, NEPSAP (Non-linear Elastic Plastic Structural Analysis Program) used by Shariffi and

Sable computes strains at the nodal points. Since the element integration point is slightly removed from the edge, the DIAL solution has a smaller value. The shear stress values shown in Figure 10 show very good agreement since the stress-strain curve is not very steep at this strain value, thereby diminishing any variation in the shear strains.

3.0 ISPAN Modules Development

The ISPAN (Interactive Stiffened Panel ANalysis) module is an interactive design tool that is intended to provide a means of performing simple and self-contained preliminary analysis of aircraft primary structure using composite materials. The advantage of this module lies in that it gives an inexperienced finite element code user a direct way of creating and solving a finite element model without the need to acquire in-depth knowledge about the code; in the mean time it does not limit experienced users from doing any modifications and in-depth analysis once the model is created. The term "generic model" has been applied to the finite element models created by this process.

This program combines a series of modules with the finite element code DIAL as the backbone. Each module can create a finite element model of a different type of primary aircraft structure, (i.e. wing panel, fuselage panel, etc). Each module consists of a set of Fortran driver programs which create DIAL generic model runstream files. The DIAL runstreams utilize the syntactic input capability of DIAL which is a Fortran-like language within the program. These elements of the generic model pre-processing are transparent to the user.

Users are instructed to input geometric properties, materials properties, load information and types of analysis that the user desires. Subsequently, the program will utilize this information to generate and solve the finite element model. The output in the form of summary tables of stress or margin of safety, contour plots of loads, stress, or strains and deflected shape plots may be used to determine the viability of the particular design. It also markedly simplifies parameter studies, as all analysis can be conducted using the same generic model. Parameter changes from the first analysis to the subsequent analyses can be trivial with the file editing or model revision capabilities.

The scope of the analysis that can be performed by this program includes conventional linear stress analysis, bifurcation buckling analysis and nonlinear collapse analysis.

At present there are four ISPAN modules; the flat and curved panel; truss core panel; and the geodesic panel. A full discussion of each module is presented in this report. Interactive examples can be found in the Advanced Composite ISPAN Modules Users Manual [23].

3.1 Flat Stiffened Panel

The flat stiffened panel module is an interactive FORTRAN program which constructs DIAL finite element models based on user selected options. The skin and stiffener components of these panel models are constructed using shell elements. Presently, the program is capable of modeling eight different types or categories of stiffener cross sections as shown in Figure 11.

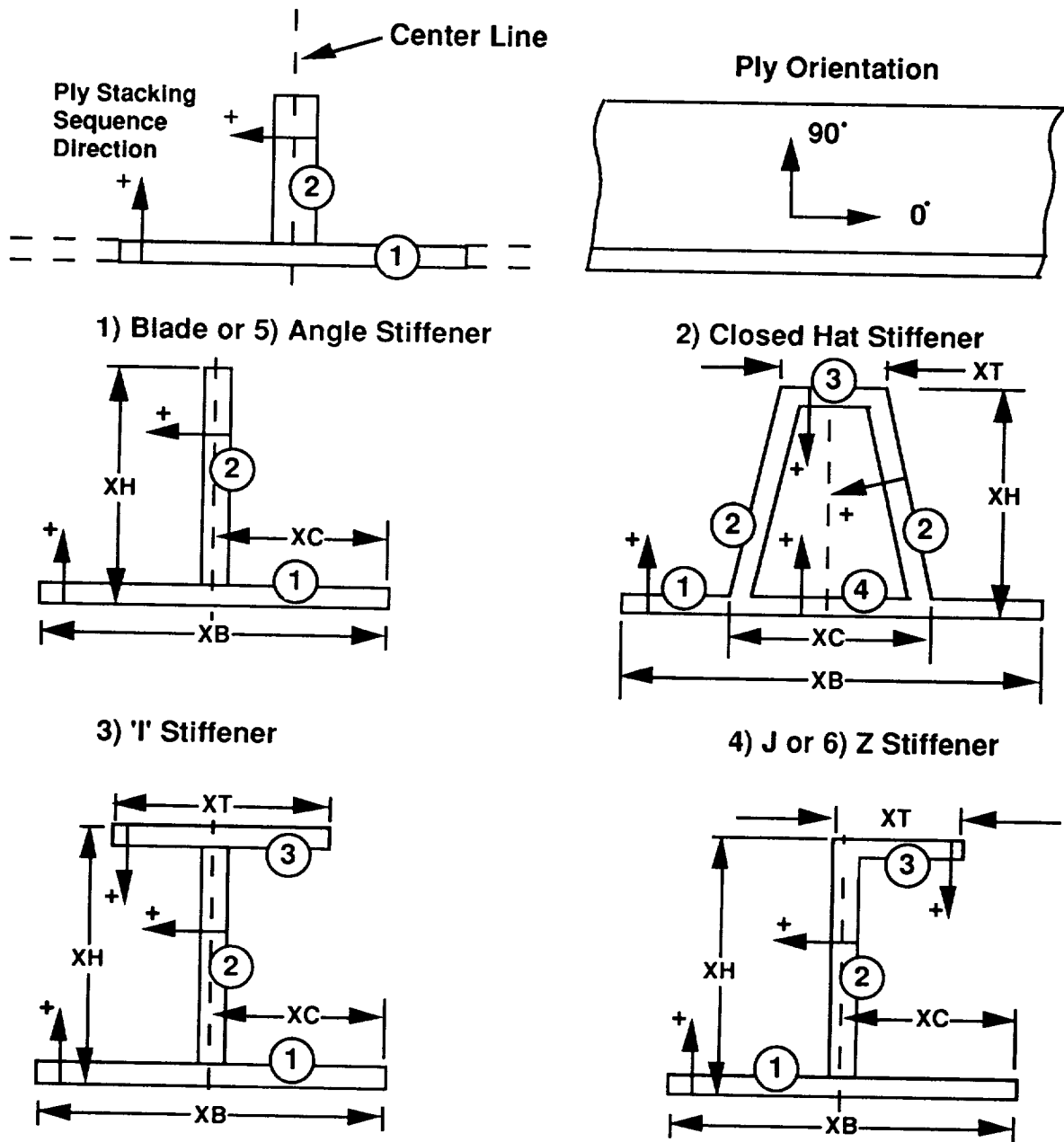
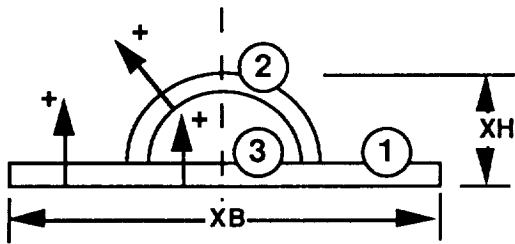


Figure 11 Flat Panel Stiffener Geometry

7) Bead Stiffener



8) Open Hat Stiffener

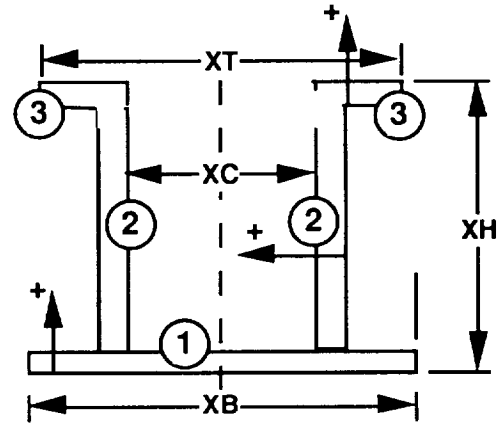


Figure 11 Flat Panel Stiffener Geometry (continued)

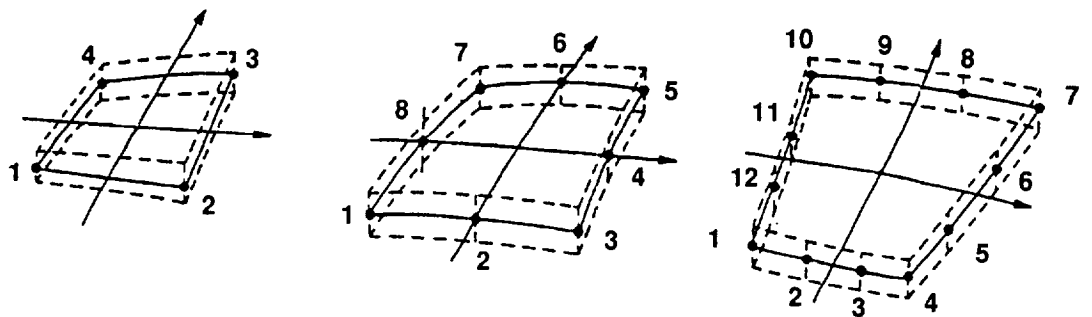
The following list describes the options available to the user. This list is presented as an overview of the capabilities of the program. These options will be discussed in more detail in the subsections which follow.

- | | |
|---------------------|------------------------------------------------------------------------------------------------------------------------------------------------------------------------------------------------------------------------------------------------------------------------------------------------|
| Stiffener | <ul style="list-style-type: none">- cross section type- number of stiffener- spacing (may be irregular)- flange widths, thickness- material, ply orientation |
| Skin | <ul style="list-style-type: none">- width, length and thickness- materials, ply orientation |
| Loading | <ul style="list-style-type: none">- axial end load, N_x (tension or compression)- lateral load (perpendicular to the stiffener direction) N_y- inplane edge shear, N_{xy}- normal pressure, p |
| Boundary Conditions | <ul style="list-style-type: none">- Each of the four panel edges may be specified separately as free, simply supported, or clamped.- Vertical translations and/or rotations may also be specified across the width of the panel to simulate the rib/frame supports. |

- Solutions
- linear static
 - bifurcation (buckling)
 - post buckling (target point analysis)

3.1.1 DIAL Shell Element

All components of the flat stiffened panel models are constructed using the modified thick shell element (MSH). This is a super-parametric doubly curved thick shell element. The element was modified from the original thick shell element by separating the membrane, bending and transverse shear responses, thus allowing the simulation of laminate and sandwich type structures. Linear, parabolic and cubic versions of this element are available in DIAL (figure 12).



Element connectivity and local coordinate system (r,s)

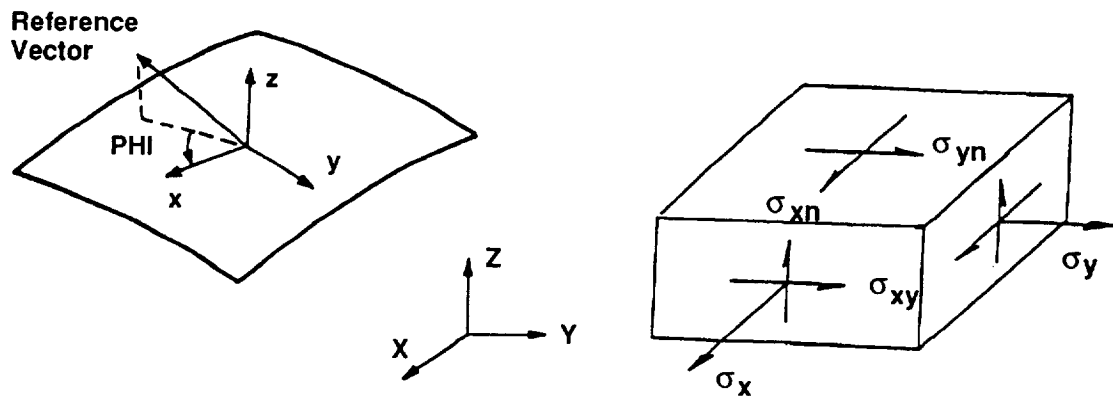


Figure 12 Shell Element Connectivities, Reference Vector and Sign Convention

The parabolic and cubic shell elements are vastly superior to the linear elements in terms of accuracy and are generally recommended. The parabolic elements were selected for use in ISPAN because they were judged to provide the optimum accuracy for a given level of complexity.

3.1.2 Model Geomerty

Stiffeners are represented in the resulting models as built-up sections comprised of parabolic shell elements. Their flange widths, thicknesses and materials are established during the interactive execution of Module 1. The stiffeners must number no more than ten, have the same cross section and be parallel to one another. An example of a typical flat stiffened panel model is shown in Figure 13.

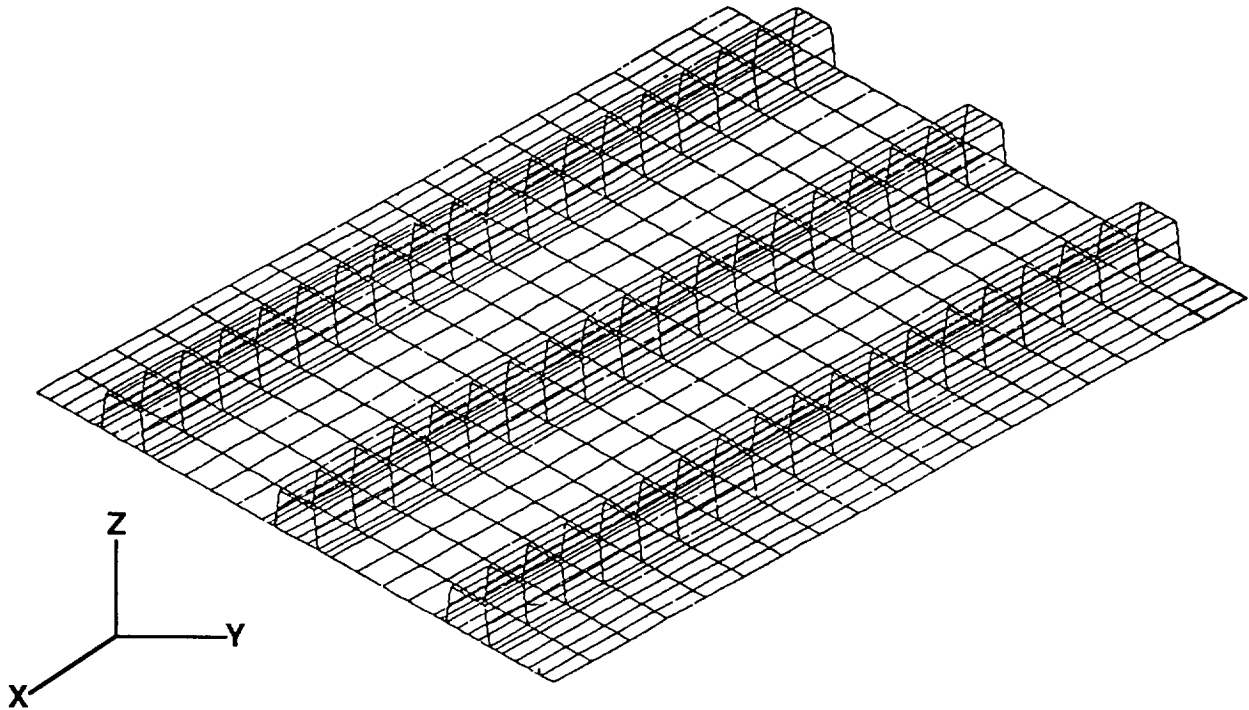


Figure 13 Typical Flat Panel Model with Closed Hat Stiffener

Although the stiffener elements are generally distinct from the base panel, it should be noted that the attached flanges are assumed to be included in the skin. Therefore, these elements in the flange attach region should be given thicknesses and orientations which reflect the sum of the flange and skin in this region as shown in Figure 14.

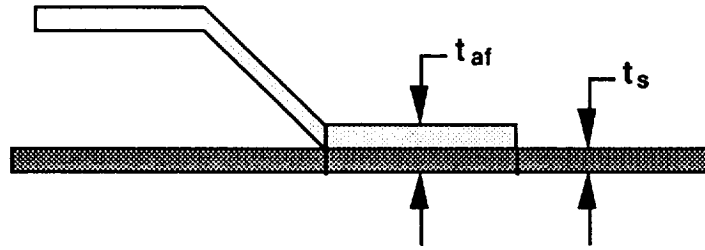


Figure 14 Flange Attach Region

The ribs (frames) are not modeled with structural elements in this analysis. However, they are represented by constraints on the degrees of freedom at the rib locations. The details of this are discussed in the sub-section on boundary conditions.

3.1.3 Loads

In-plane axial (N_x), lateral (N_y) and shear loads (N_{xy} , N_{yx}) as well as normal pressure (P) may be applied to the model. The definition and sign convention of these load components are shown in Figure 15.

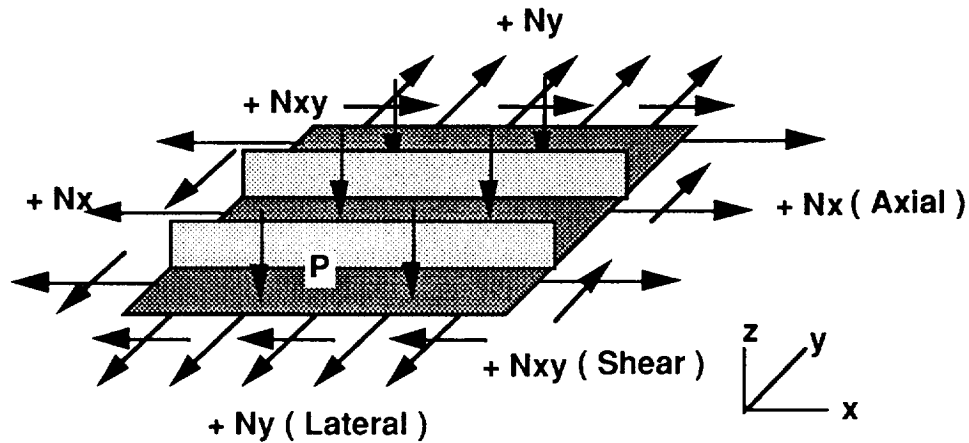


Figure 15 Applied Loads Definition

The axial loads on the panel ends (N_x) are applied in such a way as to produce uniform strain, (ϵ_x). That is, the total applied load is effectively distributed to the base panel and the stiffeners according to their relative stiffnesses. This is accomplished in DIAL by using a command called CONODE, which forces a set of edge "slave" nodes to displace as the weighted average of the displacements of the two "master" nodes at the panel corners. (Figure 16)

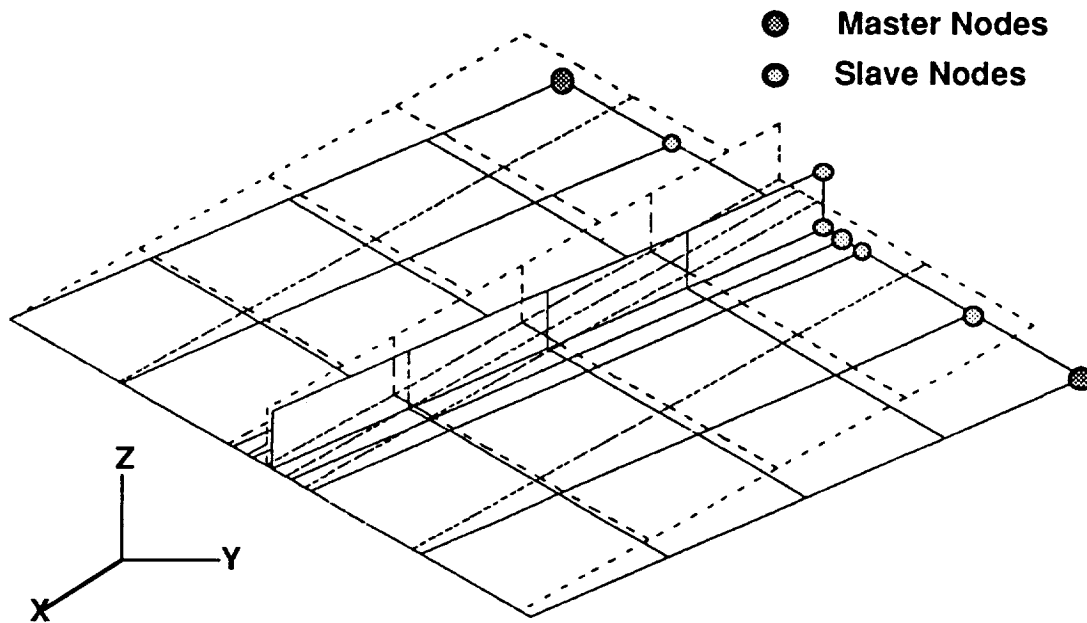


Figure 16 CONODE Command

The weights used in this CONODE command are inversely proportional to the distances of the slave nodes to the master nodes. This method of applying axial loads accurately simulates the loading produced by the surrounding wing or fuselage structure as well as in most stiffened panel test set-ups.

3.1.4 Boundary Conditions

Each edge (boundary) of the panel may be independently specified to be free, simply supported or clamped. The simple supports are simulated by using the DOFSUP command to constrain only the out-of-plane (normal to panel) degree of freedom at each node. The DOFSUP command is also used for the clamped condition to constrain both normal translations and rotations along the edge. In addition to the constraints used to simulate the structural support provided by the adjacent structure, kinematic constraints are specified to prevent rigid body motions as shown in Figure 17.

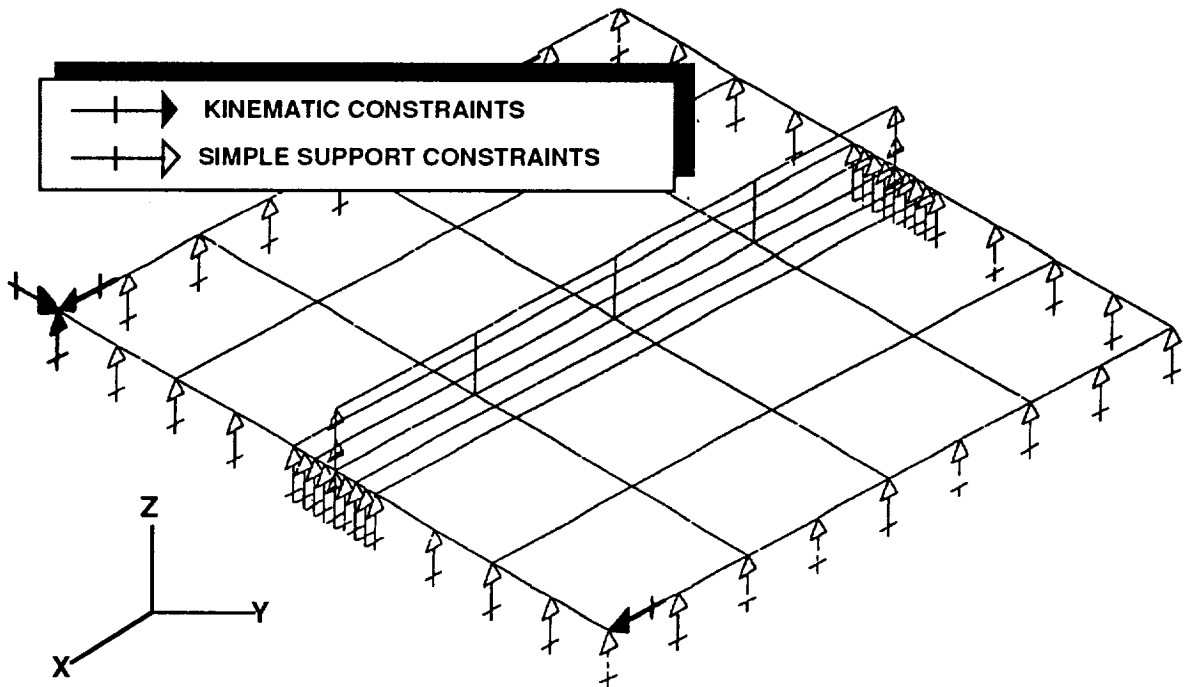


Figure 17 Typical Constraint Vectors for Flat Panel

These kinematic constraints are generated automatically by the ISPAN Module, hence user's interaction is required. Under normal circumstances the kinematic constraints will produce no internal loading in the panel. However, if two adjacent edges were unsupported and out-of-plane pressure loads were specified, for example, the constraints at the corners would react the pressure load. This undesirable situation should become obvious once the deflected shape and/or stress contours are examined.

The option exists in ISPAN to provide out-of-plane support at specified locations on the stiffened panel in such a way as to simulate a rib or circumferential frame. The support is modeled by constraining the out-of-plane displacement normal to the panel at user specified locations. The inherent assumption in this modeling technique is that the rib or frame has sufficient stiffness to enforce a node in the buckled mode shape as shown in Figure 18.

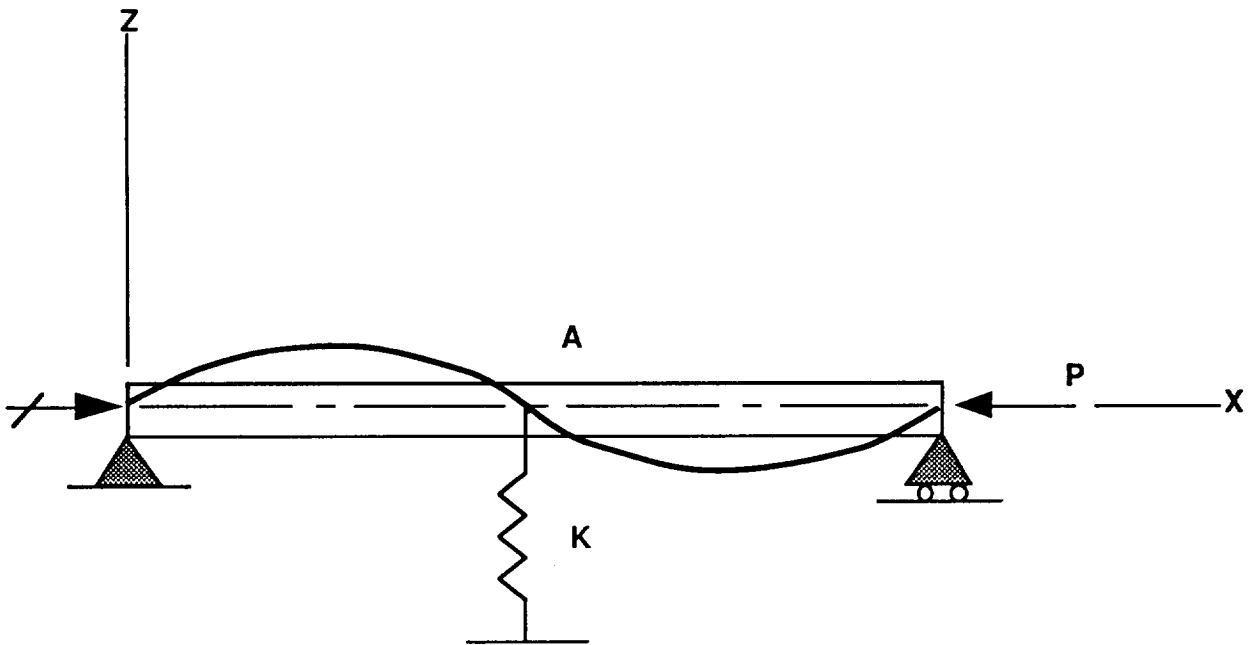


Figure 18 Rib/Frame Elastic Support, Column Analogy

The rotations (about the y-axis) may also be constrained in order to simulate a very rigid support such as a main frame. In most applications (intermediate frames or ribs), constraining these rotations will be un-conservative. At some later date, an option may be created to generate rib type support in the form of translational and rotational stiffness parameters.

3.1.5 Solutions

Three solution procedures, linear static, bifurcation (initial buckling) and post-buckling, are presently available in ISPAN. The linear static solution is straightforward and needs no explanation.

The initial buckling solution is an analysis to determine the multiplier on the applied load load (eigenvalue) at which any part of the structure first becomes unstable. Neither knockdown factors nor initial imperfections are accounted for in this analysis.

The post-buckling solution allows the user to determine the ultimate load capability of the structure. Some flight vehicle structures are permitted to buckle locally at load levels below ultimate provided

they retain the capability to carry the ultimate load without complete collapse. The post-buckling solution in DIAL permits the user to conduct such a non-linear analysis to investigate the integrity of the structure, after initial buckling, to establish the ultimate allowable load based on strain cutoff, strain interaction or general instability - total collapse. The DIAL program uses the Arc-Length method to perform the non-linear analysis. This method, which was discussed in more detail in section 2.2 requires the user to select a target point in the form of either load factor or a maximum displacement at a certain location (grid point). Since strength, rather than displacement is the criterion most often used for design, the load factor option is recommended for this type of analysis.

It is also recommended that the user conduct an initial buckling calculation first, and use the resulting load and mode shape as the starting point for the non-linear post-buckling analysis. This will save time and expense compared to running non-linear through the entire range of loads.

3.2 Curved Stiffened Panel

The curved stiffened panel program was developed from the flat panel module, by adding the capability of specifying curvature about one axis (parallel to the stiffeners). This type of geometry is intended to represent fuselage panels and wing covers. The effect of this curvature is, in general, an increase in the critical buckling loads over that of the flat, but otherwise identical stiffened panels.

For the most part, the changes to the program (from flat panel to curved panel) will be transparent to the user; ie, the panel dimensions and stiffener spacings are input as distances along the arc rather than specifying an angle in the cylindrical coordinate system. The conversion of the geometry to a cylindrical system is performed within the curved panel module of ISPAN. Figure 19 shows the definition of the variables used to specify the panel geometry.

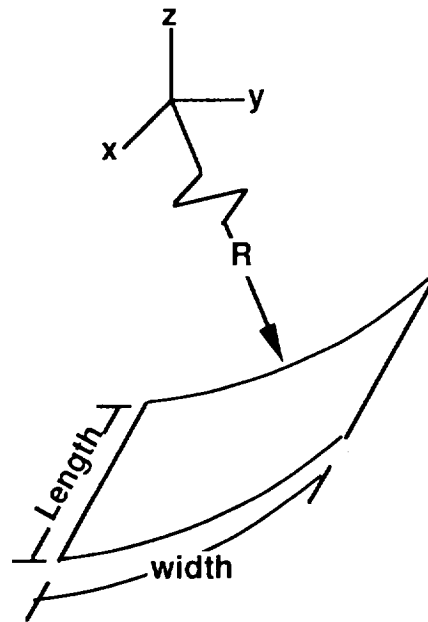


Figure 19 Geometry of Curved Panel

The radius of curvature, R , is specified on the same card image as the panel length and width. Note that the width is now the arc length of the curved panel.

The mechanics of running the curved stiffened panel module are the same as for the flat panel version. The program capabilities and limitations described in the Flat Stiffened Panel discussion in Section 3.1 applicable to the curved panel as well.

The results obtained from running example problems and comparing the results to other available solutions will be presented.

3.2.1 Example Problems

Two example problems will be solved to illustrate the features and options of the Curved Stiffened Panel module. The first example is an “I” stiffened panel with pure compression loads. A linear elastic solution will be obtained using a Lockheed laminate strength analysis program called LAMSTR and compared to results obtained from ISPAN. The second example is a buckling solution for combined compression and shear loads applied to a bead stiffened curved panel.

3.2.1.1 Example 1: Linear Static Analysis

The stiffened panel in this example has overall dimensions of 40” by 40”, and radius = 60”. Two “I” stiffeners, each 2.5 inches high with 2.0 inch flange width are integral with the panel; ie, the stiffener webs and flanges have the same construction (thickness, orientation, etc) as the base skin panel.

Figure 20 shows the DIAL model geometry of this panel and the applied compression load vectors.

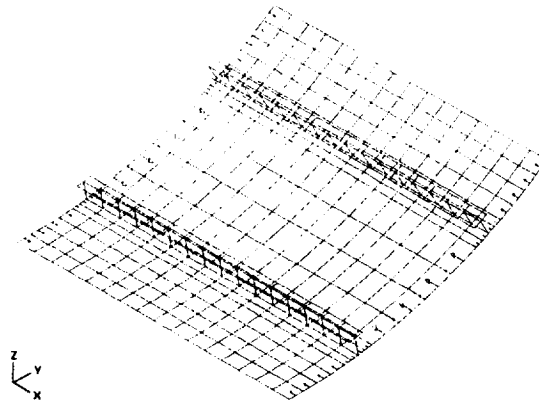


Figure 20 Curved Panel, DIAL Model with Applied Load, Example 1

Figure 21 shows the deflected shape under these compression loads.

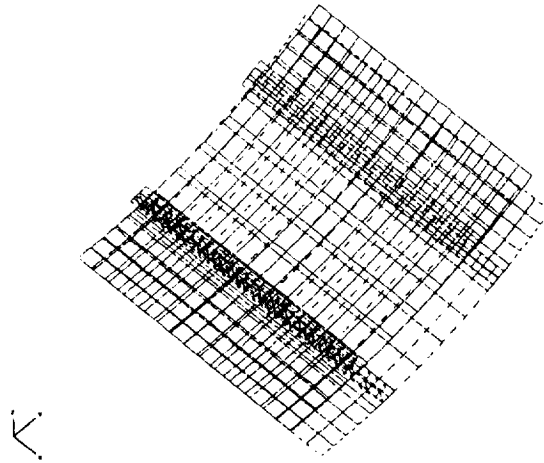


Figure 21 Curved Panel Deflected Shape, Example 1

Mechanical properties:

Average room temperature elastic properties of AS4/3501-6 used for the example.

E_1	E_2	G_{12}	ν_{12}	AML	ϵ_T	ϵ_C
19.8×10^6	1.47×10^6	$.867 \times 10^6$.30	-40	.00620	-.00645
				0	.00635	-.00675
				+40	.00650	-.00705

Table 1 Curved Panel Material Properties, AML Values and Strain Allowables

Laminate Description:

For this example, a 14 ply laminate was selected, which resulted in a total thickness of 0.070 inches. The stacking sequence utilized for LAMSTR and DIAL-A-MATIC was a $[\pm 45/0/\pm 45/0/90]_S$. This stacking sequence was used for the stiffener and skin of the curved panel.

Applied Loads:

A total compressive load of 180 kips was applied to the ends of the panel. The stiffener elements in this example have the same stiffness as the panel elements and therefore will have the same running load, N_x . The magnitude of N_x may then be calculated as:

$$N_x = (-180000 \text{ lb}) / (40.0 \text{ in} + 2(2.0 \text{ in} + 2.5 \text{ in}))$$

where 40 inches is the width of the panel, 2.0 inches is the height of the web, and 2.5 inches is the length of the top flange.

$$N_x = -3673.5 \text{ lb/in}$$

Compressive stress:

$$\sigma_c = -3673.5 \text{ lb/in} / .070 \text{ in}$$

where .070 in is the thickness of the laminate used for the skin and stiffeners.

$$\sigma_c = -52478 \text{ psi}$$

Compressive strain:

LAMSTR was used to calculate the compressive strain values which will then be compared to the DIAL results. The printout from this program, which includes a summary of the ply level mechanical properties data, stacking sequence and input loads, as well as output laminate modulus and strain values, is presented in this section following the comparison of DIAL and LAMSTR results. The compressive strain calculated by LAMSTR was,

$$\epsilon_c = -.006252 \text{ in/in}$$

Allowable strains:

The laminate chosen for this analysis consists of 57.1% 45 degree plies and 28.6% 0 degree plies resulting in an AML value of 28.5. The allowable compressive strain from interpolation of the mechanical properties (AML) data presented in Table 1, is -0.00696.

Margin of safety (LAMSTR results):

$$\text{M.S. compression} = -.00696 / -.00625 - 1 = +.114$$

DIAL Model results:

Figures 22 through 25 are contour plots of running loads, strains and margins of safety for skin elements and stiffener elements. These plots were obtained during an interactive post-processing session using DIAL-A-MATIC.

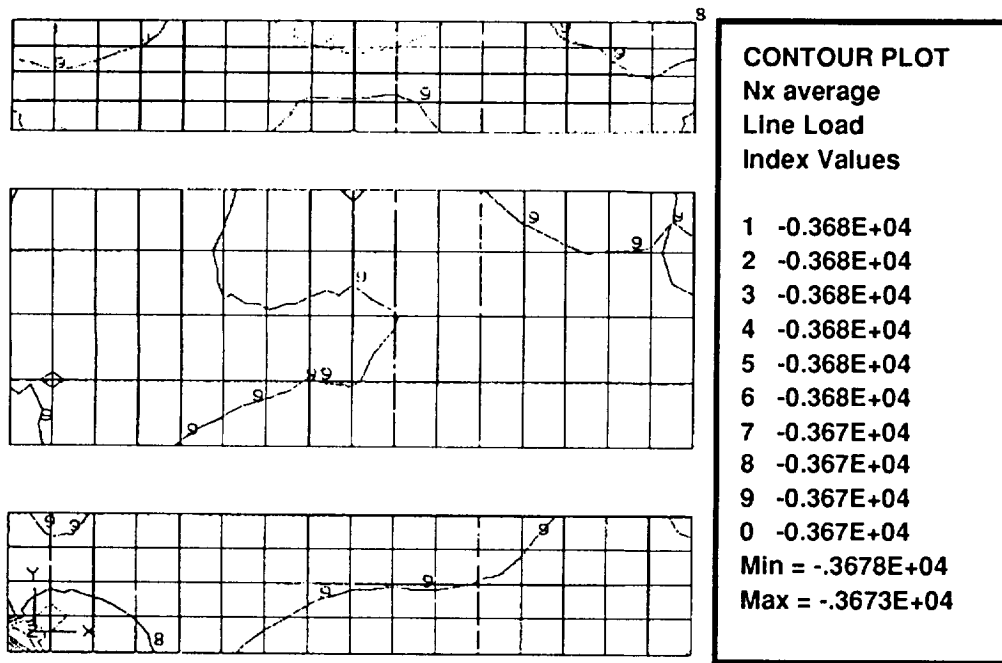


Figure 22 Curved Panel Contour Plots N_x Average, Example 1

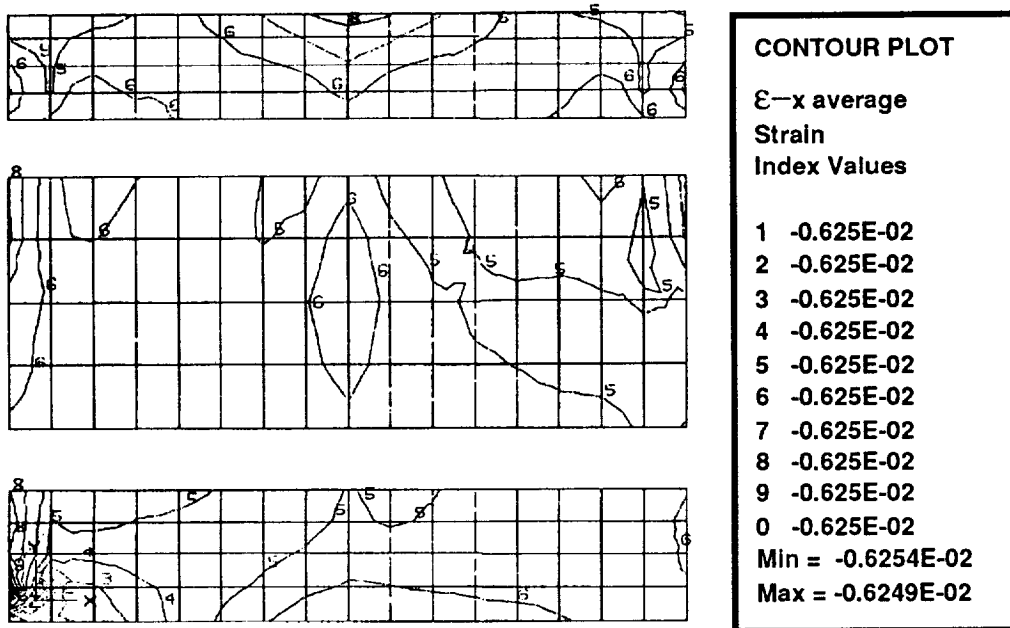


Figure 23 Curved Panel Contour ϵ_x Average, Example 1

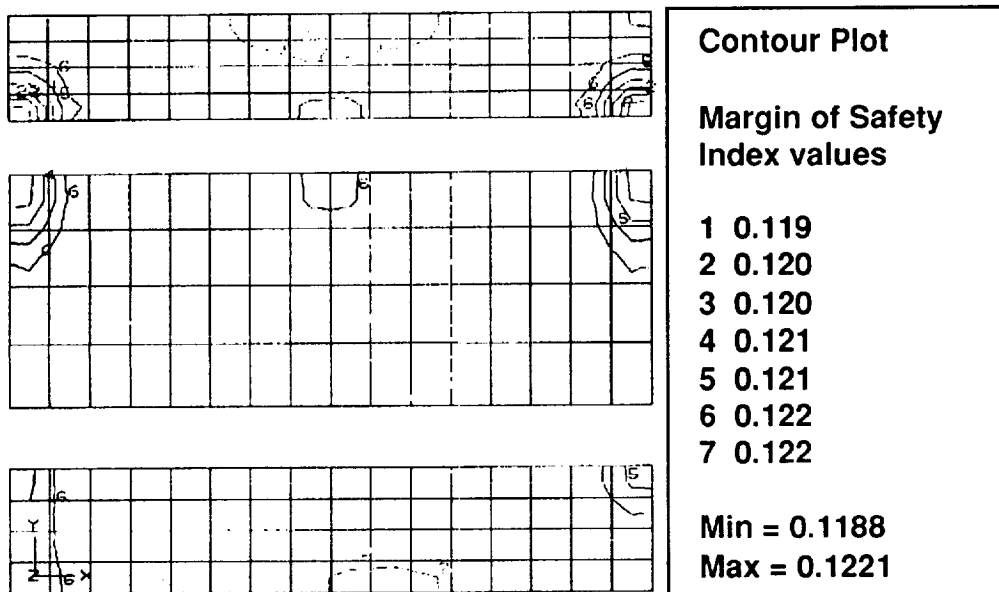


Figure 24 Curved Panel Margin of Safety, Example 1

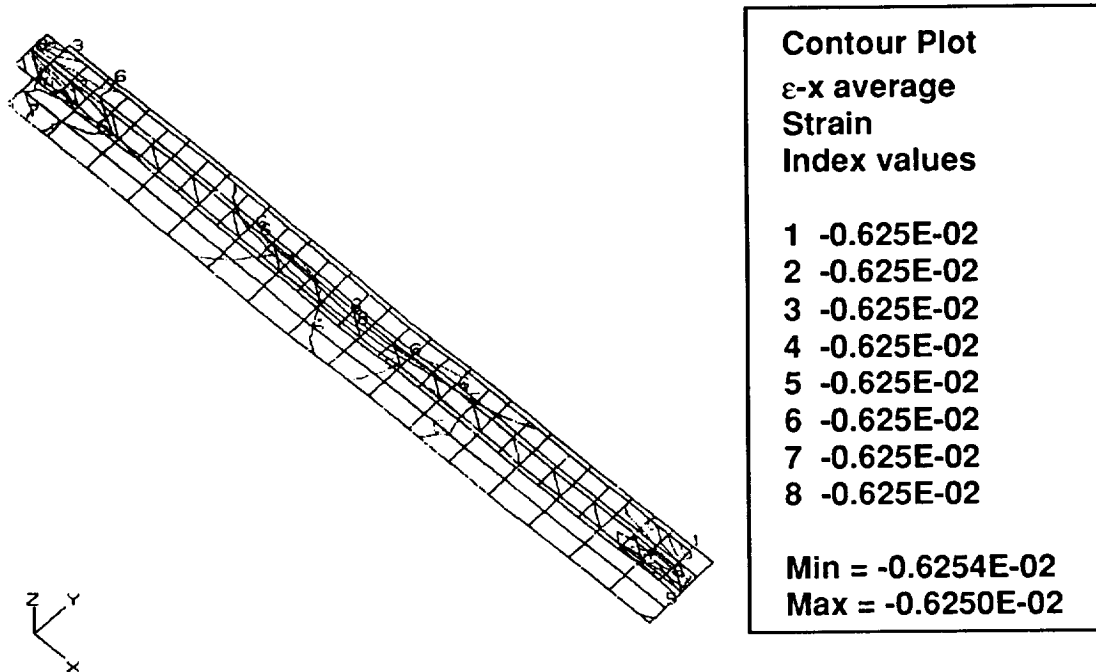


Figure 25 Curved Panel ϵ_x Average Typical Stiffener, Example 1

At first glance, the contours seem to indicate an unsymmetric solution for what should be a symmetric problem. Examination of the legend, however, shows that the maximum and minimum strain values (in the panel, for example) range from -0.006249 to -0.006254 , a $.08\%$ difference. Similarly, the margins of safety range from $+1.119$ to $+1.122$. A comparison of the average results from the ISPAN module to the LAMSTR calculations is presented in the following table:

	Strain	Margin of Safety
LAMSTR	-0.006252	$+1.113$
ISPAN	-0.006252	$+1.121$

Table 2 Comparison of Average Results from LAMSTR and ISPAN: Curved Panel

3.2.1.2 Example 2: Bifurcation Buckling Analysis

The second example is a buckling analysis of a bead-stiffened, curved panel. The applied load for this problem is 1000 lb uniform compression combined with 1000 lb/in shear flow. The geometry and applied load vectors are shown in Figure 26.

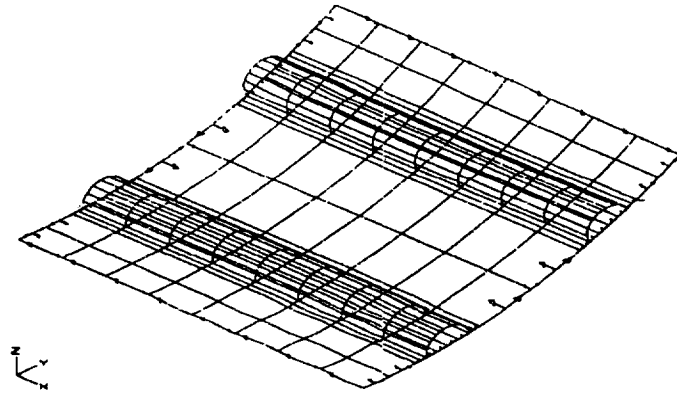


Figure 26 Curved Panel Geometry and Applied Load Vectors, Example 2

The boundary conditions were arbitrarily selected to be simple supports along the panel ends (perpendicular to stiffeners) and clamped edges on the sides. The mesh density in this example was less than that used in example 1 in order to speed up the run time for the (non-linear) buckling solution. Figures 27 through 29, show the deflected shape and strain contours when the buckling solution is complete.

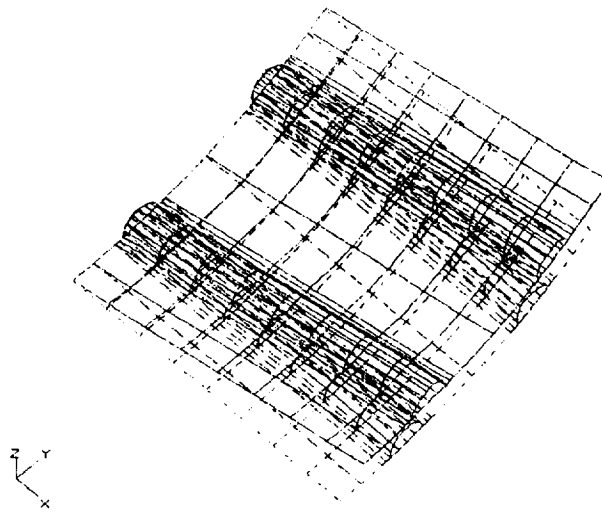


Figure 27 Curved Panel Deflected Shape, Example 2

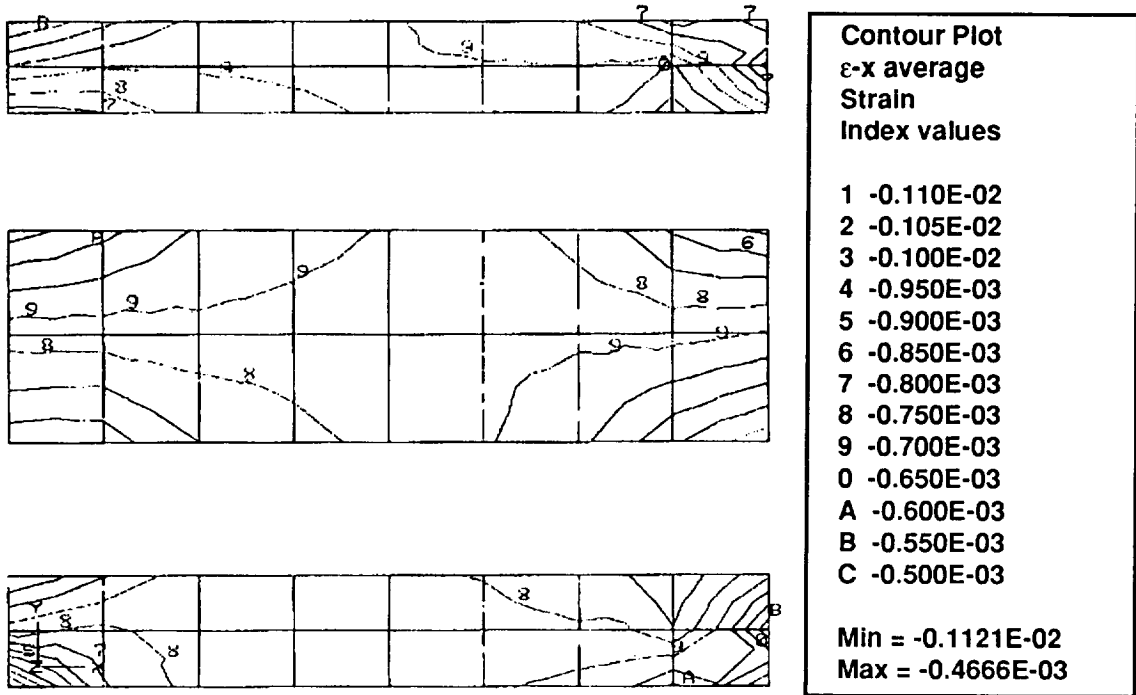


Figure 28 Curved Panel Contour Plot, ϵ_x , Example 2

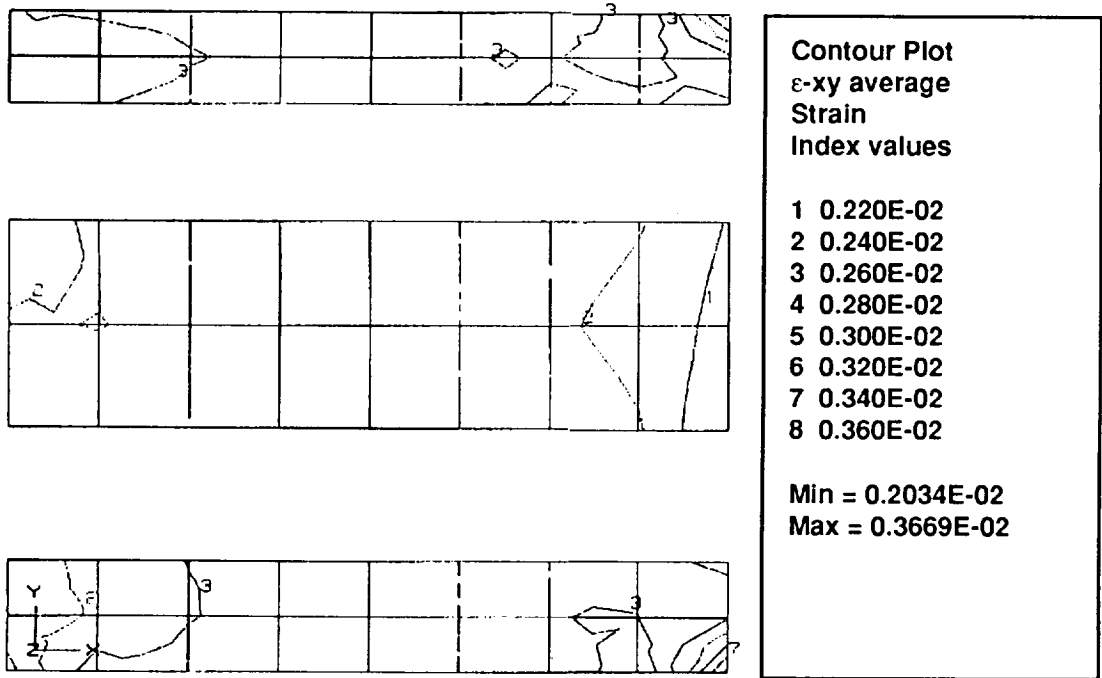


Figure 29 Curved Panel Contour Plot, ϵ_{xy} , Example 2

Only the first buckled mode shape was requested, although the option exists in ISPAN to request up to 50. The plot of this mode shape is presented in Figure 30.

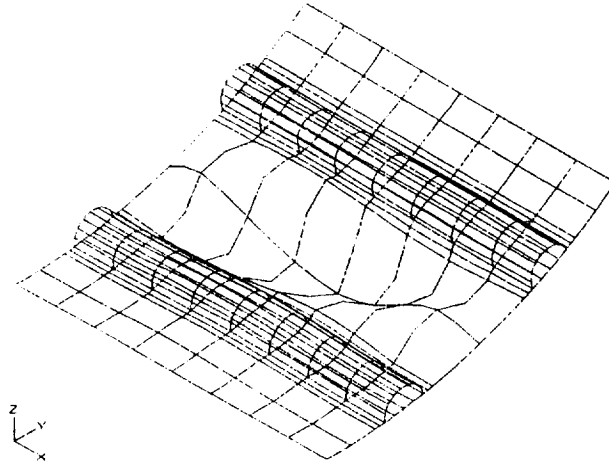


Figure 30 Curved Panel Buckled Mode Shape, Example 2

As expected, the skin between the stiffeners buckles in a diagonal pattern due to the presence of the applied shear. Very little deflection is observed in the stiffeners, which, by virtue of being closed sections, are very rigid. The printout of the eigenvalue (critical load factor) determined from this solution is found in a file called **cluster.out**, which is automatically generated when either the bifurcation buckling or post-buckling solution is requested. The eigenvalue calculated for the first mode in this example (where compression and shear flow are applied in equal magnitudes) is 1.273, indicating that initial elastic instability will occur at 1,273 lb compression combined with 1,273 lb/in shear flow.

3.3 Flat Rectangular Tubular Truss Core Panel

This ISPAN module creates a finite element model of a flat sandwich composite panel as shown in Figure 31. The panel is composed of trapezoidal tubes bonded side by side to form the core which is bonded to the top and bottom skins of the tube-skin assembly. All tubular stiffeners are identical, while the top and bottom skins may have different layups.

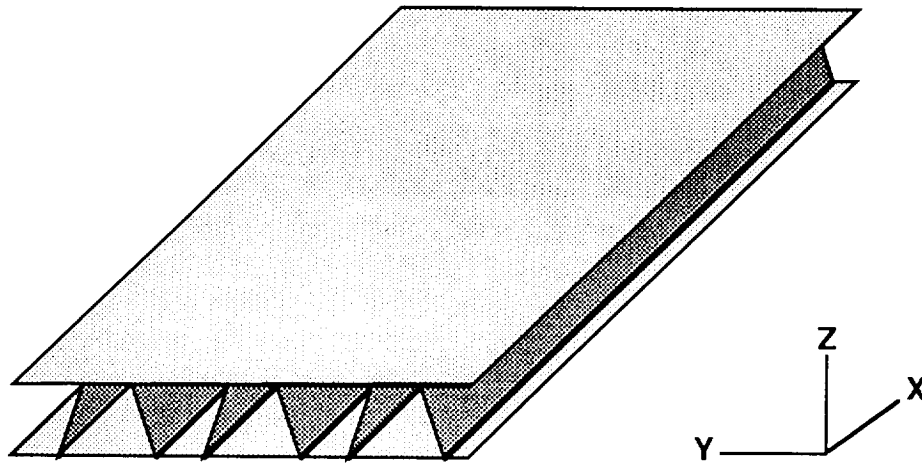


Figure 31 Truss Core Panel

Linearly elastic static and overall buckling analyses may be performed. For the static analysis, the panel may be loaded by any combination of uniformly distributed inplane axial and shear loads. The results of the analyses can be reviewed using the post processor.

Although the program does not consider initial damage and disbond, and it does not perform post buckling or thermal stress analyses, the runstreams and post-processor can be modified to perform these tasks.

3.3.1 Programs Components

The program consists of three parts, the command module and pre- and post-processors.

3.3.1.1 Command Module

The command module serves as a program driver. It permits the user to enter or exit the program at various stages of the task including input entry, input update, runstream generation, runstream review, geometry check, solution, and post-processing. It also allows the user to designate input and output file names.

3.3.1.2 Pre-processor

The pre-processor prompts the user for various geometry parameters, materials, layups, boundary conditions, loading data, and solution options. It lists inputs, accepts updates, and finally stores them in user designated files. It then proceeds to generate DIAL runstreams that allow for linear static and bifurcation analyses. The model geometry may be checked after the runstreams are executed and before the solution run is made.

3.3.1.3 Post-processor

The post-processor consists of several options that generate 3-D plots of undeformed and deflected shapes, load vectors, contours of average laminate strains, ply stresses and strains, and laminate margins of safety based on the AML failure criterion. It also generates summary tables of average laminate loads and strains, ply stresses and strains, and laminate margins of safety.

The user has an option of the viewing direction, among other things. The parts that can be reviewed include the top skin, bottom skin, top tube wall, bottom tube wall, webs, fillers, and combinations of these.

3.3.2 Modeling Concepts

3.3.2.1 Shell Model

The load carrying parts of the panel are represented by 3-D thick shell elements having membrane, bending, and transverse shear capabilities. Fillers on the panel sides, which serve as restraints, are simulated by 3-D solid elements.

Figure 32 shows a generic truss-core panel. The orientation for the ply lay up are also shown for the panel.

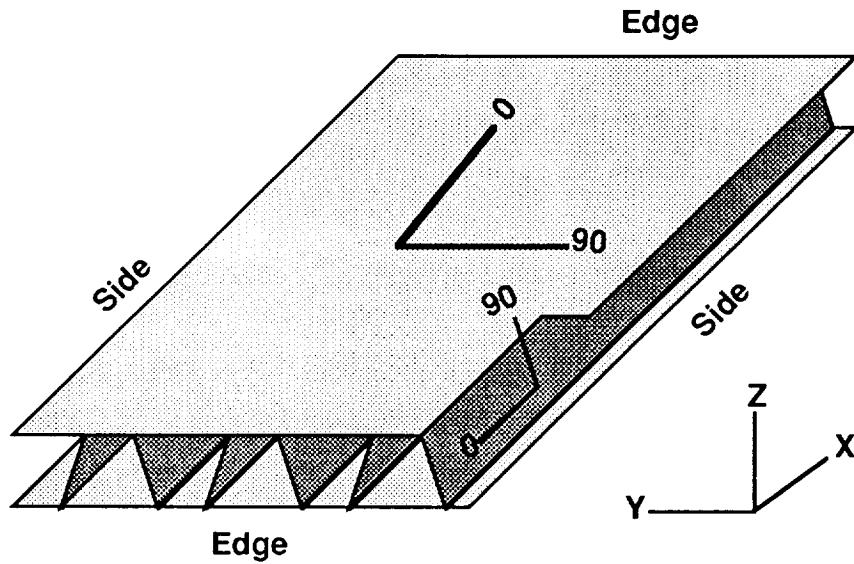


Figure 32 Generic Truss Core Panel with Ply Orientations.

The skin and tube wall laminates are defined separately about the midplane of the bond line. This will tend to decrease the stiffness locally. While bifurcation solutions will be accurate, improved accuracy could be obtained by correcting this decrease in local stiffness.

3.3.2.2 Mesh Generation

A coarse mesh is generated for static analysis and a finer mesh is generated for buckling analysis. The mesh generation begins with a basic pattern consisting of two halves of a skin/tube segment, which is created and then duplicated in the transverse and longitudinal directions, this sequence is illustrated in Figure 33.

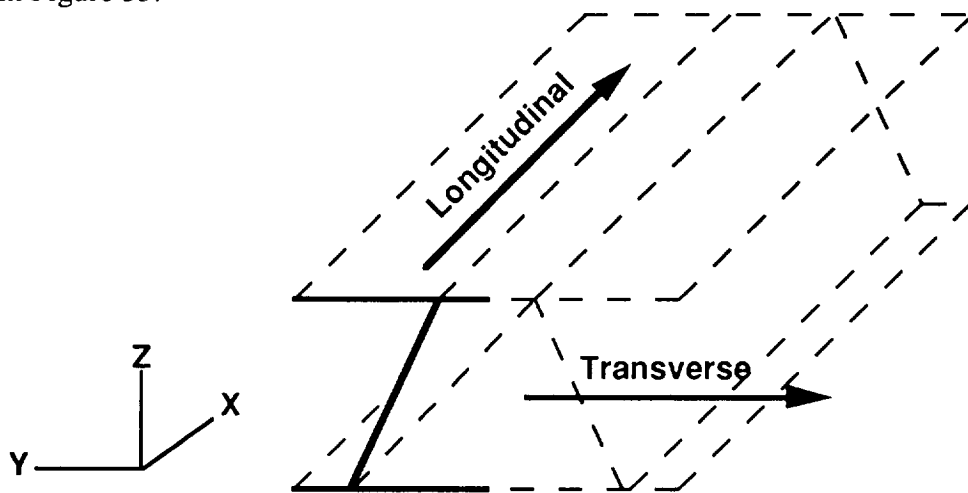


Figure 33 Truss Core Mesh Generation Sequence

The duplication is accomplished by the use of syntactic variables and subroutines in the DIAL runstreams, which include the DITTO, TRANS, MIRROR and MERGE routines. Side fillers, if called for, are generated separately and merged with the panel shell model.

3.3.2.3 Boundary Conditions

The boundary conditions consist of two parts; kinematic boundary conditions that prevents rigid body motions and user specified boundary conditions.

The kinematic boundary conditions specifies that all displacements in the x direction of the front edge be equal to zero. Additionally, the y direction displacement at point 'A' and the z direction displacements at points 'A' and 'B' are equal to zero (Figure 34).

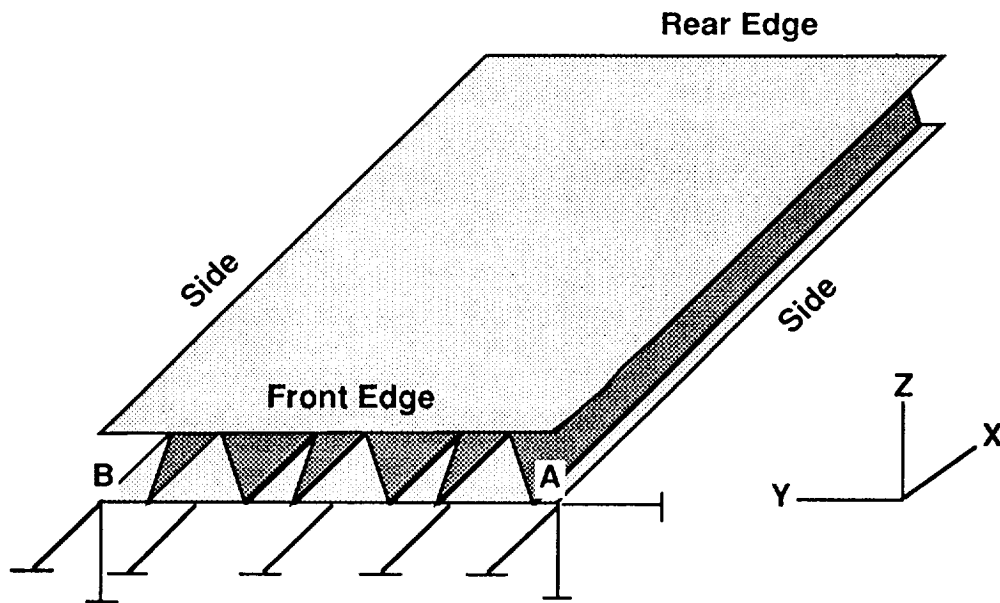


Figure 34 Truss Core Panel, Kinematic Boundary Conditions

The user selected boundary conditions consist of three conditions, very large panel, simply supported sides, or clamped edges. The implementation of these boundary conditions is outlined below.

1) Very Large Panel - For the top and bottom skins all rotations about the local y axis are equal to zero for the front and rear edges of the panel. All rotations about the local x axis are equal to zero for the sides of the panel.

2) Simply Supported Sides with and without fillers - All z-displacements and rotations about the local y axis for the bottom skin on the sides are zero.

3) Clamped Edges - For the top and bottom skins all y- and z-displacements on the front and rear edges and rotations about the local x and y axes are equal to zero.

3.3.2.4 Load Application and Displacement Coupling

The side sections of a truss core panel contain the top and bottom skins, and the edges contain the core and top and bottom skins. The test setup will be such that the inplane axial and shear loads to the panel sides are transmitted via the top and bottom skins. The inplane axial and shear loads to the panel front and rear edges will be transferred via the truss core and top and bottom skins.

In the model, line loads representing axial and shear loads are applied at the midface of the skin elements along the edges and sides. In addition, the CONODE and DOFEQ commands are used so that the applied loads can be properly distributed over the entire section of a side or edge.

The CONODE command dictates that a certain displacement of a node be the slave whose value is the weighted average of two master node displacements. The weights are inversely proportional to the slave node distances from the two master nodes. This displacement coupling ensures that the line loads onto a section are distributed over the entire section according to the cross sectional area stiffness of each component. This is necessary to accurately model displacement controlled tests such as compressive and picture shear frame tests.

3.3.3 Examples

Static and bifurcation buckling analyses were performed to verify the truss core module.

The first example involves a small strip of a truss core panel. It was used for verifying the results of static analysis, including the margins of safety computation. The panel strip has no side fillers. However, side fillers could be added if so desired.

The next four examples are intended to verify available features and show that the results are reasonable for static and bifurcation analyses. The examples are summarized below.

- 1) Static analysis of a small strip of truss core panel subjected to axial loading. Results include average laminate strain and margin of safety contour plots.
- 2) Square panel model subjected to inplane shear loads.
- 3) Variation of the first example, with the dimensions chosen so that the local buckling occurs before global buckling.
- 4) Variation of the first example, with the dimensions chosen so that global buckling occurs before local buckling.
- 5) Square panel experiencing overall buckling. A perspective view of the first mode is presented.

3.3.3.1 Material Properties

The mechanical properties for the composite materials that will ultimately be used by the truss core panel are not available at this time. To expedite analytical work in order to obtain a preview of the panel performance, typical property values of similar materials were used in the analyses.

The average RTD elastic properties for an AS4/3501-6 laminae in tension were used for both tensile and compressive loads. The average RTD laminate tensile and compressive strengths as functions of AML for the AS4/1806 fabric laminates were used for computing the margins of safety.

The average RTD elastic properties for the AS4/3501-6 laminae [used] are,

$$\begin{array}{ll} E_1 = 19800 \text{ ksi} & E_2 = 1470 \text{ ksi} \\ G_{12} = 867 \text{ ksi} & \nu_{12} = 0.3 \end{array}$$

The average RTD AML based tensile and compressive strengths are listed in Table 3.

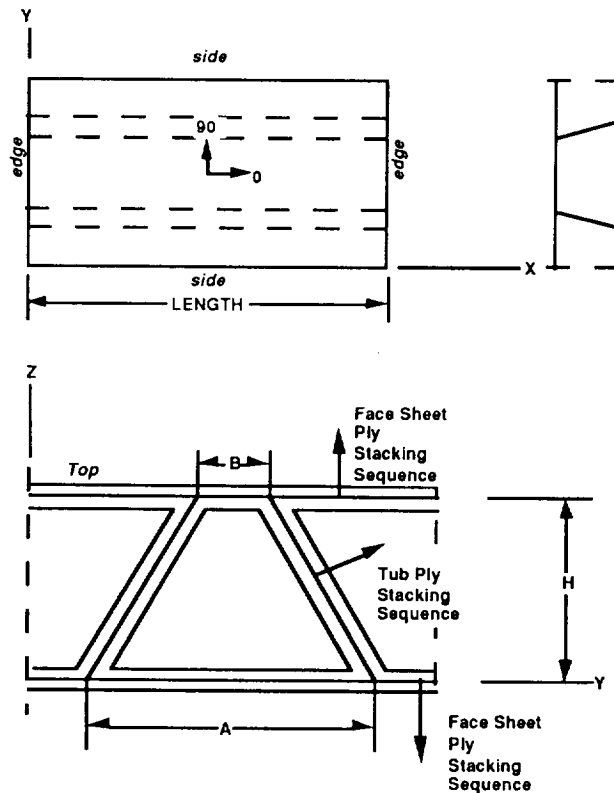
AML	Tensile Strain*	Compressive Strain**
-40	0.00620	-0.00645
0	0.00635	-0.00675
40	0.00650	-0.00705

Note: * Based on 1/4 inch filled hole tests. ** Based on 1/4 open hole tests without impact damages.

Table 3 AML Values, Tensile and Compressive Strains

3.3.4 Example 1. Static Analysis of a Panel Strip

This problem was defined so that the DIAL solutions can be verified by non-finite element calculations. The panel part is six inches in length and consists of top and bottom skins with one interior tube plus two exterior tube halves for the core. It is simply supported in its skin normal direction z along its two sides. Axial compression loading of 32623 lbs/inch in the x-direction are applied at the front and rear edges. There are no fillers on the two sides (Figure 35)



where B, A, and H are equal to .231 inches, 1.231 inches and 1 inches, respectively.

Figure 35 Truss Core Example Panel Geometry

The top and bottom skins and tube webs are made of identical quasi-isotropic laminate having 25% 0°, 50% of ±45°, and 25% of 90° plies. There are 8 plies across the thickness, the ply thickness being 0.0125 inches per ply.

3.3.4.1 Non-Finite Element Calculations

The section details were calculated to be:

thickness of each component	=	0.100 inches
panel width	=	1.462 inches
transverse cross section area	=	1.040 square inches

In this example, all components in a cross section have the same axial stiffness. Hence, the edge loads will be uniformly distributed over the cross sections at the edges of the panel, and the average axial laminate stress and strains in the x-direction will also be uniformly distributed over any section x equal to a constant. The average laminate stress is given by:

$$\sigma_x = (-32623 \text{ lbs/inches})(1.462 \text{ inches})/1.040 \text{ square inches} = -45.88 \text{ ksi.} \quad (3.3.1)$$

Using Lockheed programs HOLSTR and LAMSTR, the equivalent modulus in the global x direction E_x was found to be equal to 7800 ksi.

Utilizing (3.3.1) the uniform strain becomes:

$$\epsilon_x = -45.88/7800 = -0.00588 \text{ in./in.} \quad (3.3.2)$$

In order to calculate the margin of safety, recall that the percentages of 0,±45 and 90 were 25%, 50%, and 25%, respectively. The calculated AML value is 25. By interpolation of the values in Table 3, the allowable strain associated with this AML is equal to -0.00694 in/in. The margin of safety for the top and bottom of the laminates for the skins, webs and thus the panel with uniform strain is given by:

$$MS = 694/588 - 1. = 0.18. \quad (3.3.3)$$

3.3.4.2 DIAL Solution

Figure 36 shows the geometry of the truss core and the optional fillers.

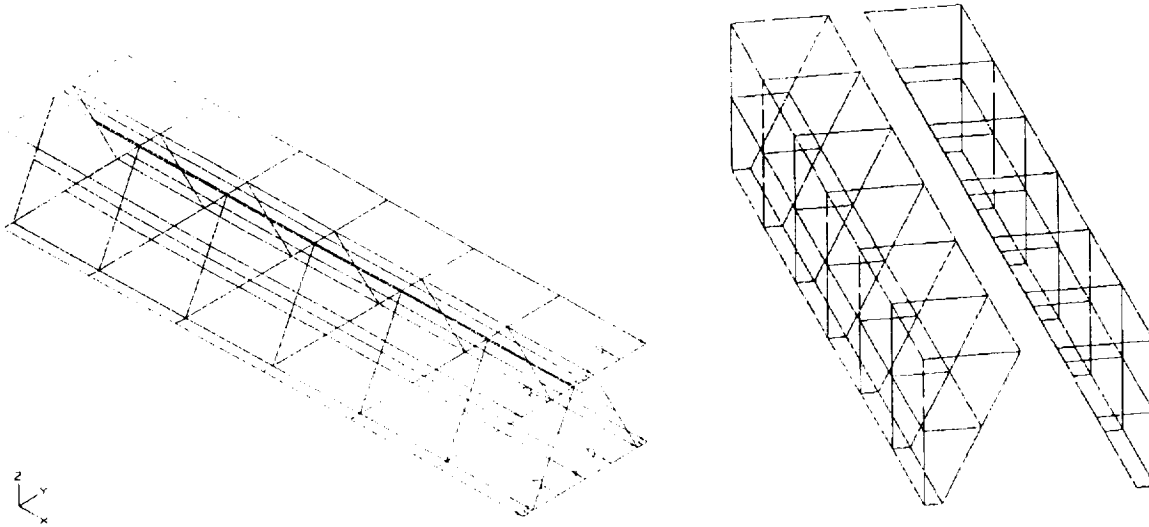


Figure 36 Finite Element Model of Truss Core Panel, Example 1

Note that in this example the fillers are not included. Figure 37 shows the deflected geometry under axial compression loading for this example. Note that the deformed shape is denoted by the solid lines.

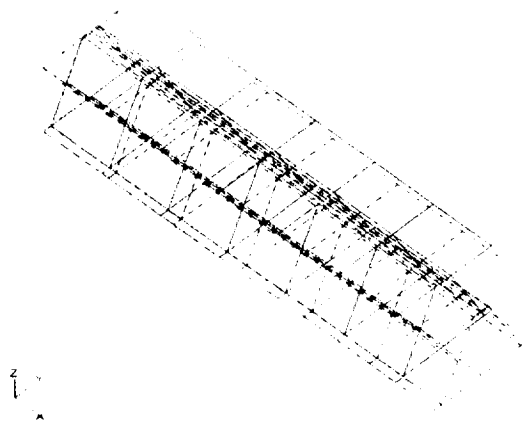


Figure 37 Truss Core Panel Deflected Geometry, Example 1

Figures 38 and 39 are the ϵ_x average and margin of safety contour plots for the top skin and tube wall.

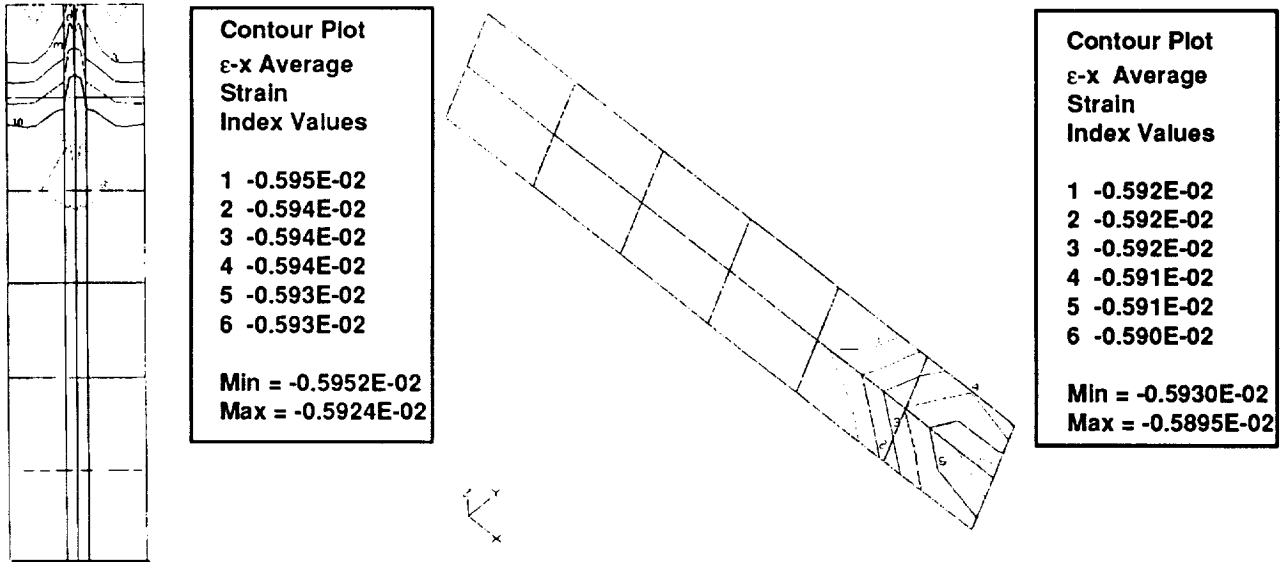


Figure 38 Truss Core Panel Contour Plot, ϵ_x , Example 1

The values of strain are essentially uniform. Slight differences are attributed to the kinematic constraints. The average percent difference is under one percent for the skin and webs of the panel.

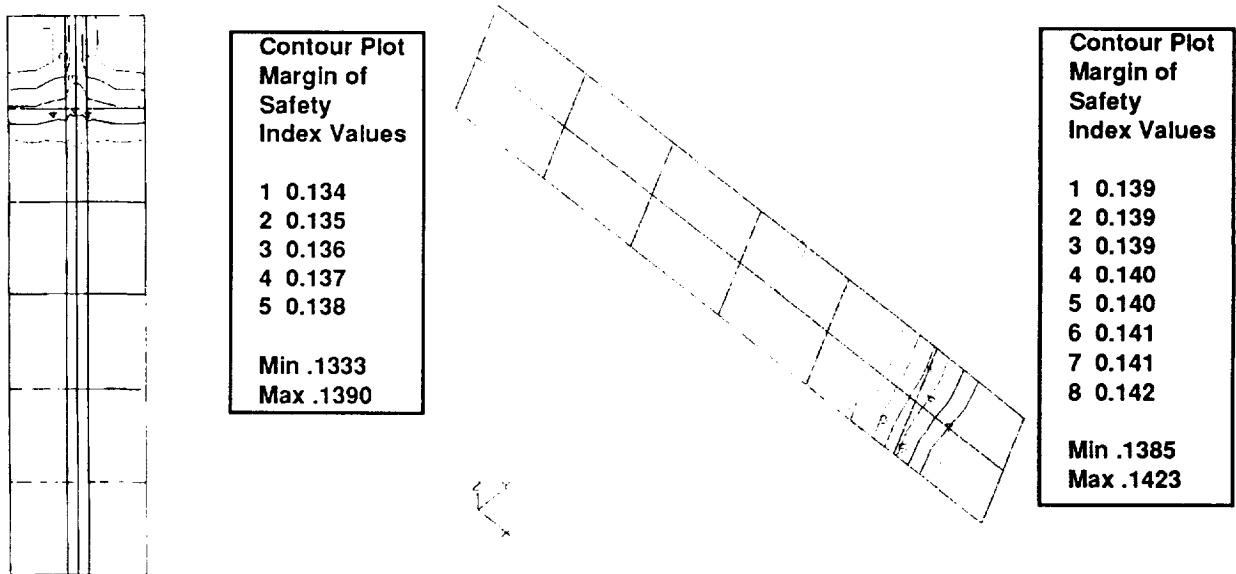


Figure 39 Truss Core Panel Contour Plot, M.S., Example 1

The minimum margins of safety shown in the plots are

0.134, 0.134, and 0.138

for the top and bottom skins and core web, respectively. These values are slightly lower than the hand calculated value.

It was judged that the local bending at the free standing skin edges in the truss core section is the reason for the difference. To see this, a separate solution was made of the same case with clamped edges. The minimum margins of safety shown in the plots are

0.176, 0.170, and 0.150

for the top and bottom skins and core web, respectively. The deviations are only 0.4% to 3%. Note that at the clamped edges, the skins are clamped and core webs remain free.

This case study shows that DIAL calculates local bending which the hand calculation shown above ignores. It also suggests that in a compression test where buckling is not critical, failure is likely to occur at the grip ends.

3.3.5 Example 2. Static Analysis of a Panel Subjected to Inplane Shear Loads

This example involves a square panel 5.85 inches in length consisting of the top and bottom skins, 7 interior tubes and two exterior tube halves. There are no fillers on its sides. The inplane shear loads are 23077 lbs/inch. All other details are the same as those listed in Example 1.

Figures 40 to 42 show the geometry, deflection, and strain plots. The deflection shape is as expected. No verification was made for the deflection and strain levels. However, the contour plots of average laminate ϵ_x and ϵ_{xy} are shown.

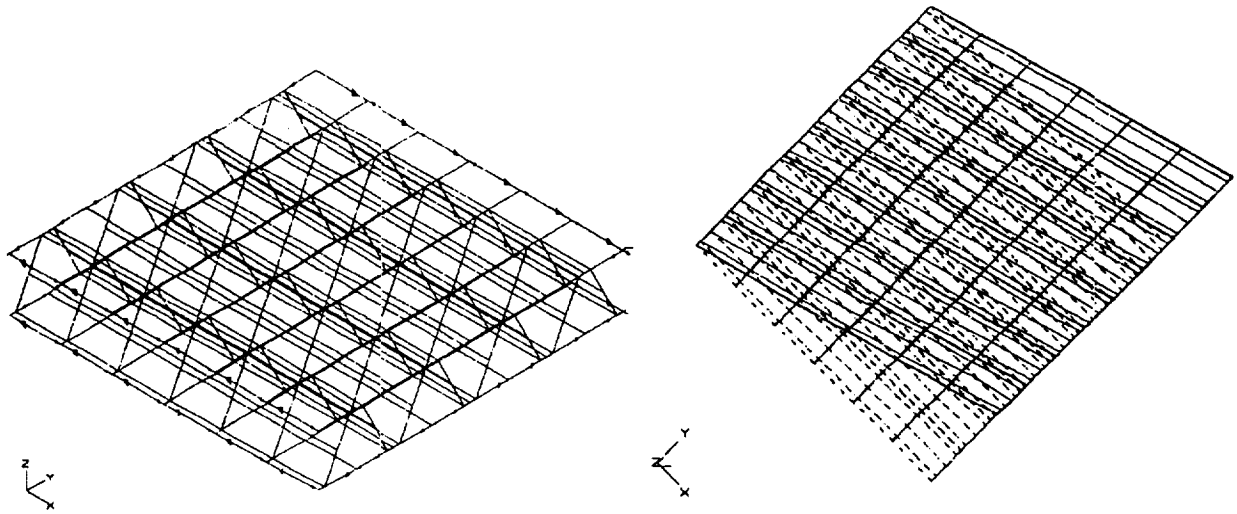


Figure 40 Truss Core Panel Geometry and Deflected Plot, Example 2

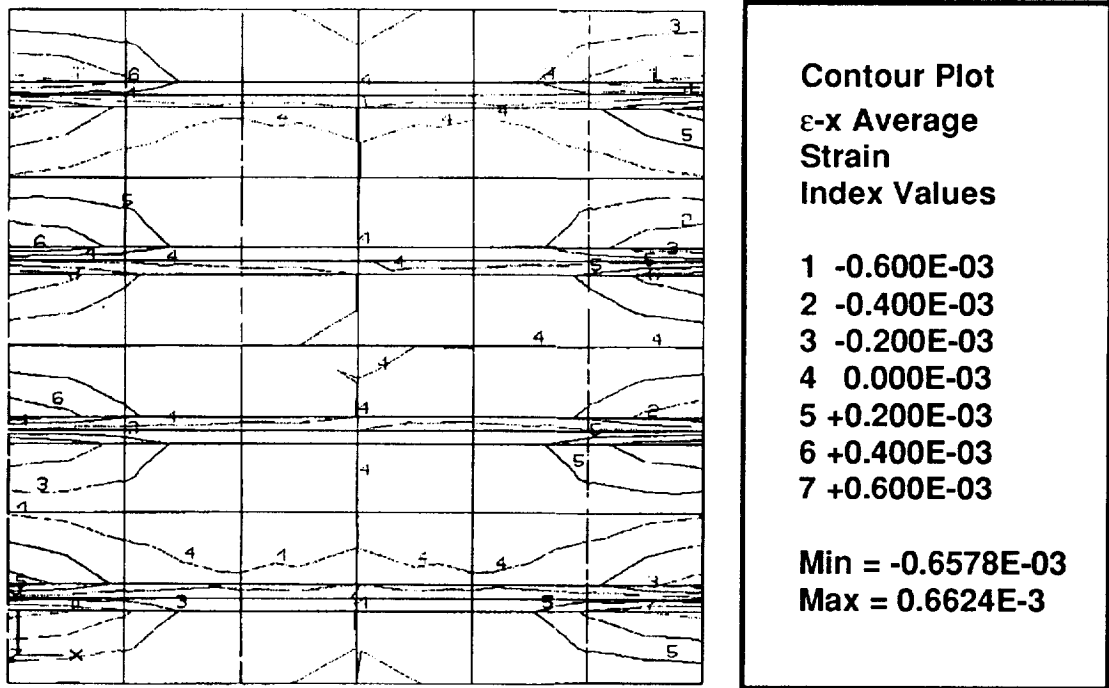


Figure 41 Truss Core Panel Contour Plot, ϵ_x , Example 2

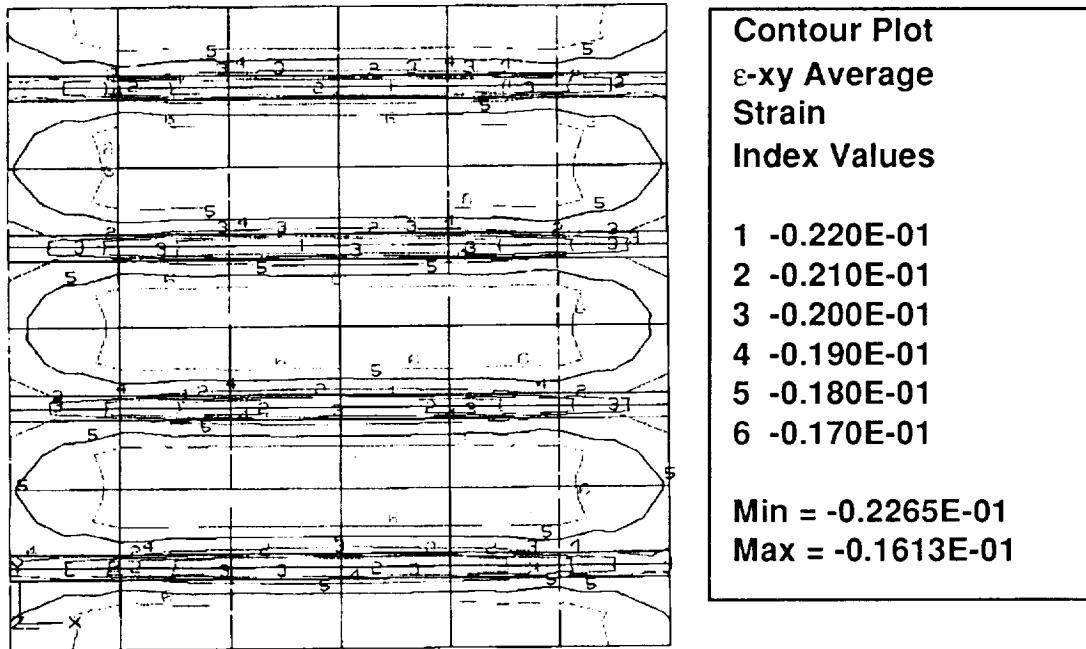


Figure 42 Truss Core Panel Contour Plot, ϵ_{xy} , Example 2

3.3.6 Example 3. Local Buckling of a Panel Strip

The panel strip is a variation of Example 1. The edges are clamped, and there are no side fillers. The tube dimensions are reduced by a half, and the thickness per ply is 0.005 inches for all parts. The panel length is 12 inches. Axial compressive loads are applied at the two edges. Figure 43 shows the geometry.

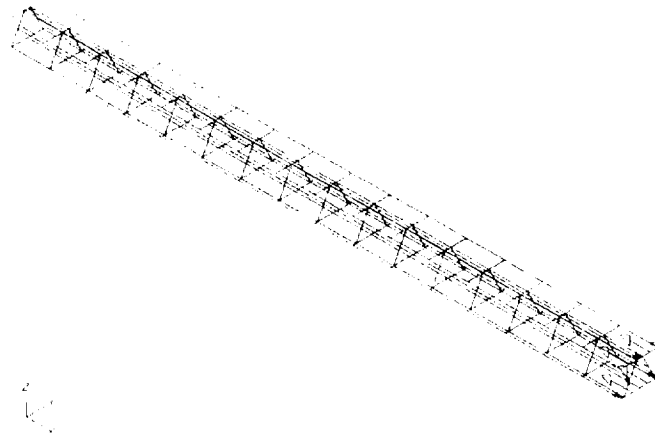


Figure 43 Truss Core Panel Strip Geometry, Example 3

Figures 44 and 45 show the mode shape plots. From these plots and printouts, it was found that local buckling occurred at the free standing portions of the skins on the two panel sides. No verification was made for the critical buckling load.

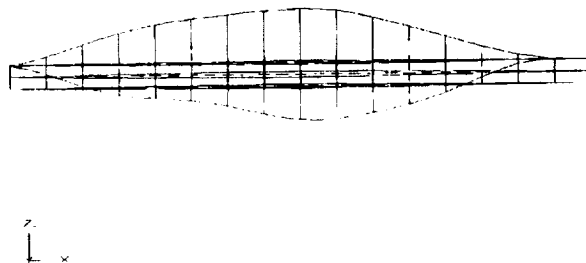


Figure 44 Truss Core Panel Strip First Mode Shape, Example 3

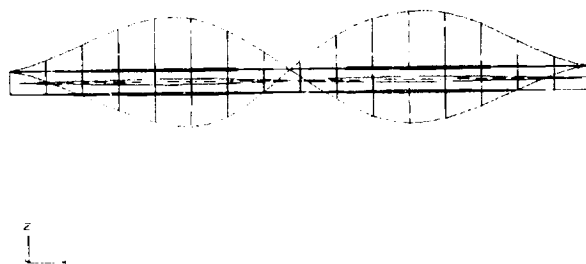


Figure 45 Truss Core Panel Strip Second Mode Shape, Example 3

3.3.7 Example 4. Overall Buckling of a Panel Strip

The panel strip is also a variation of Example 1. Its edges are clamped, and there are side fillers. The tube top and bottom widths are reduced by one half, while the panel height is reduced to 0.32 inches. The thickness per ply is 0.020 inches.

Figures 46 and 47 show the geometry and first and second mode shape plots. Based on the mode shape plots and printouts, it was found that overall buckling occurred. No verification was made for the critical buckling load.

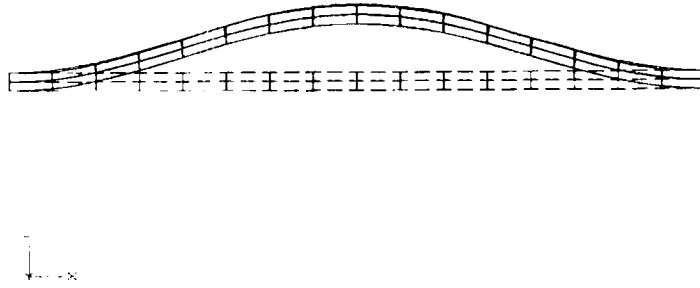


Figure 46 Truss Core Panel Strip First Mode Shape, Example 4



Figure 47 Truss Core Panel Strip Second Mode Shape, Example 4

3.3.8 Example 5. Overall Buckling of a Square Panel

This example involves a 12 inches by 12 inches square panel consisting of the top and bottom skins, 5 interior tubes and two exterior tube halves. The panel height is 0.32 inches and the thickness per ply is 0.020 inches. There are side fillers with assumed high stiffness.

Figure 48 shows the geometry and mode shape plot. Based on the mode shape plot and printouts, it was found that overall buckling occurred. No verification was made for the critical buckling load.

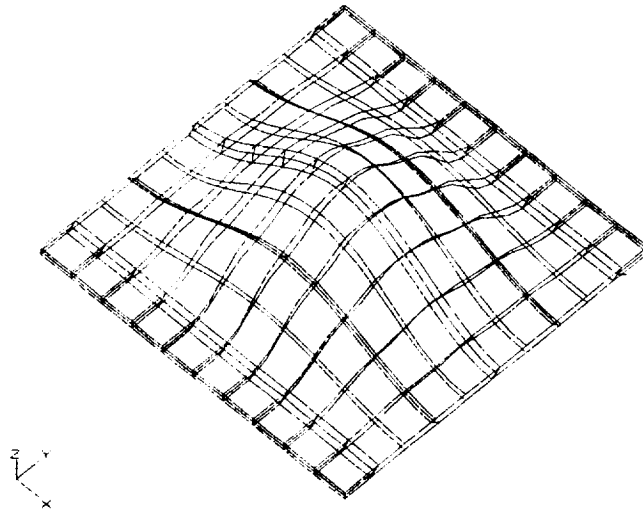


Figure 48 Truss Core Panel, Geometry and Mode Shape, Example 5

3.3.9 Closure

Based on the DIAL runstreams generated by the pre-processor, test runs, and results of the analyses including plots, it is found that the processors function as intended and they generate correct models, runstreams, and deflections/mode shapes, as well as accurate static analysis results.

The mesh fineness is judged to be adequate for the purpose of predicting the first mode of the overall panel buckling. Since DIAL has been verified for its accuracy in predicting the bifurcation buckling in a number of smaller structural problems, the examples presented here suggest that the truss core models would likely result in accurate prediction of the overall buckling. As discussed previously, the prediction of the local buckling will be on the conservative side but improvements can be made.

3.4 Curved Geodesically Stiffened Rectangular Panel

This ISPAN module creates a DIAL model of a curved panel with geodesically arranged stiffeners. The stiffeners are assumed to be filament wound with syntactic layers such that at the intersections the syntactic filler squeezes out to create continuous filament intersections without layer thickness buildup. The general structural arrangement is shown in Figure 49.

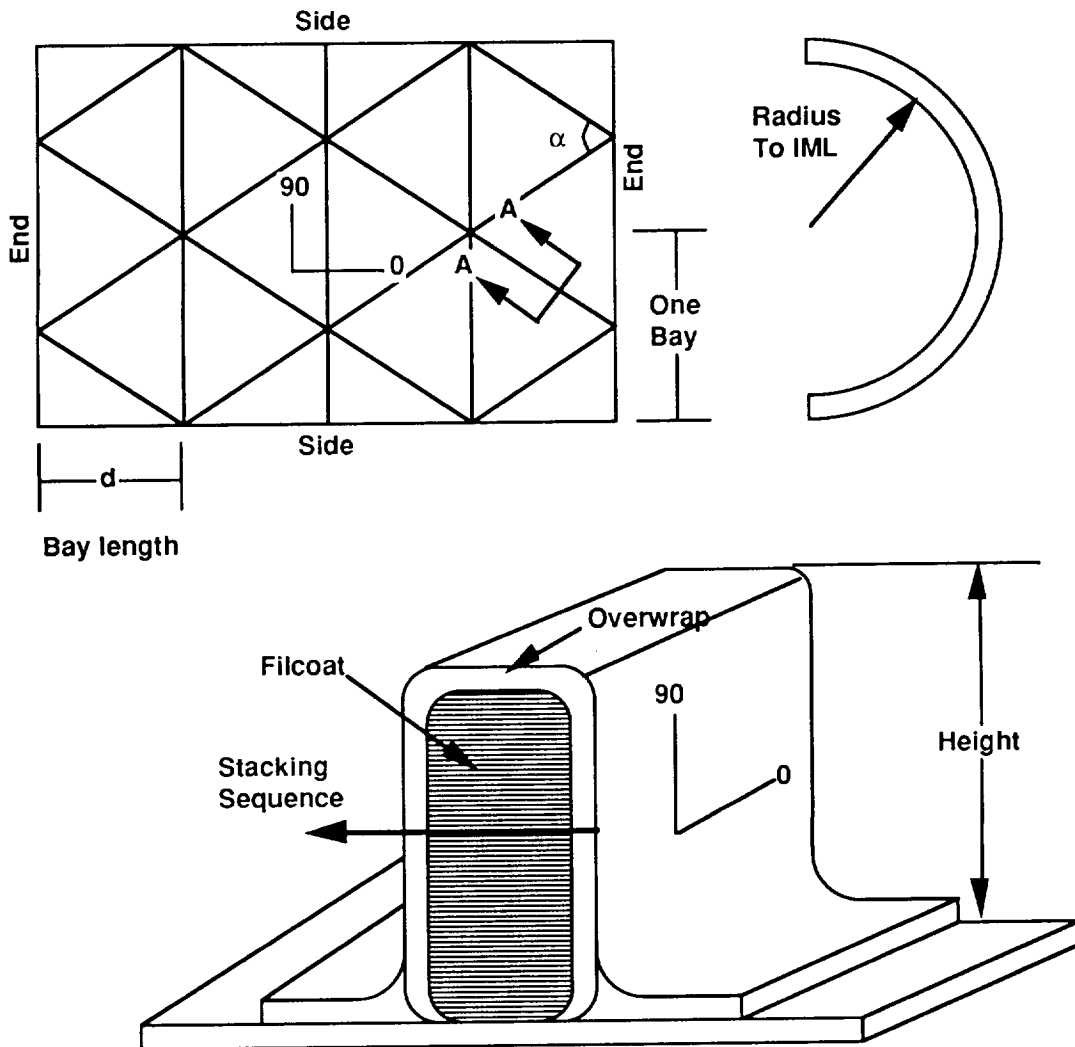


Figure 49 Geodesic Panel General Structural Arrangement

The stiffeners may have non-filament wound overwraps if desired. Because of the curvature, normal pressures may be applied to the panel which will be reacted with a hoop tension load in the

panel. All elements of the model are created with thick shell elements and analyses can include linear stress analysis and a bifurcation buckling analysis, if desired.

Current capabilities and restrictions of this module include:

- 1) Number of axial bays (must be an even number) $N > 2$
- 2) Number of lateral bays (Hoop direction) $1 < N < 5$
- 3) Stiffener angle $40^\circ < \alpha < 60^\circ$
- 4) All stiffeners, both diagonal and hoop, must have similar layups.
- 5) Model cannot exceed 180 degree arc circumferentially
- 6) All bays are geometrically similar
- 7) Any hoop load (N_y) is determined based on the applied pressure.
- 8) Option to perform either a linear stress analysis or buckling analyses. The buckling model is necessarily more refined than the stress model and as a consequence will require longer solution times.

Material input procedure is common to all modules. A full three dimensional set of orthotropic properties is not required since all models use shell elements for analysis.

3.4.1 Example

The following example is a static stress analysis of a single bay of a curved geodesically stiffened panel. The panel is assumed to be infinite, that is to say it is part of a fuselage. The loading consists of axial, shear and pressure loading.

The material properties used in this example are orthotropic and area listed in Table 4.

Material #	E_1	E_2	ν_{12}	G_{12}	G_{23}	G_{31}
1	7.E6	6.8E6	.15	3.E6	.5E6	.4E6
2	20.E6	2.E6	.06	1.E6	.3E6	.35E6

Table 4 Geodesic Panel Material Properties

The skin and stiffener layups are listed in Table 5.

Skin laminate			Stiffener laminate		
Material #	Ply Thickness	Orientation	Material #	Ply Thickness	Orientation
1	.014"	0	1	.014"	45
1	.014"	45	2	0.20"	0
1	.014"	0	1	.014"	45

Table 5 Laminate Layups for Skin and Stiffeners

Figure 50 shows the DIAL finite element model used for the static solution, as compared with its deflected shape under the action of the combined loading.

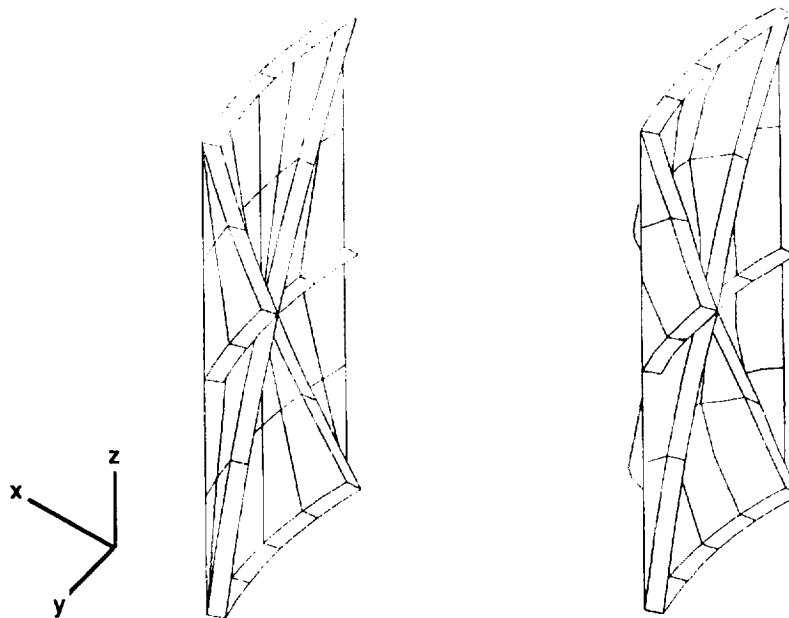


Figure 50 Geodesic Panel, Geometry and Deflected Shape

Figure 51 is a contour plot of N_x .

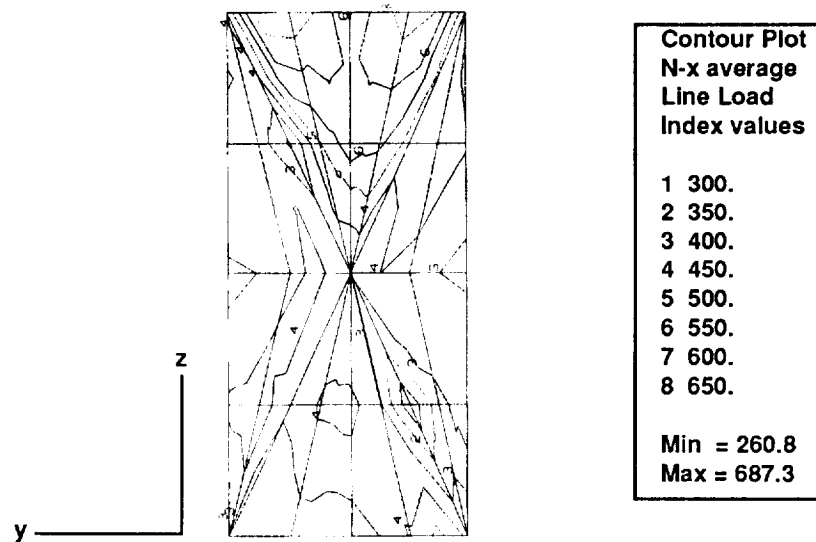


Figure 51 Geodesic Panel N_x Contour Plot

3.4.2 Closure

This example represents a fraction of the curved geodesically stiffened panel's capability. However, due to the selection of the skin/stiffener concept for the fuselage development, and due to the reorientation of the Task II, this module is not as advanced as the others. In the event that, a geodesically stiffened structure need be analyzed in the future of this program, this module can be used in its present form to perform linear static or bifurcation analyses. Additionally, improvements could be added to give the module the capability to analyzes post-buckled structures.

4.0 Failure Analysis

Two failure theories are utilized in the ISPAN modules. The Angle-Minus-Load (AML) and Hashin's failure theories. These theories have been included the DIAL finite element package. DIAL computes margins of safety based on strain allowables (AML) or strength criterion (Hashin).

The AML theory was developed by R.F. Zabora at Boeing, and applies to the laminate as a whole, and not to an individual lamina. This method was developed within the aircraft industry for composite construction and attempts to define strain allowables in a laminate with an assumed amount of damage. This laminate failure theory is advantageous for design due to its simplicity and ease of use. However, the AML criterion only defines failure of the laminate without identifying the ply level failure or the mode of failure.

Hashin's failure theory was developed by Z. Hashin of Tel Aviv University[8] for unidirectional fiber composites. This theory considers failure at the ply level. A piecewise smooth quadratic failure surface is defined where each piece of the surface represents a unique mode of failure. The possible failure modes checked are 1) tensile fiber mode, 2) compressive fiber mode, 3) tensile matrix mode, and 4) compressive matrix mode.

Utilizing the AML and Hashin's failure theories, a balance is achieved between ease of structural design and detailed analysis. The AML theory provides the designer a simple empirically based tool that can determine failure for the entire composite laminate. Hashin's failure theory provides a ply level approach that defines the specific mode in which the lamina failed. These two failure theories provide an effective tool for the design and detailed failure analysis of composite structures.

4.1 AML Failure Procedure

The Angle-Minus-Load (AML) failure methodology is empirically based and is used for laminated composites only. This method applies to the laminate as a whole and not to the individual lamina within the composite.

The ply-level maximum strain failure criterion is based on comparing the components of strain in each ply of a laminate to a set of allowable strains. Experimental determination of allowable ply-level strains, particularly in compression, is very difficult. Furthermore, the maximum strain criterion predicts failure at a strain that is independent of ply percentages in the laminate, contrary to experimental evidence.

The AML criterion, on the other hand, is a laminate failure criterion, as opposed to a ply-level criterion. The procedure is recommended for symmetric, balanced laminates composed of 0° , 90° , and $\pm 45^\circ$ plies with a minimum of 10% plies in each direction. It is based on an allowable curve of laminate failure strain as a function of the AML parameter, defined as percentage of angle plies minus the percentage of longitudinal plies. Hence, laminates with either a low percentage of angle plies or a high percentage of longitudinal plies will both have low AML values.

The AML parameter reflects the ability of a laminate to redistribute the load in the vicinity of a defect or discontinuity. It has long been realized that the higher the percentage of angle plies in a laminate, the higher is the post-impact and open-hole compression failure strain. Experimental evidence supports the contention that allowable strains are higher for laminates rich in $\pm 45^\circ$ plies. Test data obtained over the past few years shows distinct differences in the strength of damaged laminates as a function of ply layup.

The AML parameter can also be interpreted as a stability index related to ply buckling under compression loading. The 0° plies which carry the majority of load require 45° plies to stabilize them against ply buckling. Laminates with a high percentage of 0° plies and/or a small percentage of 45° plies will tend to exhibit lower compression failure strains. Therefore, as opposed to a ply-by-ply theory, the AML criterion provides a method that deals with the ability of the laminate to survive in the presence of damage.

AML allowables are obtained experimentally from tension and compression tests conducted on laminates with varying values of the AML parameter. Several conditions are evaluated, a .25" diameter open-hole, a .25" diameter filled hole, combined with various environmental conditions.

The .25" diameter open hole has been shown to be a reasonable simulation of barely visible impact damage. In addition, compression after impact specimens may be used depending on the requirement. Data obtained from these tests is used to determine knock-down factors per MIL Handbook 17 statistical approach of data reduction. Design allowables based on gross area strains are then plotted as a function of the AML parameter (% $\pm 45^\circ$ plies minus 0° plies). A hypothetical pair of design allowable curves is presented in Figure 52.

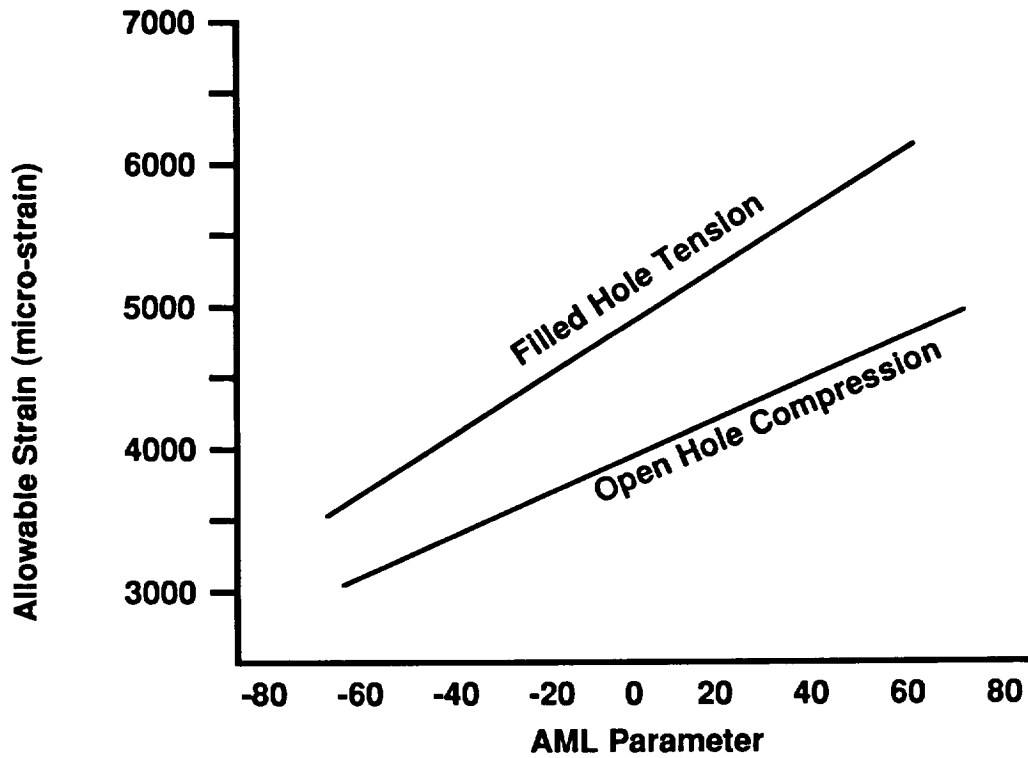


Figure 52 AML: Hypothetical Allowable Strains

4.1.1 Example

For a given laminate, the method involves analyzing for failure in each fiber direction. Therefore the AML parameter is determined for each of the fiber directions. Consider a $[\pm 45/0_2/\pm 45/90_2/\pm 45/0_2]_s$ laminate. Out of a total of 24 plies, there are eight 0° , six $+45^\circ$, six -45° and four 90° plies.

For analysis of failure in the 0° direction, the longitudinal direction is the 0° direction, and the angle directions corresponding to the $\pm 45^\circ$ plies. Therefore,

$$AML_0 = [(6 + 6) - 8]/24 \times 100 = 17$$

For analysis of failure in the +45° direction, the longitudinal direction is the +45° direction, and the angle directions correspond to the 0° and 90° plies. Therefore,

$$AML_{+45} = [(8 + 4) - 6]/24 \times 100 = 25$$

Similarly,

$$AML_{-45} = [(8 + 4) - 6]/24 \times 100 = 25$$

$$AML_{90} = [(6 + 6) - 4]/24 \times 100 = 33$$

Note that, for a balanced laminate, AML_{+45} is equal to AML_{-45} .

4.1.2 AML within DIAL

The AML theory as implemented in DIAL will compute AML values for laminates composed of layers at arbitrary angles. This is accomplished by computing equivalent layers at angles of 0°, ±45°, and 90° degrees. For example, a layer oriented at 30° degrees would be assumed to furnish 1/3 of a layer at 0° degrees and 2/3 of a layer 45° degrees. In this manner an equivalent layup consisting of 0°, ±45° and 90° degrees is computed.

The strains in each of the four load directions are computed at the top and bottom of the laminate. These strains are computed by adding the midsurface membrane strains to the bending portion of the strain divided by a factor of 1.3. These eight computed strains are compared to the allowable strains given the appropriate AML value for the load direction, and margins of safety are computed. The minimum margin of safety and its load direction are printed out.

The AML failure analysis can be performed quickly, which is of great value with respect to initial design. However, we need a failure analysis criterion that can check ply level failure and distinguish between modes of failure.

4.2 Hashin's Failure Criterion

This theory is based on a piecewise smooth quadratic surface. This piecewise approach allows this theory to distinguish between various failure modes of the composite. The possible failure modes that are checked are 1) tensile fiber mode, 2) compressive fiber mode, 3) tensile matrix mode, and 4) compressive matrix mode. Margins of safety are computed for each possible mode where the minimum margin defines the mode in which the composite failed. The failures parameters are coded to be temperature dependent. The effects of interlaminar shear stresses are ignored.

The following represents a brief outline of the methodology in order to show the benefits of this theory as opposed to previous theories [6].

Tsai and Wu [7] represented the failure theory as a smooth quadratic function in terms of stresses:

$$F_{ij} \sigma_i \sigma_j + F_i \sigma_i = 1 \quad i, j = 1, 2, \dots, 6 \quad (4.2.1)$$

For an orthotropic material with unequal strengths in tension and compression, the coefficients in general have the following form:

$$F_{11} = \frac{1}{N_1^+ + N_1^-}$$
$$F_1 = \frac{1}{N_1^+} - \frac{1}{N_1^-} \quad (4.2.2)$$

The failure theory as shown in equation (4.2.1) is a definite improvement over previous criteria because of its generality, versatility and because it provides a good fit with experimental test data. However, for composite materials there are some intrinsic problems.

Underlying these is the fact that a fiber composite consists of mechanically very dissimilar phases; stiff elastic fibers and a yielding compliant matrix. Consequently, the failure occurs in very different modes. The fibers may rupture in tension or buckle in compression, or the matrix may fail due to load transfer from the fibers. It is not evident that all of the distinct failure modes can be represented by a single smooth function such as the one given proposed by Tsai and Wu [7].

To illustrate some difficulties specific to fiber composites, let equation (4.2.1) be specified for a unidirectional reinforced lamina in plane stress as given by equation:

$$F_{11} \sigma_{11}^2 + F_{22} \sigma_{22}^2 + 2F_{12} \sigma_{11} \sigma_{22} + F_{66} \sigma_{12}^2 + F_1 \sigma_{11} + F_2 \sigma_{22} = 1 \quad (4.2.3)$$

where the 1 and 2 denote directions that are in the fiber and transverse directions, respectively.

All coefficients except F_{12} are determined by expressions of the type (4.2.2). Assuming that F_{12} has been determined by a biaxial failure test, we can utilize equation (4.2.3) to predict failure for the biaxial tensile state of stress given by equation (4.2.4):

$$\sigma_{11} = \sigma \quad \sigma_{22} = \alpha\sigma \quad \text{and} \quad \sigma_{12} = 0 \quad (4.2.4)$$

where α is a constant.

Substituting equation (4.2.4) into equation (4.2.3) will result in a quadratic equation in σ . Because of the form of equation (4.2.2), the coefficients of the quadratic depend on N_1^+ , N_1^- , N_2^+ , and N_2^- .

It follows that the failure under biaxial tensile loading depends on the values of compressive failure stresses which is physically unacceptable. These difficulties provide the motivation to represent the failure criterion of a unidirectional fiber composite in a piecewise smooth form where each smooth branch represents one distinct failure mode. This is physically more realistic than previous theories.

Hashin's failure theory provides a marked improvement over previous theories due to the fact that separate failure modes are considered. Furthermore, recognition of separate modes identifies certain troublesome interaction coefficients as being of secondary importance, thereby facilitating experimental determination of significant failure parameters.

This theory will allow for inclusion of additional failure modes, therefore as textile composites and an understanding thereof progresses additional modes of failure can be added as necessary.

4.2.1 Hashin's Criterion within DIAL

For laminated Shells each layer is checked for all four modes. The minimum margin of safety can be printed or stored for subsequent contour or section plots. Since Hashin does not consider interlaminar shear stresses to compute margins of safety in the shell lamina, the decision was made to ignore the interlaminar shear stresses in the computations. However, DIAL does compute approximately interlaminar shear stresses. The coding was planned so that interlaminar shear stresses could be incorporated in the margin of safety calculations if so desired in the future.

5.0 Bolted Joint Strength Prediction

Many bolted joint strength prediction models have been developed and reported in the literature. Most of these models were developed based on the concept of characteristic distance which evaluated the stress state away from the stress concentration points. Many assumptions are inherent in these approaches, and applicability to different modes of failure of the bolted composite joint has been unsuccessful in all cases. Alternatively, to obtain bearing/by-pass design allowables, too many test were required to address all the parameters influencing the bolted joint strength. Flexibility of providing design data was not cost-effective or timely. An analytical method, to accurately predict a bolted joint strength was needed and was developed under this program.

The effort was undertaken and the approach was conceived to develop and implement a progressive failure analysis for analyzing double lap shear composite joints. Composites made of unidirectional prepreg only, were considered. However, the code could be further developed for other forms of structural materials such as textile composites.

The progressive failure analysis consists of a stress analysis and a failure analysis. The stresses and strains were calculated by a finite element method based on a two-dimensional plane stress assumption with the consideration of finite strain deformations and the ply shear stress-strain nonlinearity. Failure was predicted by a set of failure criteria, and loss of material properties due to failure was estimated by the material degradation models. Out-of-plane failures including delamination and extensive bearing failure were not considered in the analysis. Failure prediction was on a ply-by-ply basis.

Accordingly, the new code, designated TEXTJOINT, is capable of characterizing the response of the bolted joints in laminated composites. Numerical calculations were also performed and compared with the available test data for T300/934 and IM8/APC-HTA composites. The results of this comparison showed that the predictions by the code agreed well with the test data.

The following subsection documents the effort undertaken to develop and verify the TEXTJOINT code.

5.1 Introduction to Bolted Joint Prediction

The bolted joint is one of the most common joining methods connecting two pieces of structure together. Considerable work has been performed to study the response of bolted composite joints [8-13]. The basic failure modes in bolted composite joints, which are related to the material failure, can be characterized as net-tension, shear-out, and bearing failures [13]. The failure mode, strength, and response of the joints depends strongly upon several factors, including geometry, ply orientation, material properties, fasteners types, and bolt tightening, etc.

Several analytical models have been developed in the literature [8-13]. Most of the analyses were developed based on the concept of the characteristic curve (distance) [12,13] which evaluates the stresses at a distance away from the stress concentration points. For instance, the BJSFM computer code[12] utilizes the orthotropic elasticity solutions combined with a characteristic curve with one parameter for analyzing the strength of the bolted composite joint with a single hole. The model has been demonstrated to provide reasonable predictions for joints failed in the bearing mode. The BOLT code developed by Chang et al [13] adopted a finite element analysis and a characteristic curve with two parameters for analyzing joints with a single hole, and two holes in parallel or in series. The code has been shown to provide good agreement with the test data for predicting failure load and the three failure modes.

However, these characteristic parameters have to be determined from experiments and have been found to be sensitive to laminate configuration and geometry of the joint. In addition, no information can be obtained from these models on the response of the joints to the damage accumulated inside the materials as a function of the applied load. Such information is critically important for the optimal design of a composite joints. Recently, a progressive failure analysis has been developed for analyzing the response of laminated composites containing an open hole. The model can estimate the response of the composites from initial loading, through damage development, to final failure. No delamination was considered in the model.

In this investigation the major objective was to implement the progressive failure analysis into the BOLT code. The new code is designated as TEXTJOINT. In the following, the analytical model and the TEXTJOINT code will be described and the comparison between the predictions and the available test data will also be presented.

5.2 Statement of Problem

Three types of double-lap bolted joints were considered in the study; single hole, two holes in parallel, and two holes in series, as shown in Figure 53

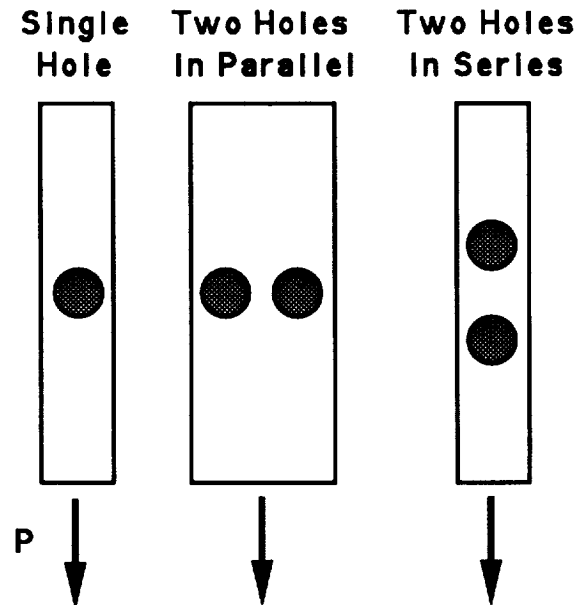


Figure 53 Description of Bolted Composite Joint Problem

The joints were made of unidirectional prepreg composites. The ply orientation of the laminate could be arbitrary but must be symmetric with respect to its middle plane. A uniform tensile load was applied at one end of the specimen. It was desired to obtain the following information.

- 1) The extent and the types of damage as a function of applied load
- 2) The ultimate failure mode and failure load of the joint

5.3 Analysis

The progressive failure analysis [14,15] consists of a stress analysis and a failure analysis. Stresses and strains in the plates are calculated based on a finite deformation theory with consideration of material and geometric nonlinearities. Plane stress condition (lamination theory) is used.

The type and size of damage in composites is predicted in the failure analysis which includes a set of proposed failure criteria and property degradation models for each mode of failure. Only in-plane ply failure is evaluated and delamination is not considered.

Stresses and strains are calculated at each incremental step, and evaluated by the failure criteria to determine the occurrence of failure and the mode of failure. Mechanical properties in the damage area are degraded appropriately according to the property degradation models. Stresses and strains are then recalculated to determine and damage as a result of stress redistribution at the same load. This procedure continues until no additional damage is found, and the next increment is then pursued. The final load is determined when the plates can not sustain any additional load or the joint has exceeded the allowed deformation.

5.3.1 Stress Analysis

The variational form of a two-dimensional equilibrium equation of a composite plate based on the plane stress condition can be generalized as equation (5.3.1.1):

$$V = \int_A \sigma_{ij} \epsilon_{ij} da - \int_{S_\sigma} T_i u_i ds \quad (i,j = 1,2) \quad (5.3.1.1)$$

where σ_{ij} and ϵ_{ij} are the stress and strain components and T_i and u_i are the surface traction acting on the surface S_σ and the displacements, respectively. A is the total surface area of the structure.

For fiber-reinforced laminated composites, the in-plane stress-strain relations on each ply can be expressed as:

$$\begin{Bmatrix} \sigma_x \\ \sigma_y \end{Bmatrix} = \begin{bmatrix} \frac{E_x}{1 - \nu_x \nu_y} & \frac{E_y \nu_x}{1 - \nu_x \nu_y} \\ \frac{E_x \nu_y}{1 - \nu_x \nu_y} & \frac{E_y}{1 - \nu_x \nu_y} \end{bmatrix} \begin{Bmatrix} \epsilon_x \\ \epsilon_y \end{Bmatrix} \quad (5.3.1.2)$$

$$\sigma_{xy} = f(\gamma_{xy}) \text{ or } \gamma_{xy} = f^{-1}(\sigma_{xy})$$

where x and y are coordinates parallel and normal to the fibers, respectively. Note that the material nonlinearity on a ply-by-ply level is introduced through the shear stress-strain relationship. The nonlinear relationship is chosen to have the following form [16]:

$$\gamma_{xy} = \left(\frac{1}{G_{xy}} \right) \sigma_{xy} + \alpha \sigma_{xy}^3 \quad (5.3.1.3)$$

where G_{xy} is the initial shear modulus and α is the nonlinear parameter of the material that has to be determined experimentally.

From equations (5.3.1.2) and (5.3.1.3), the on-axis stiffness, Q_{xy} , of a unidirectional layer of composite materials can be deduced as:

$$\begin{aligned}
[Q_{xy}] &= \begin{bmatrix} Q_{xx} & Q_{xy} & 0 \\ Q_{xy} & Q_{yy} & 0 \\ 0 & 0 & Q_{ss} \end{bmatrix} \\
&= \begin{bmatrix} \frac{E_x}{1 - \nu_x \nu_y} & \frac{E_y \nu_x}{1 - \nu_x \nu_y} & 0 \\ \frac{E_x \nu_y}{1 - \nu_x \nu_y} & \frac{E_y}{1 - \nu_x \nu_y} & 0 \\ 0 & 0 & G_{xy} \end{bmatrix}
\end{aligned} \tag{5.3.1.4}$$

where G_{xy} is the tangent shear modulus obtained by taking the partial derivative of equation (5.3.1.3) with respect to γ_{xy} as shown in equation (5.3.1.5):

$$G_{xy} = \frac{\partial f(g_{xy})}{\partial \gamma_{xy}} \tag{5.3.1.5}$$

Thus, the off-axis stiffness $[Q_{ij}]$ of a unidirectional composite can be related to $[Q_{xy}]$ by tensor transformation which depends upon the ply orientation of the layer in a laminate [19]. By combining equations (5.3.1.4) and (5.3.1.5), the laminate stiffness matrix can be calculated based on the lamination theory. Due to the nonlinearity of the ply shear stress-shear strain relationship, the laminate stiffness matrix is not constant but depends upon the amount of the applied load and the ply orientation of the laminate. As a result, equation (5.3.1.1) is combined with equation (5.3.1.2) through (5.3.1.5), and is solved numerically.

A nonlinear finite element analysis is developed based on the analysis and a four-node isoparametric element is used. Since the bolt contacting force distribution on the hole boundary can affect significantly the stress distributions inside the composite near the hole boundary, the bolt-hole contact condition has to be modelled properly. By assuming rigid bolts and no friction between the bolt and the hole boundary, the contact conditions can be expressed mathematically as follows:

$$u_T(D/2) \geq 0 \tag{5.3.1.6.1}$$

$$T_n \leq 0 \quad (5.3.1.6.2)$$

where $u_r(D/2)$ are the normal displacements of the plate along the hole boundary of a diameter D , and T_n are the normal surface tractions along the contact surface Γ . Equation (5.3.1.6.1) ensures the impenetrability of the rigid bolts, and Equations (5.3.1.6.2) enforces contact pressure be negative along the contact surface. A schematic description of a finite element mesh is shown in Figure 54.

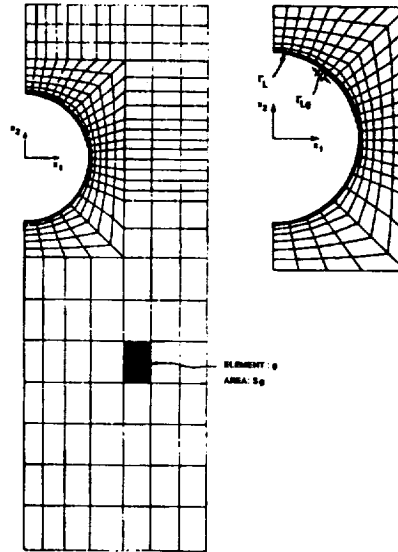


Figure 54 Bolted Joint Typical Finite Element Mesh

The above conditions have to be satisfied along the contact surface between the bolts and hole boundaries of the composites. Accordingly, equation(5.3.1.1) and (5.3.1.6) have to be solved together. Details of the derivation of the finite element analysis can be found in [16].

5.3.2 Failure Analysis

Failure prediction is performed on a ply-by-ply basis. A set of failure criteria was adopted for predicting the failure and material degradation models were developed for estimating the reduction of mechanical properties due to the damage in the layer. Since failure of bolted joints involves multiple stress components, all the basic failure modes in unidirectional composites have to be considered in order to accurately predict the damage in bolted joints. Basically, the failure modes in unidirectional composites can be classified as matrix cracking, fiber-matrix shearing, fiber breakage, matrix compression, and fiber-matrix compression failure. It is noted that matrix cracking, fiber-matrix shearing and fiber breakage in each layer contribute primarily to the net-tension and fiber-matrix compression failure are associated with bearing failure of bolted joints.

5.3.2.1 Failure Criteria

A set of failure criteria incorporated with *in situ* ply strength distributions is presented to predict failure and mode of failure of each ply in laminated composites[14].

Matrix Cracking Failure

For predicting matrix cracking ($\sigma_y \geq 0$), the criterion has the form:

$$\left(\frac{\sigma_y}{Y_t} \right)^2 + \frac{\int_0^{\gamma_{xy}^u} \sigma_{xy} d\gamma_{xy}}{\gamma_{xy}^u} = e_{M+}^2 \quad (5.3.2.7)$$

where σ_y and σ_{xy} are the transverse tensile stress and shear stress in each layer, respectively. γ_{xy}^u is the ultimate shear strain and Y_t is the *in situ* transverse tensile strength.

By introduction the ply shear stress-shear strain relationship of equations (5.3.1.3) and equations (5.3.2.7) yields:

$$\left(\frac{\sigma_y}{Y_t} \right)^2 + \frac{\frac{\sigma_{xy}^2}{2G_{xy}} + \frac{3}{4} \alpha \sigma_{xy}^4}{\frac{S_c^2}{2G_{xy}} + \frac{3}{4} \alpha S_c^4} = e_{M^+}^2 \quad (5.3.2.8)$$

At $\alpha = 0$, equations (5.3.2.8) reduces to the two-dimensional form of the tensile matrix failure criterion proposed by Hashin [5]

It is noted that the matrix tensile strength Y_t in the above equations is not a constant but can be expressed as [14,17]:

$$Y_t = Y_t^0 \left(1 + A \frac{\sin(\Delta\theta)}{NB} \right) \quad (5.3.2.9)$$

where Y_t^0 is the transverse tensile strength of a $[90_n]_s$ laminate ($n \geq 6$), $\Delta\theta$ is the minimum ply angle change between the ply under consideration and its neighboring plies (above and below), and N is the number of consecutive (clustered) plies of the same orientation. A and B are the material parameters which have to be determined by curve fitting the tensile strength data corresponding to the first matrix cracking of $[0_n/90_m]_s$ specimens from experiment.

Matrix Compression Failure

For predicting matrix compression failure ($\sigma_y < 0$) the criterion has the form:

$$\left(\frac{\sigma_y}{Y_c} \right)^2 + \frac{\int_0^{\gamma_{xy}^u} \sigma_{xy} d\gamma_{xy}}{\int_0^{\gamma_{xy}^u} \sigma_{xy} d\gamma_{xy}} = e_{M^-}^2 \quad (5.3.2.11)$$

where the Y_c is the in-plane matrix compressive strength of a unidirectional ply.

Fiber Breakage or Fiber-Matrix Shearing Failure

For fiber-matrix shearing or fiber breakage ($\sigma_x > 0$), the criterion has the form:

$$\left(\frac{\sigma_x}{X_t} \right)^2 + \frac{\int_0^{\gamma_{xy}} \sigma_{xy} d\gamma_{xy}}{\gamma_{xy}^u} = e_{fs}^2 \quad (5.3.2.12)$$

where X_t is the longitudinal tensile strength of a unidirectional composite. Note that as e_{fs}^2 approaches unity, Equation (5.3.2.12) predicts fiber breakage dominated failure when the first term is greater than or equal to the second term of equation (5.3.2.12); otherwise, it indicates fiber-matrix shearing dominated failure.

Fiber Matrix Compression Failure

For fiber-matrix compression failure ($\sigma_x < 0$), the criterion has the form:

$$\left(\frac{\sigma_x}{X_c} \right)^2 + \frac{\int_0^{\gamma_{xy}} \sigma_{xy} d\gamma_{xy}}{\gamma_{xy}^u} = e_b^2 \quad (5.3.2.13)$$

where X_c is the longitudinal compressive strength of a unidirectional composite. Note that as e_b^2 approaches unity, equation (5.3.2.13) predicts fiber-matrix compression failure.

5.3.2.2 Property Degradation Models

Once damage is predicted, material degradation models were proposed for predicting the response of the bolted composite joints containing the damage. It was assumed that the degradation of

mechanical properties of fiber-reinforced composites depends upon the failure and the damage area.

Matrix Failure

Due to stress concentration effect, matrix failure in tension or compression could occur at an early loading stage. Although the effect of such localized matrix failure on the global response of the bolted joints is minimal, it could reduce the local matrix properties significantly. It is well known that matrix failure can affect transverse modulus E_y and poisson's ratio ν_y of the layer in the laminate, depending upon the amount of the cracks accumulated within the damage area. Based on the shear lag analysis, the effect of matrix cracking over an area at the saturated state (maximum crack saturation) could reduce the transverse modulus by more that sixty percent under a uniform loading condition [18]. It was belived that such a reduction would further increase the stress concentration area.

Therefore, in the finite element analysis, for matrix failure, the transverse modulus E_y and poisson's ratio ν_y within an element are reduced by a degradation factor. A factor of 0.1 was used in the study. It was found, however, that based on the numerical simulations, the results of calculations were quite insensitive to the change of the degradation factor once it is smaller than 0.4. The longitudinal modulus E_x and the shear tangent modulus are unchanged, the in-plane properties are reduced as follows:

For $\sigma_y > 0$ and $e_M^+ = 1$

$$\left[\begin{array}{ccc} \frac{E_x}{1 - \nu_x \nu_y} & \frac{E_y \nu_x}{1 - \nu_x \nu_y} & 0 \\ \frac{E_x \nu_y}{1 - \nu_x \nu_y} & \frac{E_y}{1 - \nu_x \nu_y} & 0 \\ 0 & 0 & G_{xy} \end{array} \right] \longrightarrow \left[\begin{array}{ccc} \frac{E_x}{1 - \nu_x \nu_y} & \frac{E_y^d \nu_x}{1 - \nu_x \nu_y} & 0 \\ \frac{E_x^d \nu_y}{1 - \nu_x \nu_y} & \frac{E_y^d}{1 - \nu_x \nu_y} & 0 \\ 0 & 0 & G_{xy} \end{array} \right] \quad (5.3.2.14)$$

where E_y^d and ν_y^d are the reduced transverse modulus and Poisson's ratio, respectively.

Fiber Breakage and Fiber-Matrix Shearing Failure

For fiber breakage and fiber-matrix shearing failure, material degradation is critical because damage associated with these failure modes would significantly affect the performance of the joints carry the load.

For a unidirectional composite subjected to uniform tensile loading, the severity of the fiber damage within the composite, as the load increases, is proportional to the ratio between the damaged are (fiber breakage) and the area under consideration. This implies that failure of a few fibers in a composite would have a very limited effect on the properties on the composites unless the area (or number of broken fibers) has reached a critical value. Therefore, the residual properties of a composite, due to fiber failure, strongly depend on the damaged area in which fiber breakage has occurred.

Accordingly, for fiber breakage dominated failure, the stiffness matrix $[Q_{xy}]$ of a unidirectional composite within the damaged area was reduced as follows [16]:

$$[Q_{xy}] = \begin{bmatrix} \frac{E_x}{1 - \nu_x \nu_y} & \frac{E_y \nu_x}{1 - \nu_x \nu_y} & 0 \\ \frac{E_x \nu_y}{1 - \nu_x \nu_y} & \frac{E_y}{1 - \nu_x \nu_y} & 0 \\ 0 & 0 & G_{xy} \end{bmatrix} \longrightarrow \begin{bmatrix} E_x^d & 0 & 0 \\ 0 & 0 & 0 \\ 0 & 0 & G_{xy}^d \end{bmatrix} \quad (5.3.2.15)$$

where the longitudinal modulus E_x and the tangent shear modulus G_{xy} degenerate according to the Weibull distribution as follows:

$$\frac{E_x^d}{E_x} = \exp \left[\left(- \frac{Af}{A_o} \right)^\beta \right]$$

$$\frac{G_{xy}^d}{G_{xy}} = \exp \left[\left(- \frac{Af}{A_o} \right)^\beta \right] \quad (5.3.2.16)$$

where E_x^d and G_{xy}^d are the reduced tensile and shear moduli, respectively. A^f is the damage zone predicted by the failure criterion, and A_0^f is defined as the critical damage area. A_0^f can be considered to be a material parameter and is associated with the critical fiber interaction zone δ corresponding to the longitudinal tensile strength X_t [21]. The critical fiber interaction zone δ is defined as an effective length of a fiber break on the surrounding fibers [16]. Here, the value of A_0^f is taken to be $\delta \times \delta$ (i.e. $A_0^f = \delta \times \delta$).

The fiber interaction zone, δ can be estimated by considering the effect of stresses near the tip of a broken fiber in a matrix [19,20]. By assuming a rigid-perfectly plastic behavior of the matrix at the interface and applying the fiber bundle theory [19,20], the fiber interaction zone can be estimated by equation (5.3.2.17):

$$\delta = 2d \left(\frac{x_f}{4\tau_y} \right)^{\frac{\beta}{\beta+1}} \left[\frac{(\beta + 1)L}{d} \right]^{\frac{1}{\beta+1}} \quad (5.3.2.17)$$

where d is the diameter of the fibers, x_f is the average fiber strength, and τ_y is the yielding stress of the matrix. L is the length of the fibers under consideration (typically one inch long).

Note that the value of δ thus calculated from equation (5.3.2.17) can only be used as an approximation, because of the assumptions that were made for the analysis and variations of the material parameters required in equation (5.3.2.17). For example, depending upon the material properties of the fibers and matrix, the values of δ for graphite/epoxy composites can vary from .025 to .06 inches [21,22.] During the investigation, a value of .05 inches was selected for the graphite/epoxy composites considered in the study, because it provided the best fit of the predictions with test data.

β is the shape parameter of the Weibull distribution functions, equation (5.3.2.16). The value can be correlated with the shape parameter of the fiber bundle strength distribution [19,20]. For graphite fiber bundles, the value of β may vary from 7 to 10.

For fiber-matrix shearing dominated failure, a material degradation model similar to the one that was used for fiber failure was proposed. It was assumed that poisson's ratio, ν_y and the

transverse modulus E_y would reduce to zero, and the tangent shear modulus G_{xy} degenerates according to equation (5.3.2.15). However, it was assumed that the longitudinal modulus E_x is not affected by fiber-matrix shearing failure. Hence, the stiffness matrix $[Q_{xy}]$ of a unidirectional composite within the damaged area is reduced as follows.

$$[Q_{xy}] = \begin{bmatrix} \frac{E_x}{1 - \nu_x \nu_y} & \frac{E_y \nu_x}{1 - \nu_x \nu_y} & 0 \\ \frac{E_x \nu_y}{1 - \nu_x \nu_y} & \frac{E_y}{1 - \nu_x \nu_y} & 0 \\ 0 & 0 & G_{xy} \end{bmatrix} \longrightarrow \begin{bmatrix} E_x & 0 & 0 \\ 0 & 0 & 0 \\ 0 & 0 & G_{xy}^d \end{bmatrix} \quad (5.3.2.18)$$

Fiber-Matrix Compression Failure

Bearing failure is one of the important failure modes appeared in bolted composite joints. Unlike the other two failure modes, it proceeds progressively which is the major characteristic of the failure mode. Bearing failure is a combination of multiple failure modes associated with matrix compression, fiber-matrix compression failure, and delamination. Material near the hole boundary is crushed by the bolt through compression positively. Due to the lateral constraint introduced by the bolt tightening pressure through washers, the material damaged under the bearing load could still carry load depending upon the amount of the tightening force, washer size and properties, and bolt joint configuration.

Accordingly, the bolt bearing strength strongly depends upon bearing area, tightening force, washer size, and bolt properties, in addition to the material properties of composites. Hence, it was assumed that material degradation due to bearing failure depends not only on the failure mode and the extent of the damage, but also on the bearing area, the tightening force, and washer size.

Therefore, the stiffness matrix $[Q_{xy}]$ of a unidirectional composite within the bearing failure area due to fiber-matrix compression failure was reduced as follows:

$$[Q_{xy}] = \begin{bmatrix} \frac{E_x}{1 - \nu_x \nu_y} & \frac{E_y \nu_x}{1 - \nu_x \nu_y} & 0 \\ \frac{E_x \nu_y}{1 - \nu_x \nu_y} & \frac{E_y}{1 - \nu_x \nu_y} & 0 \\ 0 & 0 & G_{xy} \end{bmatrix} \longrightarrow \begin{bmatrix} E_x^b & 0 & 0 \\ 0 & 0 & 0 \\ 0 & 0 & G_{xy}^b \end{bmatrix} \quad (5.3.2.19)$$

where the longitudinal modulus E_x and the tangent shear modulus G_{xy} degenerate according to the Weibull distribution as follows:

$$\frac{E_x^b}{E_x} = \exp \left[\left(- \frac{A^b}{A_0^b} \right)^\gamma \right]$$

$$\frac{G_{xy}^b}{G_{xy}} = \exp \left[\left(- \frac{A^b}{A_0^b} \right)^\gamma \right] \quad (5.3.2.20)$$

where E_x^b and G_{xy}^b are the reduced longitudinal compressive and shear moduli, respectively. A is the damage zone predicted by the fiber-matrix compression failure criterion, and A_0^b is defined as the critical damage area which is strongly related to the bearing area. Here, $A_0^b = \eta D^2$ was chosen to relate the damage area to the hole diameter of the joint. η is a coefficient related to the joint configuration and the material properties of composites and bolts. The value can be determined through experiments. A value of 0.35 was selected for graphite/epoxy and graphite/PEEK composites in the study.

The shape parameter of the above distributions is γ . The value of γ is strongly dependent upon the lateral constraint of the joints. Its value may vary with the amount of tightening force applied to the joint and the washer size. Therefore, the value has to be determined experimentally. For finger-tight bolted graphite/epoxy or graphite/PEEK composite joints, a value of 1.0 for γ provided the best fit with the experimental data. The value of γ once selected should be considered as a constant as long as the lateral constraint of the joints remains to be unchanged.

5.4 TEXTJOINT Code

In order to facilitate the aforementioned analyses, a computer code was developed by implementing the analysis into the existing BOLT code. The computer code is designated as TEXTJOINT. Basically, the code is able to provide the following information.

1. The complete response of the pin-loaded plate from initial loading to final failure.
2. The extent and mode of failure inside the composites at a given load.
3. The response of the structures as a function of joint geometries and material properties.
4. The interaction between two adjacent loaded holes on the strength and the failure mode.

A sample of the inputs to the computer code are given in Appendix A.

5.5 Numerical Results and Verifications

Numerical simulations were generated using the TEXTJOINT code and were compared with the available test data. T300/934 graphite fibers with thermoset resin composites and IM8/APC-HTA graphite fibers with thermoplastic matrix composites were considered. The material properties used in the calculations are listed in Table 6.

Material Properties		T300/976	IM8/APC-HT
<u>Moduli</u>			
Longitudinal Modulus	E_x (msi)	20.27	24.8
Transverse Modulus	E_y (msi)	1.88	1.15
In-Plane Shear Modulus	G_{xy} (msi)	1.01	0.63
Poisson's Ratio	ν_{xy}	0.23	0.33
Nonlinearity Parameter	α_s (psi) ⁻³	.8E-14	.8E-14
<u>Strengths</u>			
Longitudinal Tension	X_t (ksi)	220.00	402.3
Longitudinal Compression	X_c (ksi)	231.00	175.2
Transverse tension	Y_t^0 (ksi)	6.46	8.03
Transverse Compression	Y_c (ksi)	36.70	33.5
Logitudinal Shear, Cross ply	S_c (ksi)	15.50	22.5
<u>Parameters</u>			
Fiber Interaction Zone	δ	0.05	0.06
Shape parameter for Fiber tension Failure	β	8.00	7.6
Critical Bearing Area Coefficient	η	0.035	0.035
Shape Parameter for Bearing Failure	γ	1.0	1.0
In-situ Matrix Strength constant	A	1.30	1.3
In-situ Matrix Strength constant	B	0.70	0.70
In-situ Shear Strength constant	C	2.00	2.00
In-situ Shear Strength constant	D	1.00	1.00

Table 6 Material Properties of T300/934 and IM8/APC-HTA Composites

Figure 55 shows a comparison of the failure load of the bolted composite joint with a single hole predicted by the TEXTJOINT code and the test data.

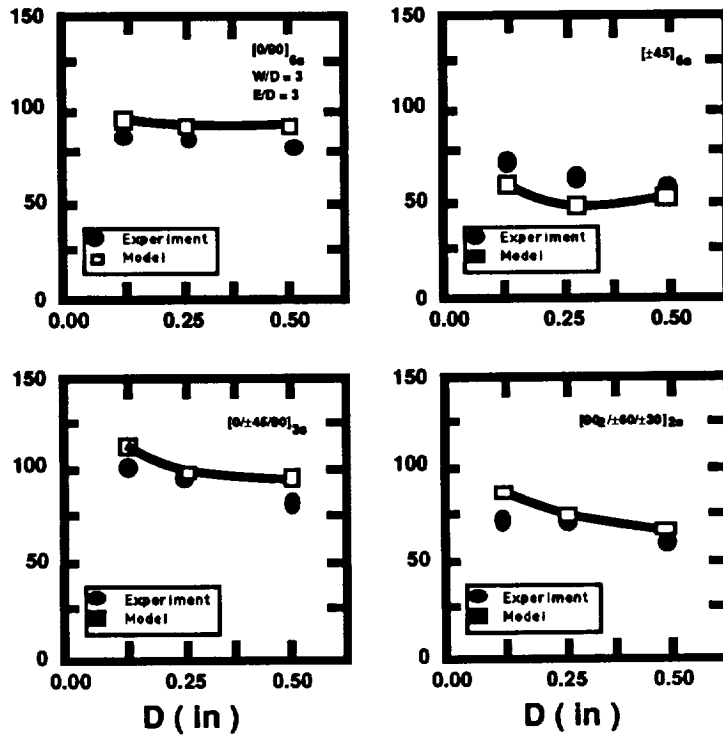


Figure 55 Measured versus Predicted Bearing Loads T300/934 Net-Tension or Shear-Out

Each box in the figure represents a different ply orientation. The data was taken from reference [6] and is indicated by solid symbols. The model predictions are shown by solid lines. The predictions agree very well with the test data.

The predicted damage progression as a function of the applied load for $[0/\pm 45/90]_{3s}$ and $[0/90]_{6s}$ laminates are analyzed. Figure 56 shows the predicted damage progression in the $[0/\pm 45/90]_{3s}$ laminate.

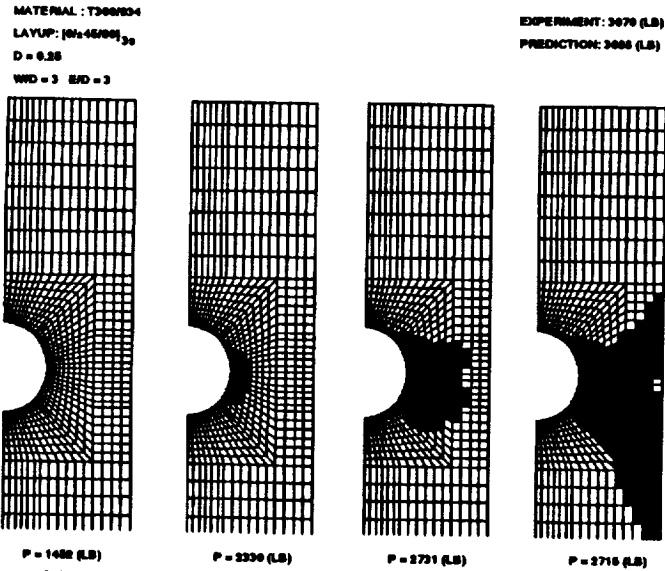


Figure 56 Predicted Damage Progression in a $[0/\pm 45/90]_{3S}$ Bolted Composite Joint

The predicted damage progression showed that the damage initiated from the hole boundary, near the stress concentrations, and propagated along the net-section of the specimen in the direction normal to the loading direction. The failure modes were initially dominated by matrix cracking and fiber-matrix shearing. Finally, a significant amount of fiber breakage occurred leading to a net-tension failure mode.

The predicted damage progression in a $[0/90]_{6S}$ laminate is shown in Figure 57.

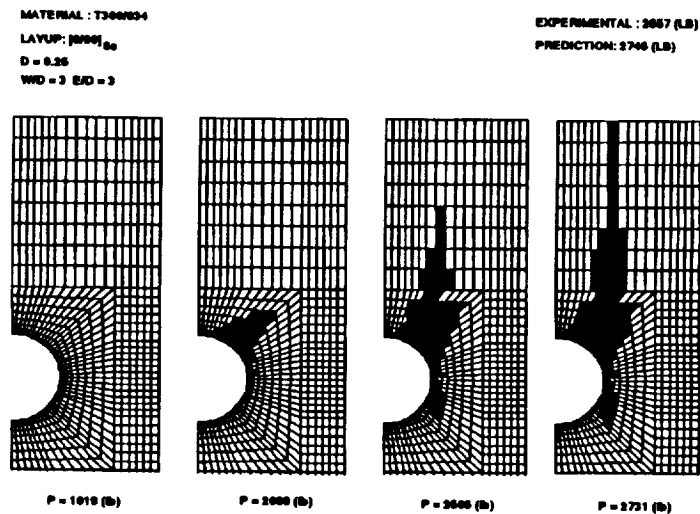


Figure 57 Predicted Damage Progression in a $[0/90]_{6S}$ Bolted Composite Joint

Matrix cracking in the 90 degree layers initiated from the hole boundary near the stress concentrations, and damage then grew in the 0 degree layers in a fiber-matrix shearing mode along the loading direction. Finally, the joint failed in a shear-out failure mode.

Figure 58 and Figure 59 present the predicted load-deflection response of IM8/APC-HTA composites containing a single hole. The test data was provided by Lockheed[9].

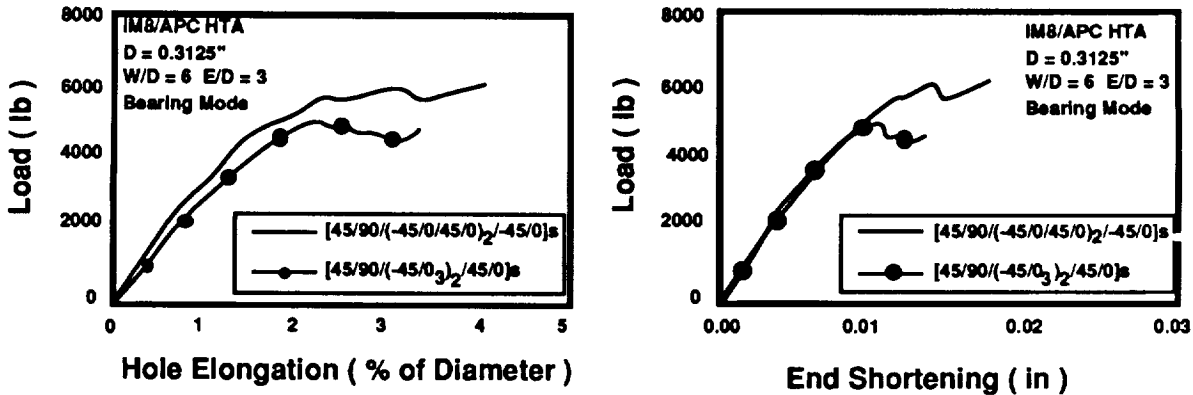


Figure 58 Predicted Load-Deflection Response of IM8/APC-HTA Bearing Failure Mode

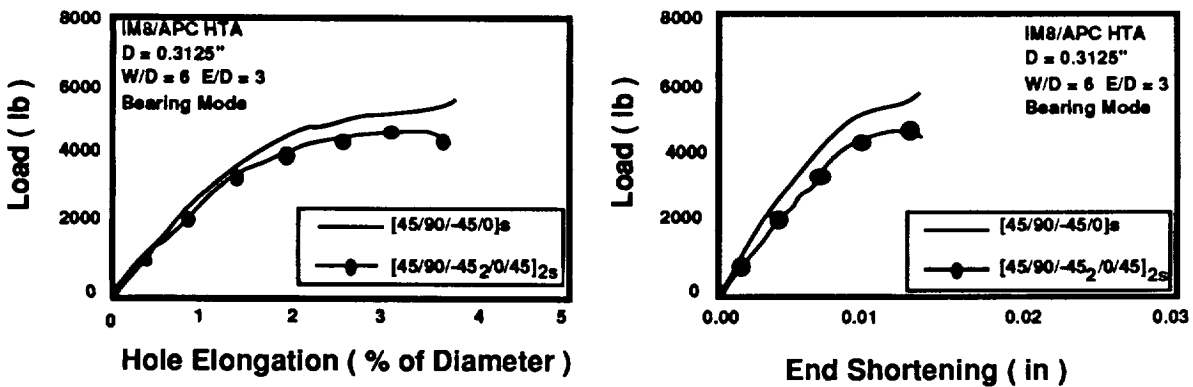


Figure 59 Predicted Load-Deflection Response of IM8/APC-HTA Bearing Failure Mode

The specimen configurations and the test data are listed in Table 7.

Ply Orientation	D(in)	$\frac{W}{D}$	$\frac{E}{D}$	H	P_{ult} lbs	P_{yield} lbs	P_{yield} 1.5	P_{model} lbs	Mode
[45/90/-45/0] _{3s}	.3215	6	3	.1248	7043	4228	6342	5738	Bearing
[45/90/-45/20/45] _{2s}	.3215	6	3	.1248	6552	4161	6242	5280	Bearing
[45/90/(-45/0/45/0) ₂ /-45/0] _s	.3215	6	3	.1248	6318	3631	5447	6070	Bearing
[45/90/-45/5/03/-45/03/45/0] _s	.3215	6	3	.1248	6236	3631	5447	5047	Bearing

Note: P_{yield} is determined by 0.5% D offset method and $1.5 * P_{yield}$ is the design strength. The predicted strength is determined as the hole elongation reaches 3% of the original hole diameter.

Table 7 Measured versus Predicted Bearing Load of IM8/APC-HTA Bearing Failure Mode.

All the specimens failed in the bearing failure mode. The response of load-hole elongation and load-end shortening curves for each ply orientation is shown in the figures. The numerical simulation was terminated when either the hole elongation exceeded three percent of the hole diameter or the load decreased continuously with the increase of the end shortening. It is noted that significant nonlinearity in the responses was predicted due to bearing failure. The failure load was predicted as the maximum load that the joint could carry before the hole exceeded the three percent requirement.

The predicted failure loads for IM8/APC-HTA composites are listed in Table 2 as compared to the measured data which was obtained from Lockheed.

The failure loads were measured by two ways, P_{ult} was the maximum load taken from the load-deflection curve measurement, and P_{yield} was measured by the 0.5% D offset method. It is noted that at P_{ult} , the joints might have suffered an excessive amount of hole elongation, which should not be used in the design as the actual bearing strength. However, there is no justification to substantiate the use of the 0.5% D offset measurement. The predicted failure loads based on the three percent hole elongation slightly under estimated the maximum bearing strength.

Figure 60 and Figure 61 show the predicted failure mode and the load-deflection curve of T300/934 composite joints containing two holes in parallel and in series, respectively. The predicted failure modes were consistent with the observed failure modes [15], and predicted failure loads agreed well with the test data [15].



[0/90]_{6s}

W/D = 8 E/D=3 Gh/D = 5 Pf = 5605 (lb)

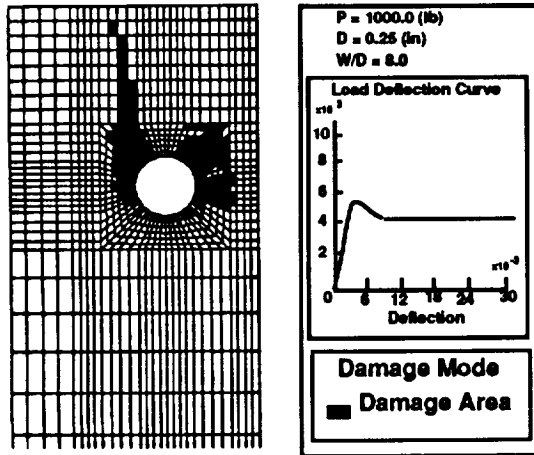


Figure 60 Predicted Load-Deflection Response of a [0/90]_{6s}, Two holes in parallel

Bolted Joints in Tandem

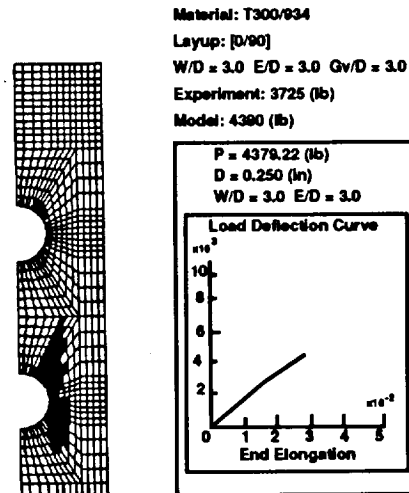


Figure 61 Predicted Load-Deflection Response of a [0/90]_{6s} with Two holes in series

5.6 Summary

A computer code TEXTJOINT was developed during this investigation by implementing a progressive failure analysis into the BOLT code. The code could be used as a design tool for analyzing the response of bolted composite joints containing a single hole or two holes in parallel or in series. Based on limited test data, the code predictions agreed well with the data. However, it is recommended that additional test data is needed to further substantiate the code. Although laminated composites were considered in this study, the code could be extended to include other composite systems.

6.0 Concluding Remarks

The objectives of developing efficient non-linear analysis capability and strength prediction methodology for combined in-plane and out-of-plane loading on the primary aircraft structures have been fully met. The development of "ISPAN" modules as pre- and post-processors to the DIAL code provided needed capability to conduct finite element analysis by an analyst with a minimum of finite element analysis experience. "ISPAN" modules may prove to be a useful analysis tool for concepts evaluation and trade studies.

The developed methodology has been verified thoroughly using benchmark problems, known solutions and correlations; however, the methods remain largely unverified for generic aircraft structures applications. The lack of experimental data, either in literature or within the scope of Phase I effort, was the prime reason for not verifying the method enhancements throughout its range of usefulness.

The following recommendations are made to increase the usefulness and confidence in the developed methods/tools:

Verify the ability of the interface element and bond material model to accurately predict skin/stiffener separation strength by performing a test correlation.

Conduct a through analytical evaluation and test verification of post-buckled stiffened panels analytically predicted failure mode(s) and failure loads.

Provide "flexible constraints" at rib/frame location to better simulate actual structural configurations.

Incorporate skin/stiffener interface elements in the "ISPAN" flat and curved stiffened panel modules.

7.0 References

1. A.C. Jackson, "Advanced Composites Structural Concepts and Materials Technologies for Primary Aircraft Structures", presented at the *First NASA Advanced Composite Technology Conference*, at Seattle Wa, October 29-November 1, 1990. NASA CP 3104, pp 39-70
2. A.C. Jackson, R.E. Barrie, B.M. Shah, and J.G. Shukla, "Advanced Textiles Applications for Primary Aircraft Structures", presented at the *Second NASA Advanced Composite Technology Conference*, at Reno NV, November 4-7,1991
3. Wempner, G.A., Discrete Approximations Related to Nonlinear Theories of Solids, *International Journal of Solids and Structures*, Vol 7, 1971, pp. 1581-1599
4. Riks, E., The Application of Newton's Method to the Problem of Elastic Stability, *Journal of Applied Mechanics*, Vol 39, 1972, pp 1060-1066
5. Shariffi and Sable, Structural Analysis of Bonded Joints using the Finite Element Method *International Conference on Composite Materials*, Honolulu, HI, 1991
6. Hashin, Z., "Failure Criteria for Unidirectional Fiber Composites," *Journal of Applied Mechanics*, Vol 47, June, 1980, pp. 329-334.
7. Tsia S.W. and Wu E.M., "A General Theory of Strength for Anisotropic Materials", *Journal of Composite Materials*, Vol 5, 1971, pg.58
8. Waszczak, J.P. and T.A. Cruse, "Failure Mode and Strength Predictions of Anisotropic Bolt Bearing Specimens," *Journal. of Composite Materials*, Vol. 5, 1971, pp. 421-425.
9. Agarwal, B.L., "Static Strength Prediction of Bolted Joint in Composite Material," *AIAA Journal*, Vol. 18, 1980, pp. 1345-1375.
10. Soni, S.R., "Failure Analysis of Composite Laminates with a Fastened Hole," *Joining of Composite Materials*, ASTM STP 749, K.T. Keward, *Am. Soc. of Testing and Materials*, 1981, pp. 145-164.
11. York, J.L., D.W. Wilson, and R.B. Pipes, "Analysis of Tension Failure Mode in Composite Bolted Joints," *Journal. of Reinforced Plastics and Composites*, Vol. 1, 1982, pp. 1412-153..
12. Garbo, S.P., and J. M. Ogonowski, "Effect of Variances and Manufacturing Tolerances on the Design Strength and Life of Mechanically Fastened Composite Joints," Flight Dynamics Laboratory, Air Force Wright Aeronautical Laboratories, Technical Report AFWAL-TR-81-3041, 1981.
13. Chang, F.K., R.A. Scott, and G.S. Springer, "Design of Composite Laminates Containing Pin Loaded Holes," *Journal. of Composite Materials*, Vol. 18, 1984, pp. 279-289.

14. Chang, F.K., K.Y. Chang, and S. Liu, "Damage Tolerance of Laminated Composites Containing an Open Hole and Subjected to Tensile Loading," *Journal. of Composite Materials*, Vol. 25, 1991, pp. 274-301.
15. Chang, F.K. and K.Y. Chang, "A Progressive Damage Model for Laminated Composites Containing Stress Concentration," *Journal. Composite Materials*, Vol. 21, 1987, pp. 834-855.
16. Chang, F.K. and K.Y. Chang, "Post-Failure Analysis of Bolted Composite Joints in Tension or Shear-Out Mode Failure," *Journal. of Composite Materials*, Vol. 21, 1987, pp. 809-833.
17. Lessard, L. and F.K. Chang, "Damage Tolerance of Laminated Composites Containing an Open Hole and Subjected to Compressive Loading, Part I - Analysis," *Journal. of Composite Materials*, Vol. 25, 1991, pp. 2-43.
18. Nuismer, R.J. and S.C. Tan, "Constitutive Relations of a Cracked Composite Laminate," *Journal. of Composite Materials*, Vol. 22, 1988, pp. 306-321.
19. Rosen, B.W., "Mechanics of Composite Strengthening," *Fiber Composite Materials*, Chapter 3, American Society for Metals, 1965.
20. Tsai, S.W. and H.T. Hahn, *Introduction to Composite Materials*, Lancaster, PA, Technomic Publishing Company, 1980.
21. Mallick, P.K., *Fiber-Reinforced Composites-Materials, Manufacturing and Design*, New York, Marcel Kekker, Inc., 1988.
22. Chamis, C.C., "Simplified Composite Micromechanics for Predicting Microstress," *Journal. of Reinforced Plastics and Composites*, Vol. 6, 1987, pp. 268-289.
23. Hairr, J.W., Huang, J.T., Ingram, J.E., and Shah, B.M., "Advanced Composites - Structural Concepts and Materials Technologies for Primary Aircraft Structures - Structural Response and Failure Analysis - ISPAN Modules Users Manual", NASA CR-4449, 1992.

Appendix A. TEXTJOINT Example Input

structures> pre-tj

-PRE-PROCESSOR FOR TEXTJOINT

THE PURPOSE OF THIS PROGRAM IS TO GENERATE AN INPUT FILE "TJ-1.DAT" FOR PROGRAM TEXTJT-1 WHICH ANALYZES A SINGLE DOUBLE LAP SHEAR JOINT OR "TJ-2.DAT" FOR PROGRAM TEXTJT-2 ANALYZING TWO DOUBLE LAB SHEAR BOLTED JOINTS IN TANDEM OR IN A ROW.

CHANG-LI HUNG, FU-KUO CHANG
STRUCTURES AND COMPOSITES LABORATORY
STANDFORD UNIVERSITY
STANDFORD CA 94305

DEC. 29, 1991

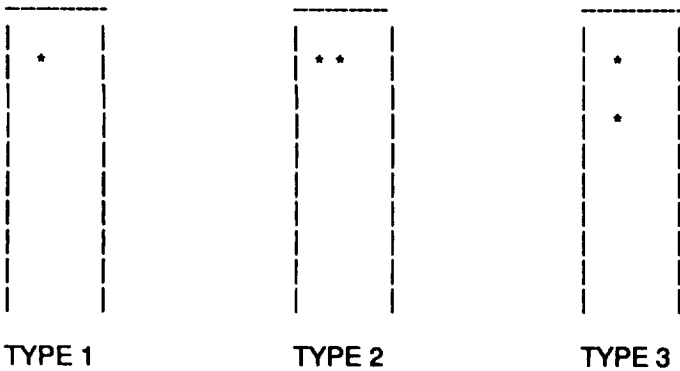
----- CAPABILITIES

TWO PROGRAMS ARE DEVELOPED TO DEAL WITH THREE TYPES OF COMPOSITES BOLTED JOINT DEFINED AS FOLLOWS:

TEXTJT-1: TYPE 1 - JOINTS WITH A SINGLE HOLE

TEXTJT-2: TYPE 2 - JOINTS WITH TWO IDENTICAL HOLES IN A ROW
 TYPE 3 - JOINTS WITH TWO IDENTICAL HOLES IN TANDEM

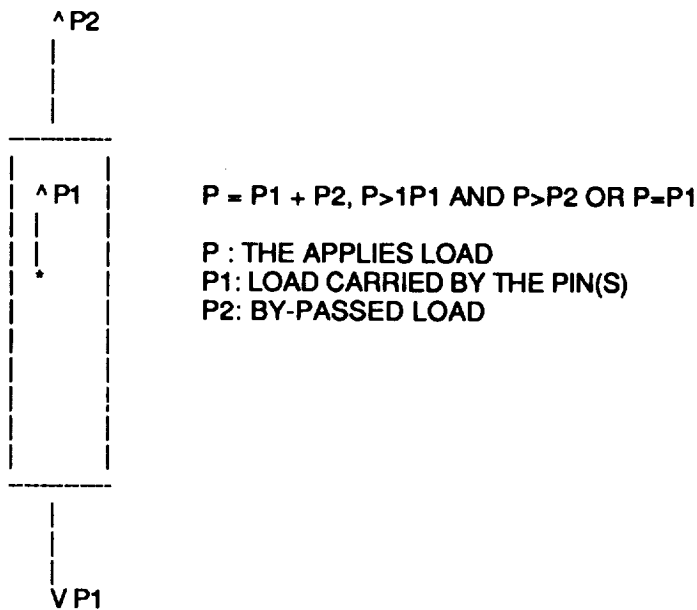
SEE FIGURE BELOW:



THIS PROGRAM CAN ALSO HANDLE THE FOLLOWING LOADING CONDITIONS:

- (A). PIN OR PINS CARRY ALL THE APPLIED LOAD
- (B). PIN OR PINS CARRY ONLY A FRACTION OF THE TOTAL LOAD APPLIED AT THE BOTTOM OF THE JOINT. THE REST OF THE LOAD IS CARRIED BY THE UPPER END

SEE FIGURE BELOW:



FOR EACH TYPE OF JOINT, THIS PROGRAM CAN HANDLE THE FOLLOWING SITUATIONS:

- (A). DIFFERENT PLY ORIENTATIONS
- (B). DIFFERENT MATERIAL PROPERTIES (SYMMETRIC LAMINATE)
- (C). DIFFERENT GEOMETRICAL CONFIGURATIONS INCLUDING DIFFERENT HOLE SIZES, HOLE POSITIONS, JOINT THICKNESS, AND JOINT LENGTHS

----- RESTRICTIONS:

THIS PROGRAM IS BASED ON THE FOLLOWING ASSUMPTIONS:

- (1). INCREMENTAL DISPLACEMENTS ARE APPLIED SYMMETRICALLY WITH RESPECT TO THE CENTERLINE OF THE PLATE
- (2). THE LAMINATE IS SYMMETRIC
- (3). HOLE SIZES ARE EQUAL IN EACH JOINT WITH TWO HOLES
- (4). PIN IS RIGID. THE PIN SUPPORT IS ALSO RIGID

----- ANALYSIS:

THE STRESSES ARE CALCULATED USING A FINITE ELEMENT METHOD FORMULATED ON THE BASIS OF TWO DIMENSIONAL CLASSICAL LAMINATION PLATE THEORY. THE FAILURE LOAD AND FAILURE MODE ARE DETERMINED BY USING PROGRESSIVE FAILURE ANALYSIS WHICH DEGRADES THE MATERIAL PROPERTIES ACCORDING TO DIFFERENT FAILURE MODES DETERMINED BYT A SET OF FAILURE CRITERIA

----- INPUT INSTRUCTIONS:

**** ENTER MATERIAL PROPERTIES ****

DO YOU WANT TO USE: <1> GRAPHITE/EPOXY T300/1034-C ?
OR <2> IM8/APC-HTA

ENTER YES OR NO

y

ENTER "1" FOR T300/1034-C

ENTER "2" FOR IM8/APC-HTA

2

JOINT TYPE SELECTION

TYPE 1: JOINT WITH A SINGLE HOLE

TYPE 2: JOINT WITH TWO HOLES IN A ROW

TYPE 3: JOINT WITH TWO HOLES IN A TANDEM

WHICH TYPE OF JOINT DO YOU WANT TO SELECT

ENTER 1, 2, OR 3.

1

DO YOU CONSIDER A BY-PASS LOAD ?

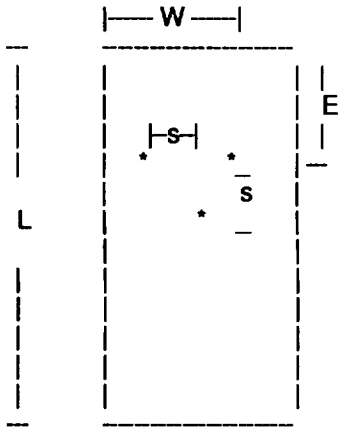
ENTER YES OR NO

no

THE FOLLOWING GEOMETRIC PARAMETERS MUST BE SPECIFIED

- (A) DIAMETER OF THE HOLE, D (D SHOULD BE LESS THAN 1 INCH FOR DEPENDABLE RESULTS)
- (B) WIDTH OF THE JOINT, W
- (C) LENGTH OF THE JOINT, L
- (D) EDGE DISTANCE OF THE JOINT, E
- (E) DISTANCE BETWEEN THE CENTERS OF THE HOLES, S

SEE FIGURE BELOW:



THE DIAMETER MUST BE INPUTED IN INCHES, OTHER GEOMETRIC PARAMETERS MUST BE RATIOS TO DIAMETER (PARAMETER/DIAMETER)

ENTER THE HOLE DIAMETER IN INCHES

0.3125

ENTER THE WIDTH TO DIAMETER RATIO:

6

ENTER THE EDGE TO DIAMETER RATIO:

3

ENTER THE LENGTH TO DIAMETER RATIO:

12

INPUT THE JOINT THICKNESS AND THE PLY ORIENTATIONS (SYMKMETRIC LAMINATE ONLY)
THE PLY ORIENTATIONS AND THE NUMBER OF PLIES IN THE PLY GROUP BY REPEATING IT.

EXAMPLE:

[(45/90/-45/0/45/-45)2]s

TOTAL NUMBER OF PLIES: 24

NUMBER OF PLIES IN THE PLY GROUP: 6

[(0/45/-45/90/90)2] s

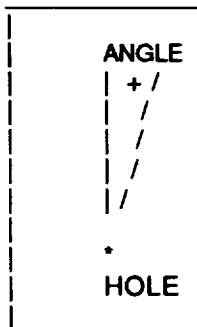
TOTAL NUMBER OF PLIES: 20

NUMBER OF PLIES IN THE PLY GROUP: 5

*2. EACH PLY ORIENTATION IS MEASURED FROM THE LOADING DIRECTION TO THE FIBER DIRECTION.

THE ANGLE IS POSITIVE CLOCKWISE AND NEGATIVE COUNTERCLOCKWISE

SEE FIGURE BELOW:



ENTER THE THICKNESS OF THE LAMINATE IN INCHES

0.1248

ENTER THE TOTAL NUMBER OF PLIES

** MAKE SURE THAT THE C.L.T IS APPLICABLE

INPUT AN INTEGER

24

ENTER THE THE NUMBER OF PLIES IN THE PLY GROUP.

INPUT AN INTEGER

4

ENTER THE PLY ORIENTATION OF PLY NUMBER 1

IN DEGREE (I.E., -90 <= ANGLE <= 90)

0

ENTER THE PLY ORIENTATION OF PLY NUMBER 2
IN DEGREE (I.E., -90 <= ANGLE <= 90)
45

ENTER THE PLY ORIENTATION OF PLY NUMBER 3
IN DEGREE (I.E., -90 <= ANGLE <= 90)
-45

ENTER THE PLY ORIENTATION OF PLY NUMBER 4
IN DEGREE (I.E., -90 <= ANGLE <= 90)
90

ENTER THE LOADING CONDITION

THE PROGRAM ALLOW USER TO CHOOSE 2 DIFFERENT LOAD INCREMENTS IN ORDER TO
SHORTEN THE TIME OF EXECUTION.

** INPUT INSTRUCTION

DEFINITION:

dP1: FIRST LOAD INCREMENT
dP2: SECOND LOAD INCREMENT
PL1: THE LOAD AT WHICH THE LOAD INCREMENT
SWITCHES FROM dP1 TO dP2

FOR TOTAL LOAD < PL1, TOTAL LOAD = dP1 ,* STEP NUMBER
FOR TOTAL LOAD > PL1, TOTAL LOAD = PL1 + dP2*STEP NUMBER

EXAMPLE:

dP1 = 400 (LB) dP2 = 200 (LB) PL1 = 4000 (LB)

THE PROGRAM CAN REACH 4000 (LB) IN 10 STEPS
AND USE SMALLER LOAD INCREMENT (200 (LB)) BEYOND
4000 (LB) TO REACH THE FINAL VALUE

ENTER THE FIRST LOAD INCREMENT dP1
200

ENTER THE SECOND INCREMENT dP2
100

ENTER THE LOAD PL1 (BEYOND PL1, dP2 IS USED)
4000

DO YOU WANT TO HAVE A LIST OF THE INPUT DATA ?
ENTER YES OR NO
yes

----- LIST OF DATA -----

JOINT TYPE SELECTION = 1
LOAD TYPE SELECTION: 0.00% OF BY-PASSED LOAD

< GEOMETRY >: (INCHES)

DIAMETER	WIDTH	EDGE	THICKNESS	LENGTH
0.3125	1.8750	0.9375	0.1248	3.7500

TOTAL PLY NO. = 24

< GROUP ORIENTATION >:

LAYER 1 ORIENTATION = 0.00 THICKNESS = 0.005200 INCH
LAYER 2 ORIENTATION = +45.0 THICKNESS = 0.005200 INCH
LAYER 3 ORIENTATION = -45.0 THICKNESS = 0.005200 INCH
LAYER 4 ORIENTATION = 90.0 THICKNESS = 0.005200 INCH

< MATERIAL PROPERTIES >:

LONGITUDINAL YOUNG'S MODULUS : 24800000.0 PSI
TRANSVERSE YOUNG'S MODULUS : 1155000.0 PSI
SHEAR MODULUS: 630000.0 PSI
POISSON RATIO: .330
LONGITUDINAL TENSILE STRENGTH 402300.0 PSI
TRANSVERSE COMPRESSIVE STRENGTH 175200.0 PSI
LAMINATE SHEAR STRENGTH: 22500.0 PSI

SHAPE PARAMETER FOR FIBER BREAKAGE FAILURE = 7.60
SHAPE PARAMETER FOR FIBER MATRIX SHEARING FAILURE = 7.60
SHAPE PARAMETER FOR BEARING FAILURE (FIBER COMP.) = 1.0
IMPIRICAL CONSTANT FOR CRITICAL BEARING AREA = 0.36

FIBER INTERACTION ZONE DELTA = 0.0600

DO YOU WANT TO MAKE ANY CHANGE IN YOUR DATA
ENTER YES OR NO

no
composite>

REPORT DOCUMENTATION PAGE			Form Approved OMB No. 0704-0188	
Public reporting burden for this collection of information is estimated to average 1 hour per response, including the time for reviewing instructions, searching existing data sources, gathering and maintaining the data needed, and completing and reviewing the collection of information. Send comments regarding this burden estimate or any other aspect of this collection of information, including suggestions for reducing this burden, to Washington Headquarters Services, Directorate for Information Operations and Reports, 1215 Jefferson Davis Highway, Suite 1204, Arlington, VA 22202-4302, and to the Office of Management and Budget, Paperwork Reduction Project (0704-0188), Washington, DC 20503.				
1. AGENCY USE ONLY (Leave blank)	2. REPORT DATE September 1992	3. REPORT TYPE AND DATES COVERED Contractor Report (May 1989-May 1992)		
4. TITLE AND SUBTITLE Advanced Composites Structural Concepts and Materials Technologies for Primary Aircraft Structures - Structural Response and Failure Analysis		5. FUNDING NUMBERS C NAS1-18888 WU 510-02-13-01		
6. AUTHOR(S) W.J. Dorris, J.W. Hairr, J.T. Huang, J.E. Ingram, and B.M. Shah				
7. PERFORMING ORGANIZATION NAME(S) AND ADDRESS(ES) Lockheed Aeronautical Systems Company 86 South Cobb Drive Marietta, GA 30063		8. PERFORMING ORGANIZATION REPORT NUMBER LG92ER0035		
9. SPONSORING / MONITORING AGENCY NAME(S) AND ADDRESS(ES) NASA Langley Research Center Hampton, VA 23681-0001		10. SPONSORING / MONITORING AGENCY REPORT NUMBER NASA CR-4448		
11. SUPPLEMENTARY NOTES Langley Technical Monitor: Randall C. Davis Task 2, Final Report				
12a. DISTRIBUTION / AVAILABILITY STATEMENT Subject Category 05		12b. DISTRIBUTION CODE		
13. ABSTRACT (Maximum 200 words) Non-linear analysis methods were adapted and incorporated in a finite element based DIAL code. These methods are necessary to evaluate the global response of stiffened structure under combined in-plane and out-of-plane loading. These methods include the Arc Length method and target point analysis procedure. A new interface material model was implemented that can model elastic-plastic behavior of the bond adhesive. Direct application of this method is in skin/stiffener interface failure assessment. Addition of the AML failure procedure and Hasin's failure criteria provides added capability in the failure predictions. ISPAN (Interactive Stiffened Panel Analysis) modules were developed as an interactive pre-and post-processors. Each module provides the means of performing self-initiated finite elements based analysis of primary structure such as: flat or curved stiffened panel; corrugated flat sandwich panel; and curved geodesic fuselage panel. This modules brings finite element analysis into design of composite structure without the requirement for the user to know much about the techniques and procedures need to actually perform a finite element analysis from scratch. An interactive finite element code was developed to predict bolted joint strength considering material and geometrical non-linearity. The developed method conducts an ultimate strength failure analysis using a set of material degradation models.				
14. SUBJECT TERMS Non-Linear Analysis; Post buckling analysis, skin-stiffener interface; Failure Predication; Interactive generic structure analysis; bolted composite joint analysis; Progressive damage predictions.		15. NUMBER OF PAGES 107		16. PRICE CODE
17. SECURITY CLASSIFICATION OF REPORT Unclassified	18. SECURITY CLASSIFICATION OF THIS PAGE Unclassified	19. SECURITY CLASSIFICATION OF ABSTRACT	20. LIMITATION OF ABSTRACT	